CHALMERS
UNIVERSITY OF TECHNOLOGY

# Alternative Methods for Quick-Clay Mapping

Master's thesis in the Master's Programme Infrastructure and Environmental Engineering


LISA SUNDSTRÖM
ALEXANDER WAERME

DEPARTMENT OF ARCHITECTURE AND CIVIL ENGINEERING
DEVISION OF GEOLOGY AND GEOTECHNICS



CHALMERS UNIVERSITY OF TECHNOLOGY
Gothenburg, Sweden 2022
www.chalmers.se

MASTER'S THESIS ACEX30

# Alternative Methods for Quick-Clay Mapping

*Master's Thesis in the Master's Programme Infrastructure and Environmental Engineering*

LISA SUNDSTRÖM
ALEXANDER WAERME

Department of Architecture and Civil Engineering
*Division of Geology and Geotechnics*
CHALMERS UNIVERSITY OF TECHNOLOGY

Göteborg, Sweden 2022

Alternative Methods for Mapping Quick Clay

*Master's Thesis in the Master's Programme Infrastructure and Environmental Engineering*

LISA SUNDSTRÖM

ALEXANDER WAERME



Examensarbete ACEX30
Institutionen för Arkitektur och Samhällsbyggnadsteknik
Chalmers Tekniska Högskola, 2022

Department of Architecture and Civil Engineering
Division of Geology and Geotechnics
Chalmers University of Technology
SE-412 96 Göteborg
Sweden
Telephone: + 46 (0)31-772 1000

Cover:
Collage including: Geotechnical field work at Åseberget, remoulded clay before shear strength testing and a T-bar penetrometer mounted on the drilling rig. Pictures taken by the authors during the project.

Department of Architecture and Civil Engineering
Göteborg, Sweden, 2022

Alternative Methods for Quick-Clay Mapping

*Master's thesis in the Master's Programme Infrastructure and Environmental Engineering*

LISA SUNDSTRÖM
ALEXANDER WAERME

Department of Architecture and Civil Engineering
Division of Geology and Geotechnics
Chalmers University of Technology

ABSTRACT

Construction and development in quick-clay areas is often associated with great challenges. The conventional method for confirming quick-clay deposits in Sweden is undisturbed soil sampling and subsequent laboratory testing. Reliable geotechnical field investigation methods that could reduce the need for time consuming and costly undisturbed soil sampling with following laboratory work has for a long time been desired in the geotechnical industry. The overall objective of this thesis has been to test three methods that potentially could be used to simplify the process of quick-clay mapping. Two of the methods focused on refining existing geotechnical field investigation methods. First, multiple cone penetration tests (CPT) were performed in the exact same location. Second, a cyclic T-bar penetration test (TPTc) was performed by letting the T-bar penetrometer circulate between two predefined depths before being penetrated down to another cyclic level. Both methods were executed to obtain data that was then used to evaluate the undisturbed and remoulded undrained shear strengths. The main finding when performing three consecutive CPT soundings were that it could not be seen as a reliable method for evaluation of the remoulded undrained shear strength. A decrease in penetration resistance was however noted, which is implying that the clay gets disturbed. Uncertainties related to difficulties with performing all soundings following the same path and uncertainties regarding if the consecutive soundings are remoulding the clay enough, where the main difficulties found. The evaluated undrained shear strength from the TPTc proved to give reasonable results for the undisturbed undrained shear strength. For the remoulded conditions the results showed that at depth where sufficiently many cycles were made, the remoulded undrained shear strength corresponded well with the laboratory results. There are uncertainties regarding the correction factor for evaluation of the undrained shear strength since there is yet no empirical relation for what correction factor to use. The third and last method was focusing on developing statistical tools to potentially find relations between results from field- and laboratory investigations. One method that was tested were to perform a statistical analysis using principal component analysis (PCA). The results of that analysis showed no clear relations between the parameters collected from laboratory results and parameters collected from field results, at least not on a regional scale. Another method was to evaluate the impact of draining soil layers on the formation of quick clay. The distance to a draining layer was compared to the corresponding remoulded undrained shear strength evaluated with fall cone test. The comparison did however not show any strong general correlations.

Key words: Undrained shear strength, quick clay, CPT, TPT, Cyclic T-bar penetration test, PCA.

Alternativa Metoder för Kartläggning av Kvicklera

*Examensarbete inom masterprogrammet Infrastruktur och Miljöteknik*

LISA SUNDSTRÖM
ALEXANDER WAERME

Institutionen för Arkitektur och Samhällsbyggnadsteknik
Avdelningen för Geologi och Geoteknik
Chalmers tekniska högskola

SAMMANFATTNING

Exploatering i områden där kvicklera har påvisats är ofta förenat med stora utmaningar. Den vedertagna metoden för att utvärdera förekomsten av kvicklera i Sverige kräver ostörda jordprover för att sedan utföra tester i laboratorium. Tillförlitliga geotekniska fältundersökningsmetoder som skulle kunna minska behovet av tidskrävande och kostsamma provtagningar av ostörda jordprover och laboratoriearbete har länge varit efterfrågat inom den geotekniska branschen. Det övergripande syftet med denna studie var att testa tre metoder som potentiellt skulle kunna användas för att förenkla kartläggningen av kvicklera. Två av metoderna fokuserade på att utveckla befintliga geotekniska fältundersökningsmetoder. Den ena metoden gick ut på att utföra flera spetstryckssonderingar (CPT) på exakt samma plats. Den andra metoden gick ut på att utföra cyklisk T-bar sondering (TPTc) genom att låta en T-bar tryckas ner och dras upp mellan två fördefinierade djup innan den trycktes ner till nästa nivå där ytterligare ett antal cykler utfördes. Båda metoderna utfördes för att erhålla data som användes för att utvärdera den ostörda och omrörda odränerade skjuvhållfastheten. Slutsatsen av de tre på varandra följande CPT sonderingarna var att det inte kan ses som en tillförlitlig metod för utvärdering av den omrörda odränerade skjuvhållfastheten. Dock minskade spetstrycksmotståndet mellan sonderingarna, vilket tyder på att leran störs. De största osäkerheterna med denna metod är kopplade till om alla sonderingar följer samma spår och om de på varandra följande sonderingarna stör leran tillräckligt mycket. Den utvärderade odränerade skjuvhållfastheten från TPTc visade sig ge rimliga resultat för den ostörda odränerade skjuvhållfastheten. I den störda leran visade resultaten att där tillräckligt många cykler hade gjorts, motsvarade den omrörda odränerade skjuvhållfastheten laboratorieresultaten väl. Det finns osäkerheter kring vilken korrektionsfaktor som bör användas för utvärdering av den odränerade skjuvhållfastheten eftersom det inte finns något utvecklat empiriskt samband. I den tredje och sista metoden som testades var målet att utveckla olika statistiska verktyg för att potentiellt hitta samband mellan resultat från tidigare utförda geotekniska fält- och laboratorieundersökningar. En metod som användes för att testa detta var att utföra en principialkomponentanalys (PCA). Resultaten av den analysen visade inga tydliga samband mellan parametrarna som samlats in från laboratorieresultat och parametrarna som samlats in från fältresultat, åtminstone inte på en regional nivå. En annan metod som användes var att utvärdera effekten ett dränerande jordlager kan tänkas ha för bildandet av kvicklera. I den metoden plottades avståndet från en godtycklig punkt till ett dränerande lager med motsvarande omrörda odränerade skjuvhållfasthet utvärderad med fallkonförsök. Jämförelsen visade dock inga tydliga samband.

Nyckelord: Odränerad skjuvhållfasthet, kvicklera, CPT, TPT, cyklisk T-bar sondering, PCA.

# Contents

# Preface

This Master thesis was conducted as the finalising project of our education at Chalmers University of Technology. The thesis was done together with the consultant company Norconsult AB.

We especially want to thank our supervisor Martin Persson at Norconsult AB, who came up with the idea of coordinating several studies in an interesting area and that we got the opportunity to be part of that. Martin has been very supportive and a great brainstorming partner during the process of our thesis. His knowledge and critical thinking have been very helpful.

We also want to thank the nice colleagues at the geotechnical division at Norconsult, who always answered our questions and supported us when we had doubts.

This project has partially been done as a case study. That would not have been possible without the landowner and land developer Bokab. We therefore would like to thank Bokab for funding the geotechnical field investigations performed at the Åseberget site.

We would like to thank Fredrik Andersson at Norconsult Fältgeoteknik AB for performing the geotechnical field work that was part of the project. We especially would like to thank Fredrik for explaining and letting us be part of the work and for enduring long workdays in horrible weather.

The laboratory work conducted in this project would not have been possible without the excellent support and guidance from Georgios Birmpilis at the Chalmers Geomechanics laboratory.

Last but not least, we want to thank our supervisor and examiner Mats Karlsson at Chalmers University of Technology for supporting us during the whole process.

# Notations

### Roman upper case letters

| | |
|---|---|
| $A_s$ | Surface area of the friction sleeve [mm$^2$] |
| $A_{sb}$ | Cross-sectional bottom area of the friction sleeve [mm$^2$] |
| $A_{st}$ | Cross-sectional top area of the friction sleeve [mm$^2$] |
| $A_c$ | Projected area of the cone [mm$^2$] |
| $A_p$ | Projected area of the T-bar in plane normal to the shaft [mm$^2$] |
| $B_q$ | Pore pressure ratio [-] |
| CPT | Electric cone penetration test |
| CPTu | Piezocone penetration test (with pore pressure measurement) |
| $F_s$ | Measured force acting on the friction sleeve [kN] |
| $I_p$ | Plasticity index [%] |
| JB | Soil/Rock probing |
| Kv | Piston sampler (undisturbed) |
| $M$ | Correction variable for liquid limit [-] |
| $N$ | Correction variable for liquid limit [-] |
| $N_{ke}$ | Effective cone factor for evaluation of shear strength [-] |
| $N_{kt}$ | Empirical cone factor for evaluation of shear strength [-] |
| $N_s$ | Cone factor for estimation of sensitivity [-] |
| $N_T$ | T-bar factor for evaluation of undrained shear strength [-] |
| $N_{T,rem}$ | T-bar factor for evaluation of undrained remoulded shear strength [-] |
| $N_{\Delta u}$ | Cone factor used when evaluating $c_u$ using excess pore pressure [-] |
| $OCR$ | Over consolidation ratio [-] |
| $Q_c$ | Measured force on the cone [kN] |
| $R_f$ | Friction ratio between the sleeve friction and the cone resistance [%] |
| $S_t$ | Sensitivity [%] |
| Skr | Auger sampler (disturbed) |
| TPT | T-bar penetration test |
| TPTc | Cyclic T-bar penetration test |
| Tr | Pyramid penetration test |

### Roman lower case letters

| | |
|---|---|
| $a$ | Net area ratio between the cross-sectional area of load cell or shaft, and the cross-sectional area of the cone/T-bar [-] |
| $c$ | Constant used for evaluation of shear strength from the fall cone test, dependent on the tip angle used for the specific test [-] |
| $c_u$ | Undrained shear strength estimated from CPT or TPT [kPa] |
| $c_{ufc}$ | Undrained shear strength of an undisturbed soil sample estimated by the fall cone test [kPa] |
| $c_{urfc}$ | Undrained shear strength of a remoulded soil sample estimated by the fall cone test [kPa] |
| $f_s$ | Measured sleeve friction [kPa] |

| | |
|---|---|
| $f_t$ | Corrected sleeve friction [kPa] |
| $g$ | Acceleration due to gravity at free fall [m/s$^2$] |
| $i$ | Penetration depth of the cone into the soil sample in a fall cone test [mm] |
| $m$ | Mass of the cone used in a fall cone test [g] |
| $q_c$ | Measured cone resistance [kPa] |
| $q_{c,T-bar}$ | Measured penetration resistance in a TPT [kPa] |
| $q_e$ | Effective cone resistance [kPa] |
| $q_t$ | Corrected cone resistance [kPa] |
| $q_{t,T-bar}$ | Corrected penetration resistance in a TPT [kPa] |
| $u_0$ | *In situ* equilibrium pore water pressure [kPa] |
| $u_1$ | Measured pore pressure at $u_1$ [kPa] |
| $u_2$ | Measured pore pressure at $u_2$ [kPa] |
| $u_3$ | Measured pore pressure at $u_3$ [kPa] |
| w | Water content [%] |
| $w_L$ | Liquid limit [%] |
| $w_n$ | Natural water content [%] |
| $w_P$ | Plastic limit [%] |

**Greek letters**

| | |
|---|---|
| μ | Empirical correction factor used for correcting shear strengths evaluated from the fall cone test or the field vane test [-] |
| $\Delta u$ | Excess pore pressure $(u - u_0)$ [kPa] |
| $\sigma'_c$ | Pre-consolidation pressure [kPa] |
| $\sigma_{vo}$ | *In situ* vertical stress [kPa] |
| ρ | Density [t/m$^3$] |

# 1 Introduction

Construction and developments in clay areas requires a careful evaluation of soil properties to avoid negative consequences. A traditionally important soil parameter when evaluating the suitability for construction is the sensitivity. The sensitivity is a unitless ratio between the undisturbed undrained shear strength and the remoulded undrained shear strength of the soil (Swedish Geotechnical Institute [SGI], 2018). Clays with a sensitivity of over 50 and a remoulded undrained shear strength below 0.4 kPa are classified as quick clays (Larsson, 2008).

In parts of Sweden previously submerged after glaciation, quick clay is a critical problem since the shear strength of the clay can decrease drastically if the clay is disturbed. Small initial landslides in quick-clay areas can evolve and successively cause major damage including social and economic costs. The 2006 Småröd quick-clay landslide resulted in a total societal cost of 520 million Swedish crowns (SEK) (MSB, 2009).

Today several different methods are used for indicating quick-clay presence. Sounding methods like cone penetration testing (CPT) and pyramid penetration test (Tr) are commonly used to get an overview of clay behaviour. Möller & Bergdahl (1982) found that the slope of the penetration resistance with depth normally is steep when performed in sensitive clays. The slope of the penetration resistance against depth has since then been a useful tool for evaluating the sensitivity of a clay from CPT and Tr (Lundström et al., 2009; Rankka et al., 2004).

Another method that has been used for identifying quick clay *in situ* is resistivity measurements. In marine clays that have been leached by freshwater a correlation with the salt content and the sensitivity is often found. Resistivity measurements can at these sites provide useful information on stratigraphy and clay parameters. Where high resistivity is detected, prerequisites for the clay to be quick exists (Lundström et al., 2009). However, in Sweden fall cone testing is the only method that is used to confirm the sensitivity of a clay. Geotechnical sampling followed by laboratory work constituted of fall cone testing is therefore required to verify the presence of quick clay (SGI, 2018). Drawbacks with fall cone testing is that it is costly and time consuming, since it is performed in a laboratory and requires undisturbed samples from the site. As a consequence, cost and time constraints could often result in soil samples being recovered at few locations in a typical project. The lateral density therefore often is lower than desired. The low coverage may negatively impact stability calculations and safety in the built environment. The possibility to perform cost effective methods for mapping quick clay is therefore in demand in the geotechnical industry.

## 1.1 Case study

The project will partly be done as a case study. The site that will be investigated is called Åseberget, located in the municipality of Kungälv in the south-west of Sweden, 20 km north of Gothenburg. Early-stage planning and design work is ongoing. The ambition for the area stated by the landowner and land developer Bokab is to establish a new residential area consisting of roughly 1500 to 2000 dwelling units (AL Studio, 2021). As part of the prestudies for the project, geotechnical field work will take place. Results from the geotechnical field work will be used in this project.

## 1.2 Aim and objectives

The aim of the project is to test different methods that potentially could be used to simplify the process of mapping quick clay. The overall objective with all methods is to minimise the dependency on undisturbed soil samples in the geotechnical industry, while still being able to conduct a correct mapping of quick clay. As part of fulfilling the aim of the thesis the following objectives will be researched.

- Could multiple consecutive piezocone penetration tests (CPTu) performed in the same position be used as a reliable method for evaluation of the remoulded undrained shear strength?
- Could cyclic T-Bar penetration testing (TPTc) be used as a reliable method for evaluation of the undisturbed and remoulded undrained shear strength?
- Assess the sources of error when performing the alternative field methods.
- Assess the difference in results when performing laboratory testing at two separate laboratories.
- Could a combined assessment using data from a great number of existing geotechnical field- and laboratory datasets be used as a reliable method for indicating the presence of quick clays and could this be statistically verified?

## 1.3 Scope and limitations

Several field methods were executed as part of the field study, but only cone and piezocone penetration test (CPT, CPTu), T-bar penetration test (TPT) and standard piston sampling will be explained and discussed in this study. Soil/rock probing (Swe. JB-sondering), auger sampling and pyramid penetration testing was part of the geotechnical field investigation, but the results of the tests was solely used for identification of boreholes suitable for further analysis. Some existing methods for implying the presence of quick clay from field measurements will be mentioned and partly explained but not conducted or discussed further. The reference undrained shear strength will be evaluated exclusively from fall cone test in this study. No triaxial testing, field vane test or direct simple shear tests have been performed. The undrained shear strength will hereafter be referred to as shear strength since drained shear strength is not affected or relevant in this study. The statistical analysis is a regional analysis, the datasets used is limited to south-west Sweden. The prerequisites for the collected dataset are that the test points must be within the selected area. The raw data collection from the CPT and routine laboratory testing have been performed without any further analysis of the properties or characteristics of the soil. The field measurements and laboratory results conducted in the case study part of this project is not included in the statistical analysis.

# 2 Quick clay and generalised geology in SW Sweden

This chapter includes a brief description of the geology in south-west Sweden and its implications on the formation of quick clay. Additionally, the case study site Åseberget and its geological and geotechnical prerequisites will be described. For geologist, the term soil is per definition referred to as the surficial organic-rich weathered zone. Soil will in this report, in accordance with the geotechnical engineering world, refer to the top soil, as well as glacial, glaciofluvial and marine sediments.

## 2.1 Brief geological description of south-west Sweden

The geology of the Gothenburg region is characterised by a large proportion of bedrock outcrops in the elevated parts of the region and fine-grained soils in the lower -lying fracture valleys (Bergström et al., 2022). The fine-grained material is often clayey. The quaternary geology of the region has been highly affected by the last glaciation and deglaciation. The melting of the most recent ice sheet in the region occurred between circa 14 500 to 16 000 years ago (Bergström et al., 2022). During that period the direction of the movement of the ice was for the most part from north-east (Bergström et al., 2022). In the Göta älv valley at that time, large amounts of silt and clay particles were transported by the meltwater and became deposited as glaciomarine clay (SGI, 2012).

A factor that has played a major roll on the formation of the soil stratigraphy is that a majority of the land area in the region is located below the marine limit. During glaciation, the ground surface was depressed far below the sea level. The ground level has since the deglaciation risen isostatically and keeps doing so to this day. The current post-glacial rebound is around 2 mm/year in the Gothenburg region and the highest regional marine limit is located around 90 to 100 m above the current sea level (Bergström et al., 2022). Clay is in general only expected in areas located below the marine limit even if lacustrine clays occur also. Above and around the marine limit none or very shallow clay depths is expected (Bergström et al., 2022).

The relation between the soil stratigraphy and deposition environment is closely correlated to each other. According to Stevens et al. (1984) the soil types in the south-west of Sweden could be divided into a generalised stratigraphy. Directly on the bedrock there is normally a glacial till layer. The glacial till layer often has a thickness of less than five metres, where a thickness of one or two metres is common. A gravelly-sandy glaciofluvial layer can sometimes be recorded over the glacial till. Silty clay with interbedded sand layers is generally deposited above the gravely sand. In the lowest part of this soil unit, silt and clay is frequently varved with sand. Upwards in this soil unit, sand layers occur less frequently (Stevens et al., 1984). Overlaying this soil layer is normally a silty clay layer, with the silt particles generally decreasing upward in the soil unit (Stevens et al., 1984). Silt particles is decreasing upward in the soil unit, due to the distance to the ice front becoming longer with time. The effect of the deglaciation was that only the lighter clay particles were able to be transported longer distances where they later on deposited (SGI, 2012). The largest clay depths in the Gothenburg region are found in the Göta älv valley with clay depths of around 50 to 100 metres (Bergström et al., 2022). Drilling near the Gothenburg central station and the Masthuggskajen have proven clay deposits of over 110 metres (Persson, personal communication, May 30, 2022).

Above the homogeneous clay layers a slightly silty clay layer with presence of sand is normally found. The formation of that layer could be explained by erosion of the underlaying clay layer that later on became re-deposited. The underlaying clay layer were deposited in meltwater from the receding ice front. During a period after the deglaciation these layers became vulnerable to erosion and landslides due to the great land uplift that occurred at that time. The erosion and landslides therefore led to redeposition of coarser material together with the eroded clay (Stevens et al., 1984). The formation of this so called post-glacial clay normally deposited in valleys and coastal areas. Its geotechnical properties are often similar to that of the glacial clay (Bergström et al., 2022).

Above the post-glacial clay layer, closer to the ground, clays with a higher organic content are occasionally found. This organic clay was deposited during a more recent period with warmer climate which was favourable for organic production. The soil content in this layer is however highly impacted by local processes and is therefore varying to a large extent (Stevens et al., 1984).

## 2.2 Quick clay

In south-west Sweden (including the Gothenburg region, the Göta älv valley and other valleys) quick clay is not uncommon (SGI, 2012). Clays with potential to become quick clays have normally been deposited in sea water during the end of the last glaciation (Rankka et al., 2004).

What characterises a quick clay is a clay with a soil structure that completely collapses after being remoulded. In Sweden a clay is classified as quick if it has a remoulded shear strength below 0.4 kPa and a sensitivity above 50, where the sensitivity is the ratio of the undisturbed shear strength and the remoulded shear strength (Rankka et al., 2004). In Norway a clay is classified as quick if the remoulded shear strength is below 0.5 kPa (NGS, 2011). In Canada, a clay needs to have a remoulded shear strength below 1.0 kPa and a liquidity index above 1.2 kPa to be classified as a sensitive clay (Lundström et al., 2009). The liquidity index is the ratio of the difference between the natural water content and the plastic limit of the soil to its plasticity index (Larsson, 2008).

The deposition environment of the clay particles is an important factor determining if a clay could develop quick behaviour. In south-west Sweden, clay particles have mostly been deposited in sea water (Rankka et al., 2004). Clays deposited in sea water will naturally have a high salt content. The ions found in seawater on the west coast of Sweden are normally sodium ($Na^+$), chloride ($Cl^-$), potassium ($K^+$), magnesium ($Mg^{2+}$) and sulphate ($SO_4^{2-}$) (Löfroth et al., 2011). Naturally the clay will therefore contain these ions. In addition, clay particles are normally negatively charged. Hence, positively charged ions will be adsorbed to the clay particles. Consequently, the amount of positively charged ions are normally much higher in the clay structure compared to the amount of positively charged ions in the pore water in the original clay deposit (Löfroth et al., 2011).

If the clay is exposed to groundwater flow or precipitation, leaching of ions in the pore space and on clay particle surfaces can occur. The leaching result in an overall decrease in ion contents which with time could affect the structure of the clay particles (Rankka et al., 2004). As freshwater flows through the clay deposit initiating leaching of ions (sodium in particular) the pore water will cease to be in equilibrium with the ions adsorbed to the surrounding clay particles. This will have the effect that ions adsorbed to the clay particles will move to the pore water in the clay deposit to sustain in equilibrium. With time these positively charged ions will to a large extent decrease. The ion concentration in the pore water will then also decrease until it resembles the ion concentration of the water leaching the deposit (Löfroth et al., 2011). This process will strongly weaken the structure of the clay deposit and make it sensitive to disturbance. If this weakening of the soil structure is ongoing for a longer period of time, quick clay can be formed.

### 2.2.1 Geological prerequisites for formation of quick clay

To distinguish areas where quick clay potentially could be formed, geological and hydrogeological prerequisites can be studied. One fundamental prerequisite for formation of quick clay is that the area should be located below the marine limit. This is because very little clay has been deposited above and close to the marine limit (Rankka et al., 2004). Due to the normally low permeability of a clay deposit, it is unlikely to find quick clay in deep deposits of homogeneous clay. Because the thicker the clay layer is, the longer it will take for the leaching process to reduce the salt content in the soil. Hence, quick clay is normally found in thinner deposits in direct proximity to soil layers with a higher permeability. Layers of silt and sand interbedded in a clay deposit is therefore increasing the possibility of water leaching the clay deposit and reducing the salt content (Rankka et al., 2004).

A glacial till layer interlaying the bedrock and the clay in a clay deposit could have an impact on the formation of quick clay if a sufficiently high water flow could occur. The water flow in a glacial till layer is dependent on if the hydraulic conductivity is sufficiently high. It is also dependent on if the layer is in direct contact with infiltrating precipitation or surface water like lakes, rivers and streams. Or if it is connected to the groundwater through fractures in the underlying bedrock (Rankka et al., 2004).

Based on the above mentioned prerequisites, quick clay could for example be found close to valley sides where rock outcrop is visible. Because close to rock outcrop, the clay layer often is thin. Meaning that the likelihood of high water flow in a draining layer is larger because it could be in direct contact with surface water or other water-conducting layers which are increasing the possibility of leaching (Rankka et al., 2004).

## 2.3 The Åseberget site

In Figure 1, a geological map over the Åseberget site is shown. The geological map is developed by the Geological Survey of Sweden. The marked area is showing where the geotechnical field investigations for this project were done. The project area is located in direct proximity to a bedrock hill. It is enclosed by the bedrock hill in the south-west direction and a highway in the north-east direction. According to the Geological Survey of Sweden, (SGU, n.d.) the soil type in the project area is postglacial clay. After geodetic work, it was found that the project area is located at 7 to 8 metres above the current sea level, which is clearly below the marine limit of around 90 to 100 metres above the current sea level. The peak of the bedrock hill located right next to the project area is located around 60 metres above the current sea level. The low elevation of the project area is indicating that the clay was deposited during a recent time period seeing it from a geological perspective. Based on the height above sea level it is approximated that the area has been above sea level for around 1000 years (Bergström et al., 2022). If no excessive erosion or anthropogenic process has impacted the area it is relatively safe to assume that the clay in the area is normally consolidated. Meaning that it is likely that the soil at the current time period is experiencing its highest effective vertical stress (Larsson & Sällfors, 1995).

When comparing the project area to the mentioned prerequisites for formation of quick clay it is evident that several of the specified prerequisites are fulfilled. Considering the proximity to the bedrock hill and the height above sea level it is expected that the clay layers are somewhat limited in depth. Furthermore, the proximity to the bedrock hill has the effect that an eventual glacial till layer between the clay and bedrock most likely is in direct contact with the groundwater or infiltrating water from other sources that increases the possibility of leaching.

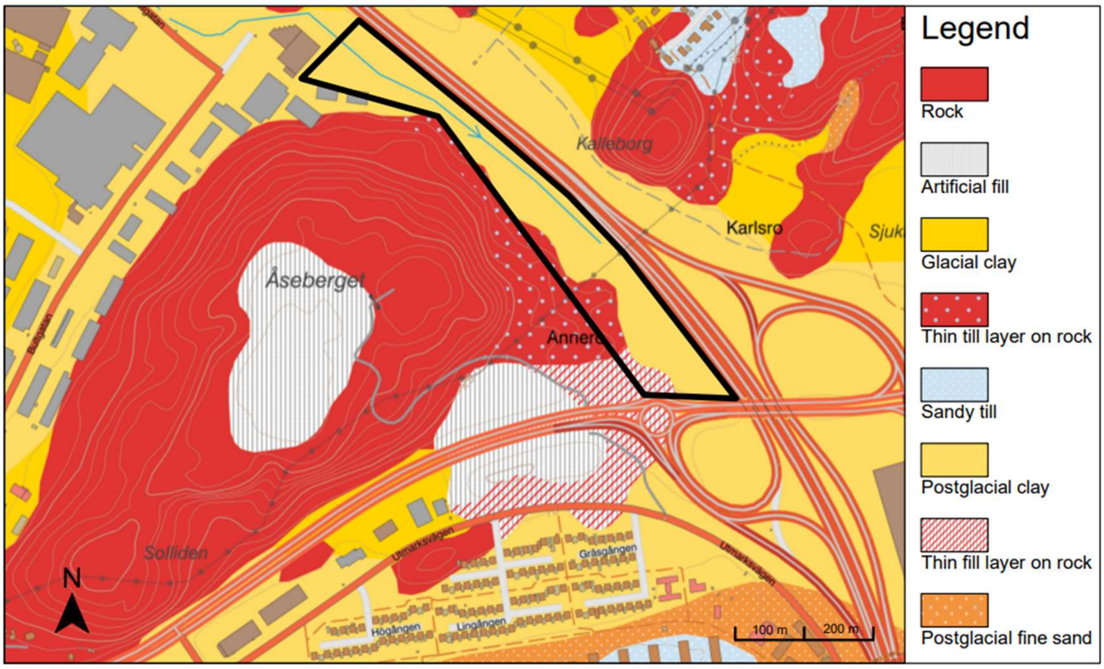


*Figure 1. Geological map over the Åseberget site with the project area marked. Modified from* SGU. (n.d.).

# 3 Field Investigation Methods

Geotechnical field investigations will be performed as part of the project. In this chapter international, European, and Swedish standards and Swedish guidelines for the field methods that will be used is described together with associated empirical relations used for correcting the parameters evaluated.

## 3.1 Piston sampling

Piston sampling is a common sampling technique used for recovering clay samples (Swedish Geotechnical Society [SGF], 2013). The purpose with the sampling is to recover undisturbed core samples for being used in tests performed in laboratory. The term "undisturbed" implies that the properties of the samples should remain intact. Meaning that the composition, water content and density of the sample should not differ much from field conditions once the core sample is recovered (SGF, 2009). The execution of the piston sampling shall in Sweden be performed according to the SGF Report 1:2009. The SGF Report 1:2009 is a guideline for the standard piston sampler used for undisturbed sampling in fine grained soils (SGF, 2009). There is a European standard (ISO 22475-1:2006) regulating undisturbed sampling. However, the European standard is not detailed enough to fulfil the quality that is sought in Sweden.

Piston sampling is performed by pushing down a cylindrical sampler equipped with a sharp edge into the soil. There are two different types of standard piston samplers described in the guideline, St I and St II. The quality of the core samples recovered using the different samplers are equivalent, but the St II is more suitable than St I for sampling in more solid clays (SGF, 2013). The difference between the two samplers is that the St II has an outer protective tube and therefore the outer diameters differ. The St I sampler has an outer diameter of 60 mm and the St II sampler has an outer diameter of 82 mm. According to the guideline (2009), the choice of sampler is mostly based on the experience of the operator and the equipment available. The sampler includes five tubes, both for St I and St II. Three tubes for recovering of the soil samples, which are 170 mm long and 50 mm in diameter. In addition, there are two short tubes, 85 mm each, which are placed above and below the sampling tubes. The purpose of the short tubes is to ensure that the soil in the sampling tubes is undisturbed, and the soil recovered from the short tubes is not aimed for testing of undisturbed properties (SGF, 2009).

Before the actual sampling can take place, the sampler is pushed down to a predetermined depth in order for the samples to be recovered at the desired depth. When pushed down, the sample tubes are enclosed by an inner piston to make sure that the sampling tubes are not filled while being pushed down. Once the predetermined depth is reached the inner piston is locked while the sampler with the sharp edge continues to be pushed down filling the empty sample tubes (SGF, 2013). Figure 2 is showing the sampling process of a piston sampler.

Directly after the samples has been cut, some time is required before the samples can be recovered. This is because directly after the samples has been cut the soil along the sample tubes is disturbed and the friction along the wall of the sample tubes is very low. The friction is however increasing instantly after the samples has been cut. Normally it is enough to wait for around 10 minutes for sensitive and quick clays and 5 minutes for clays with lower sensitivity. For very soft clays, a shutter mechanism (shutter sleeve) is sometimes used to prevent leakage of the soft clay from the sampling tubes. However, a shutter sleeve will cause an increased disturbance in the soil samples and the use of a shutter sleeve shall be avoided if possible (SGF, 2009).

After sampling, the tubes shall be sealed and placed in specific boxes that are isolated and shock absorbing. These boxes are aimed to keep the samples as undisturbed as possible during storage in field and transportation. All transport and storage must be done so that vibrations and large temperature variations are avoided. The boxes may under no circumstances be transported on the tracked geotechnical drilling rig (SGF, 2009).

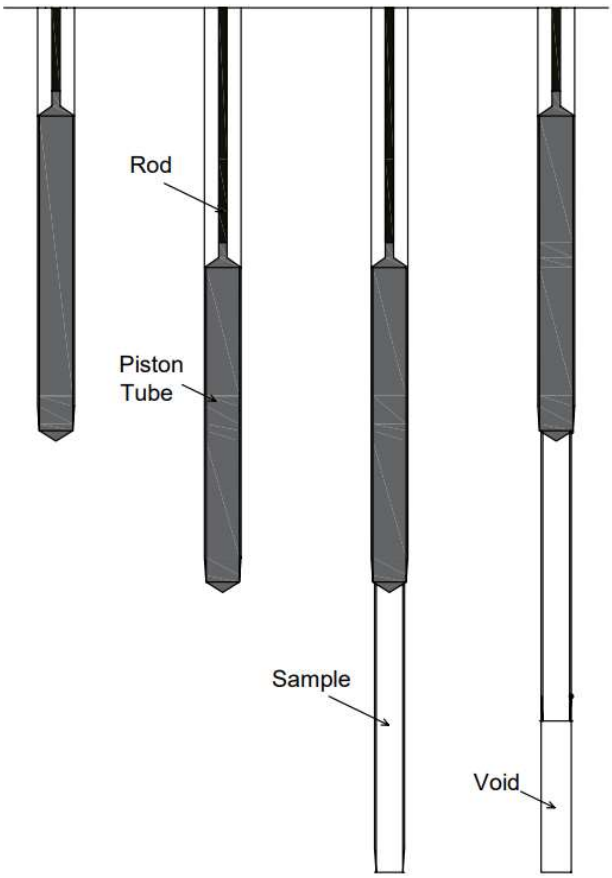


*Figure 2. Execution of standard piston sampling.*

### 3.1.1 Minimising disturbance

Minimising disturbance is one of the most important aspects to consider during the sampling procedure. Factors that affect the quality of the sample is for example sample diameter, wall thickness, cutting edge angle, inside clearance and inside and outside friction of the sampler (Jannuzzi et al., 2021). To minimise disturbance, it is preferable to use a sampler with a large diameter. The wall thickness should be as thin as possible, and the cutting-edge angle should be as sharp as possible. The inside clearance shall be kept small. The inside clarence is the difference in diameter between the cutting edge and the sample tube (SGI, 1961). It is also important that the friction on the inside of the sampler is low. The outside friction should also be kept low because a high friction on the outside of the sampler can create shear stresses in the soil below the cutting edge (Jannuzzi et al., 2021).

## 3.2 Cone penetration test

How to perform the electrical cone penetration test (CPT) and the piezocone penetration test (CPTu) is regulated in the standard SS-EN ISO 22476-1:2012. The basic concept of the CPT is that a cone penetrometer is pushed down into the soil at a constant rate (20 mm/s ± 5 mm/s) while cone resistance and sleeve friction are recorded. The execution of CPTu is the same, but the pore pressure around the cone is recorded as well as the parameters mentioned for CPT (Swedish Standards Institute [SIS], 2012). In Sweden, CPTu is more commonly used compared to CPT (SGF, 2013). When the CPT and CPTu are performed with great accuracy in accordance with the standard, the results from the soundings can be used for qualified evaluation of the stratification, geotechnical parameters and the deformations and consolidation characteristics (SGF, 2013). The CPTu is one of the standard methods in Sweden when evaluating the soil layering and soil characteristics (SGI, 2018).

An important note is that the pore pressure measured in a CPTu-sounding is not equivalent to the *in situ* pore pressure. To obtain the *in situ* pore pressure from a CPTu-sounding, a dissipation test needs to be performed. A dissipation test is carried out by measuring the pore water pressure with time during a pause in pushing the cone penetrometer where it is held stationary. The procedure of the dissipation test is regulated in the standard SS-EN ISO 22476-1:2012.

The cone penetrometer consists of the cone, a friction sleeve, three filter elements, sensors and measuring systems and an adapter for connecting the push rod. The different parts of the cone penetrometer can be seen in Figure 3. The cone (1) is the lower part of the penetrometer and internal sensors in the cone are measuring the cone resistance. The friction sleeve (2) is the cylindrical section of the penetrometer above the cone. The friction sleeve is measuring the friction between the sleeve and the soil. There are three filter elements where the pore pressure can be measured. One at the face of the cone ($u_1$), the second at the cylindrical part of the penetrometer below the friction sleeve ($u_2$) and the third above the friction sleeve ($u_3$) (SIS, 2012). In the penetrometer there is an inclinometer measuring the angle to the vertical axis when penetrating, so the inclination can be monitored and mapped (Lunne et al., 1997). The required dimensions and the tolerance requirements for all the components in the cone penetrometer is stated in the standard.

The connecting push rods shall have the same diameter as the cone penetrometer for 400 mm counted from above the cone (SIS, 2012). Behind the friction sleeve, electrodes can be mounted for measurement of the resistivity in the soil (Lunne et al., 1997). The cone penetration test with measurements of resistivity is referred to as CPT-R and CPTu-R. Measurements of the resistivity is used for several different purposes, where one of them is for implying the presence of quick clay. The theory for evaluation of quick clay from resistivity can be found in section 3.2.2.

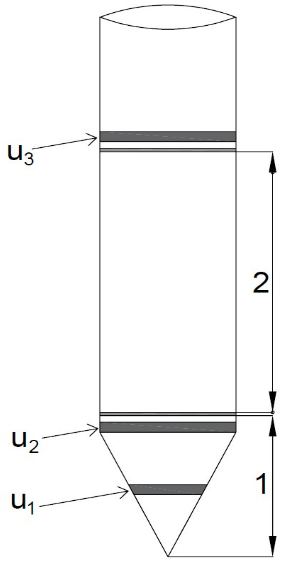

*Figure 3. Cone penetrometer for CPTu.*

Before the execution of the CPTu starts, it is required that the penetrometer shall have around the same temperature as the soil it will penetrate. If the air temperature deviates a lot from the ground temperature, the penetrometer can be held in the soil just below the ground surface for 5-15 minutes before penetrating further. The neutralization of the temperature is important in order to obtain the required accuracy of the measured parameters (SIS, 2012). Variations in temperature can affect the measurement results (SGF, 2013). After the temperature has been adjusted, zero readings of the cone resistance, sleeve friction, pore pressure and inclination shall be recorded. Before the CPTu can be used in field, the filter element and other parts of the pore pressure measurement system shall be saturated. Either distilled water or glycerine is used for saturation of the membrane, depending on the saturation of the soil. For saturated soils, distilled water is often used (SIS, 2012). The saturation of the pore pressure measure elements is crucial for the measurement results. All spaces in the penetrometer tip shall be filled with fluid to prevent air bubbles, so that the pore pressure can be measured directly without delay or loss in pressure (SGF, 2013).

According to the standard there are four different application classes that defines the test type, measurable parameters, allowable minimum accuracy for each measured parameter, and minimum logging frequency. The classification is based on the homogeneity and the grain size of the soil. The application classes are divided in order to satisfy all soil conditions over the world. It is stated in the standard that in regions with very soft soil, other accuracy requirements may apply. The accuracy requirements in these four application classes are lower than what is required in Sweden, therefore an application class 0 is implemented (SGF, 2013). Class 0 refers to very soft to soft deposits and is only performed using CPTu. Pre-drilling through dry crust or filling materials is often required for class 0. The measurable parameters for class 0 are cone resistance, sleeve friction, pore pressure, inclination, and penetration length. The maximum length between the measurements for class 0 is 10 mm for pore pressure measurements and 20 mm for the other parameters. The allowable minimum accuracy for the cone resistance, sleeve friction, pore pressure and penetration length can be found in the geotechnical field manual by SGF (2013) for class 0 and in the standard for the other classes. The requirement for the inclination of the penetrometer is that the inclination must not deviate more than 2° from the initial thrust direction (SIS, 2012).

To compute the measured sleeve friction $f_s$, from the force acting on the sleeve, equation (1) is used.

$$f_s = \frac{F_s}{A_s} \tag{1}$$

Where

$f_s$ is the measured sleeve friction [kPa]
$F_s$ is the measured force acting on the friction sleeve [kN]
$A_s$ Is the area of the sleeve [m$^2$]

The same principle applies for the measured cone resistance $q_c$, in equation (2).

$$q_c = \frac{Q_c}{A_c} \tag{2}$$

Where

$q_c$ is the measured cone resistance [kPa]
$Q_c$ is the measured force on the cone [kN]
$A_c$ is the projected area of the cone [m$^2$]

The pore water pressure effects the cone resistance and the sleeve friction, due to the geometry of the penetrometer. If the pore pressure is measured between the cone and the friction sleeve, at $u_2$ in Figure 3, the measured cone resistance shall be corrected according to equation (3) (Lunne et al., 1997; SIS, 2012). According to Lunne et al., the measured pore pressure at $u_2$ can be estimated based on the measured value of $u_1$. However, in the standard SS-EN ISO 22476-1:2012, it is stated that the correction shall only be made if the pore pressure is measured at $u_2$.

$$q_t = q_c + u_2 * (1 - a) \tag{3}$$

Where

$q_t$ is the corrected cone resistance [kPa]
$q_c$ is the measured cone resistance [kPa]
$u_2$ is the measured pore pressure at $u_2$ [kPa]
$a$ is the net area ratio between the cross-sectional area of load cell or shaft, and the cross-sectional area of the cone [-]

According to Lunne et al., (1997) the sleeve friction shall be corrected according to equation (4), due to the different pore pressure measured at $u_2$ and $u_3$ when excess pore pressure is generated. It is stated in the standard SS-EN ISO 22476-1:2012 that the pore pressure is rarely measured at location $u_3$, therefore the sleeve friction is seldom corrected.

$$f_t = f_s - \frac{u_2 * A_{sb} - u_3 * A_{st}}{A_s} \tag{4}$$

Where

$f_t$ is the corrected sleeve friction [kPa]
$f_s$ is the measured sleeve friction [kPa]
$u_2$ is the measured pore pressure at $u_2$ [kPa]
$u_3$ is the measured pore pressure at $u_3$ [kPa]

$A_{sb}$ is the cross-sectional bottom area of the friction sleeve [mm$^2$]
$A_{st}$ is the cross-sectional top area of the friction sleeve [mm$^2$]
$A_s$ is the surface area of the friction sleeve [mm$^2$]

To estimate the pore pressure ratio $B_q$, equation (5) is used. The pore pressure ratio is a parameter mostly used for soil classification and to differentiate layers in a soil. It is therefore a useful parameter in many aspects. It could for example be related to the determination of the shear strength of a soil (Karlsrud et al., 1997).

$$B_q = \frac{\Delta u}{q_t - \sigma_{vo}} \tag{5}$$

Where
$\Delta u$ is the excess pore pressure $(u - u_0)$ [kPa]
$u_0$ is the *in situ* equilibrium pore water pressure [kPa]
$\sigma_{vo}$ is the *in situ* vertical stress [kPa]

### 3.2.1 Estimation of shear strength from CPTu

From CPTu data the *in situ* shear strength of the soil can be calculated. There is however no single equation that is used to calculate the *in situ* shear strength. The reason for that is because the shearing of the soil caused during penetration of the penetrometer is dependent on a great number of different factors. For example, the mode of failure, soil anisotropy, strain rate and the stress history of the soil (Lunne et al., 1997). For this reason, empirical corrections are normally needed to calculate the shear strength. The most common empirical relations used to calculate $c_u$ can be grouped into three main categories. The first approach is estimation of $c_u$ using total cone resistance. Another approach is estimation of $c_u$ using effective cone resistance. A third approach is to estimate $c_u$ using excess pore pressure (Lunne et al., 1997).

The approach of estimating $c_u$ using total cone resistance is expressed in equation (6) where the total cone resistance is corrected for pore pressure effects (Craig & Knappet, 2012).

$$c_u = \frac{q_t - \sigma_{vo}}{N_{kt}} \tag{6}$$

Where
$q_t$ is the cone resistance corrected for pore pressure effects [kPa]
$\sigma_{vo}$ is the *in situ* vertical stress [kPa]
$N_{kt}$ is an empirical cone factor [-]

When estimating the cone factor $N_{kt}$, Figure 4 taken from Karlsrud et al. (2005) can be used. The figure is showing the cone factor determined using data from a large number of soil samples. The cone factor is plotted against the corresponding plasticity index ($I_P$) of the soil. The plasticity index is the difference between the liquid limit and the plastic limit. The shear strength used to calculate the cone factor in the figure was determined in laboratory using triaxial compression tests performed on samples that were consolidated anisotropically to the present in situ effective stress. The samples were retrieved using a 250 mm Sherbrooke block sampler, which is perceived to recover samples with minimal disturbance (Karlsrud et al., 2005). Although the results are showing a large scatter it can be seen that the cone factor generally is increasing with increasing plasticity index and that the $N_{kt}$ values are varying around 6-16 (Karlsrud et al., 2005).

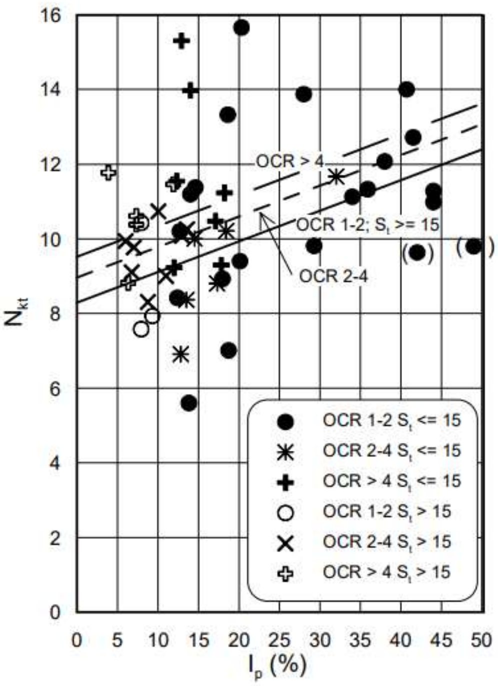


*Figure 4. Relation between plasticity index and cone factor* $N_{kt}$ (Karlsrud et al., 2005).

Figure 5 is showing another method presented in Karlsrud et al. (1997) for estimating the cone factor. In the figure the cone factor is evaluated from several different sites and plotted against the pore pressure ratio $B_q$ of the soil. The figure is showing a good correlation between the pore pressure ratio and the cone factor with $N_{kt}$ values ranging between 6-15.

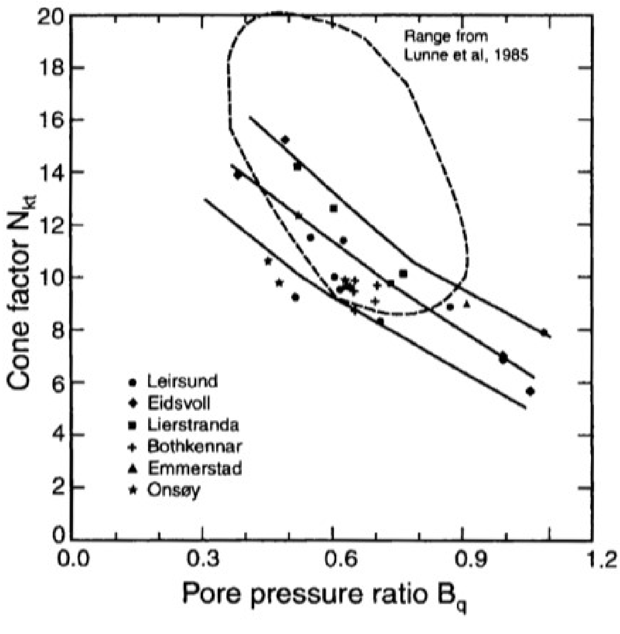


*Figure 5. Correlation between* $N_{kt}$ *and* $B_q$ (Karlsrud et al., 1997).

In Sweden an empirical relation using total cone resistance for evaluating the shear strength, $c_u$, is used. The relation is shown in equation (7). In the denominator of the equation, it can be seen that the cone factor is dependent on the liquid limit ($w_L$) of the soil. The equation has shown to be valid for normally consolidated clays and slightly overconsolidated clays (Larsson et al., 2007).

$$c_u = \frac{q_t - \sigma_{vo}}{13.4 + 6.65 w_L} \tag{7}$$

For overconsolidated clays equation (8) is used. Where $OCR$ is the overconsolidation ratio, which is the ratio of the preconsolidation stress and the vertical effective stress (Larsson et al., 2007).

$$c_u = \frac{q_t - \sigma_{vo}}{13.4 + 6.65 w_L} \left( \frac{OCR}{1.3} \right)^{-0.20} \tag{8}$$

In cases where the overconsolidation ratio not yet has been evaluated, equation (9) can be used to evaluate the preconsolidation stress ($\sigma'_c$) from the CPTu data which in turn can be used to evaluate the overconsolidation ratio (Larsson et al., 2007).

$$\sigma'_c = \frac{q_t - \sigma_{vo}}{1.21 + 4.4 w_L} \tag{9}$$

As stated earlier in the chapter, another approach for estimating $c_u$ is by using effective cone resistance. The relation is then as follows in equation (10) (Lunne et al., 1997).

$$c_u = \frac{q_e}{N_{ke}} = \frac{q_t - u_2}{N_{ke}} \tag{10}$$

Where

$q_e$ is the effective cone resistance defined as the difference between the measured cone resistance and the measured pore pressure $u_2$ [kPa]

$u_2$ is the measured pore pressure right behind the cone in the CPTu instrument [kPa]

$N_{ke}$ is the effective cone factor [-]

The effective cone factor can be evaluated using Figure 6 (Karlsrud et al., 1997). In the figure the cone factor is evaluated from different soil samples and plotted against the pore pressure ratio ($B_q$). It is clearly visible that this data is containing less scatter compared to the graphs used for the evaluation of the total cone factor.

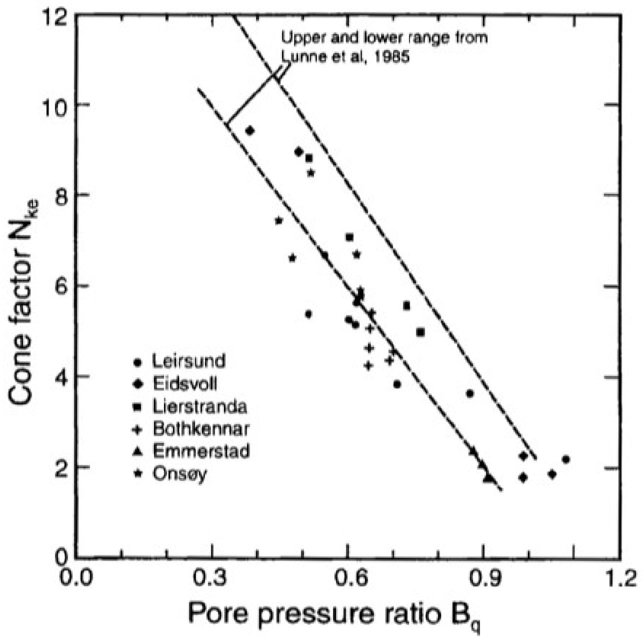


*Figure 6. Correlation between $N_{ke}$ and $B_q$* (Karlsrud et al., 1997).

In addition, it is possible to determine the undrained shear strength, $c_u$, using excess pore pressure by using equation
(11) (Lunne et al., 1997).

$$c_u = \frac{\Delta u}{N_{\Delta u}} \qquad (\Delta u = u_2 - u_0) \tag{11}$$

Where

$\Delta u$ is the difference between the measured pore pressure and the initial pore pressure [kPa]

$N_{\Delta u}$ is the cone factor used when evaluating $c_u$ using excess pore pressure [-]

Figure 7 is showing evaluated $N_{\Delta u}$ values from different soil samples. In the figure, $N_{\Delta u}$ is plotted against the plasticity index ($I_p$). The two parameters correlate to each other slightly where $N_{\Delta u}$ increases with an increasing plasticity index. The $N_{\Delta u}$ varies between 4 and 10 (Karlsrud et al., 2005).

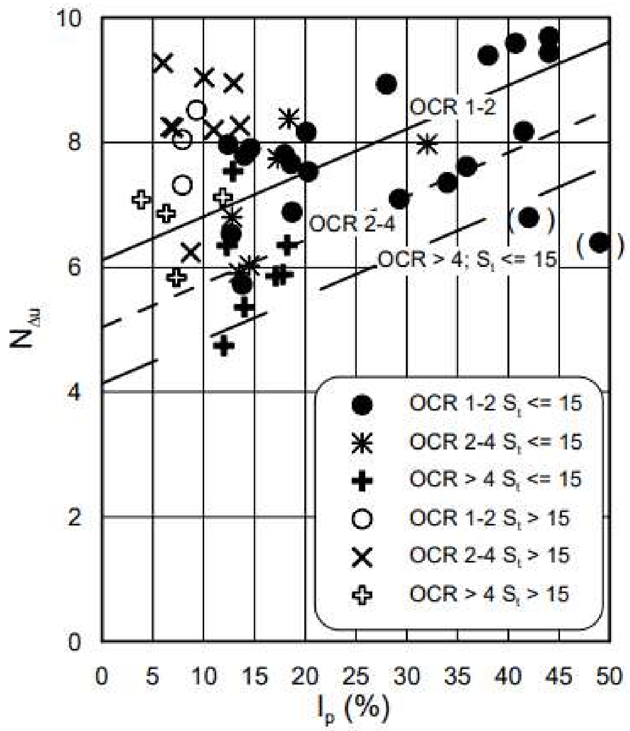


*Figure 7. Relation between plasticity index and cone factor* $N_{\Delta u}$ (Karlsrud et al., 2005).

### 3.2.2 Alternative methods for implying presence of quick clay

The presence of quick clay can be estimated using the rod friction along the rods generated when performing CPT. The rod friction is the measured penetration force together with the weight of the rods and reduced with the cone resistance (Löfroth et al., 2011). The generated rod friction is plotted together with a skin friction of 1 kPa per metre. According to the method description, quick clay may be expected where the inclination of the rod friction is lower than the inclination of the skin friction (Löfroth et al., 2011). The rod friction method tends to overestimate the presence of quick clay, which means it interprets the presence of quick clay where the clay is not actually quick. Meaning that the evaluation of the presence of quick clay using this method will be on the safe side. According to SGI (2018), the rod method is the second-best method for identifying quick clay. However, the method is not suitable for areas where the soil deposits consist alternately of silty clay, clayey silt, and silt (SGI, 2018).

The electrical resistivity of a soil is foremost determined by the salt content in the pore water. However, the resistivity can also be influenced by the porosity, grain size distribution, and possibly conductive minerals (SGI, 2018). Quick clay and highly sensitive clays have a low salt content as a result of leaching (as described in chapter 2, section 2.2). The resistivity in clays normally ranges between 1-100 Ωm (Solberg et al., 2011). Low salt content generates low resistivity. Measurements of the resistivity can therefore be used to distinguish leached clay from not leached clay (Löfroth et al., 2011). Löfroth et al., (2011) argues that to imply that the salt content is low enough for the clay to be quick, the resistivity shall be ≥5 Ωm. However, in the study from SGI (2018) quick clay was identified at locations where the resistivity was as low as 4 Ωm.

According to Lunne et al., (1997) the sleeve friction measured during CPT is a function of the remoulded shear strength. It is suggested that the sensitivity $S_t$, can be roughly estimated according to equation (12), where $R_f$ is the friction ration between the sleeve friction and the cone resistance. The constant $N_s$ ranges between 6 – 9, but an average value of 7.5 may be likely for most clays. The value of $N_s$ shall be calibrated with local experience. However, for relatively sensitive clays that generates very low sleeve friction values which may be difficult to measure with great accuracy, this method might be difficult to use for estimation of sensitivity (Lunne et al., 1997).

$$S_t = \frac{N_s}{R_f} \tag{12}$$

## 3.3 T-bar penetration test

The T-bar penetration test (TPT) is a geotechnical site investigation tool that has been developed primarily to be used in soft clays (Stewart & Randolph, 1994). The TPT is using the same technology and working similarly as the CPTu. The only difference in the setup of the two tests is that the conical tip of the CPTu penetrometer is replaced with a T-bar that is screwed on to the penetrometer. Figure 8 is showing a sketch of a T-bar. As seen in the figure the T-bar constitutes of a horizontal bar made from steel. With the T-bar screwed on to the penetrometer it has the shape of the capital letter "T" positioned upside-down (Nakamura et al., 2009). Although the TPT has been used in a relatively large number of projects, especially in offshore projects, no specific standard regulating the procedure of the TPT has been developed (Lunne et al., 2005). According to Lunne et al., (2005), the recommendation is to use a T-bar with a 250 mm long horizontal steel bar with a diameter of 40 mm. These dimensions are giving a projected area 10 times larger compared to the standard cone used for the CPT. A significant difference between the CPT to the TPT is that with a TPT it is possible to measure the resistance both when penetrating down in the soil and when the T-bar is withdrawn. The penetration and extraction rate should be the same as for CPT, 20 mm/s (Lunne et al., 2005). Since the apparatus is the same as for CPTu, the pore pressure and sleeve friction is also measured.

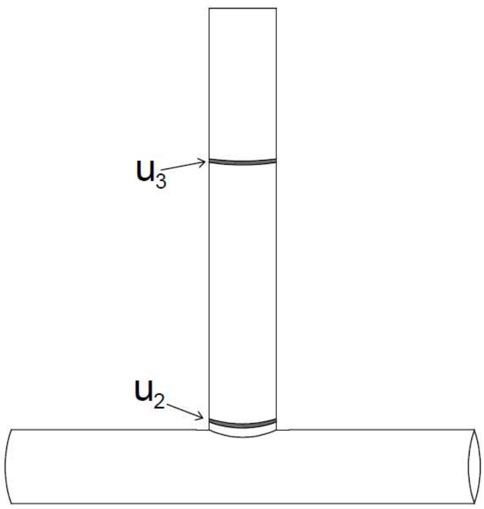


*Figure 8. Illustration of a T-bar penetrometer.*

The penetration resistance shall be corrected according to equation (13) (Low et al., 2010). The term $A_s/A_p$ is equal to approximately 0.1 for a T-bar with 250x40 dimensions and according to Nakamura et al., (2009) correction is not needed when

$A_s/A_p$ is less than 0.3. However, when performing cyclic TPT, the correction will have significant influence when the $q_{c,T-bar}$ decreases. Cyclic TPT is a method where penetration and extraction are repeated several times in the same depth interval.

$$q_{t,T-bar} = q_{c,T-bar} - [\sigma_{v0} - u_0 * (1 - a)] * A_s/A_p \qquad (13)$$

Where

| | |
|---|---|
| $q_{t,T-bar}$ | is the corrected penetration resistance [kPa] |
| $q_{c,T-bar}$ | is the measured penetration resistance [kPa] |
| $\sigma_{v0}$ | is the *in situ* vertical stress [kPa] |
| $u_0$ | is the hydrostatic water pressure [kPa] |
| $a$ | is the net area ratio between the cross-sectional area of load cell or shaft, and the cross-sectional area of the T-bar [-] |
| $A_s$ | is the cross-sectional area of the connection shaft [mm$^2$] |
| $A_p$ | is the projected area of the penetrometer in plane normal to the shaft [mm$^2$] |

One advantage with the TPT compared to the CPT is related to the much larger projected area of the tip. The larger projected area is resulting in that a higher penetration force is required, which gives a higher resolution in the measured resistance (Randolph, 2004). Another advantage with the TPT, also linked to the geometry of the T-bar, is that it is a so called “full-flow” penetrometer. The “full-flow” mechanism has the effect that the vertical stress has a small effect of the corrected resistance (Randolph, 2004). The “full-flow” mechanism is only present in very soft soils where the soil is flowing around the penetrometer, as shown in Figure 9 (Low et al., 2010; Nakamura et al., 2009). The arrows are showing how the soil is moving around the T-bar. This mechanism enables the vertical stress to act on the T-bar when penetrated downwards.

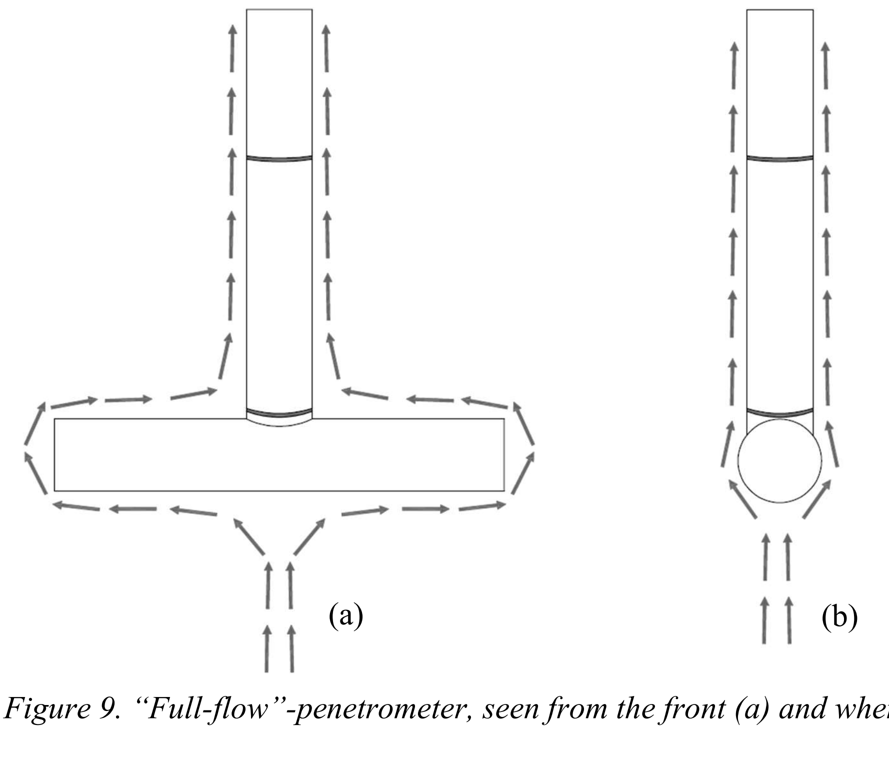


*Figure 9. “Full-flow”-penetrometer, seen from the front (a) and when rotated 90º (b).*

### 3.3.1 Estimation of shear strength from TPT

The shear strength using data from TPT is calculated using equation (14) (Lunne et al., 2005). Because of the "full-flow" mechanism, there is no need for correction with the vertical stress as is required for determination of shear strength from CPTu with the approach of using the total cone resistance (Lunne et al., 2005). The T-bar factor, $N_T$, have been evaluated and discussed in several studies (Low et al., 2010; Lunne et al., 2005; Nakamura et al., 2009). However, all authors are agreeing on that more studies are required to be able to determine the range in $N_T$ for various soil types. In the mentioned studies, $N_T$ have been determined by using shear strength from anisotropically consolidated undrained triaxial tests both in compression and extension, direct simple shear tests and field vane shear tests, as well as an average shear strength from all these tests. The results of $N_T$ from the different studies have shown that the T-bar factor varies from 7.1-14.3 (when excluding a deviating value of 17.1).

$$c_u = \frac{q_{t,T-bar}}{N_T(N_{T,rem})} \tag{14}$$

In the study by Low et al., (2010) a $N_T$ factor for remoulded conditions has been evaluated, based on cyclic TPT, referred to as $N_{T,rem}$. The sensitivity was in general lower than 6 for the soil included in the investigated database. The remoulded shear strength used in the evaluation was measured by field vane shear test, fall cone test and unconsolidated triaxial compression test. When combining these tests, the $N_{T,rem}$ is ranging between 11.38-32.44. The $N_{T,rem}$ based on when only the shear strength from the fall cone test was used ranges between 11.61-16.98. Low et al., (2010) suggests that the $N_{T,rem}$ increases when the sensitivity increases. In the article it is also mentioned that more studies are required to confirm the dependency on the $N_{T,rem}$ factor for moderate to highly sensitive soils.

# 4 Laboratory Testing Methods

Laboratory testing will be part of this project to determine reference values for the evaluated parameters from the field methods. In this chapter European and Swedish standards and Swedish guidelines for the laboratory testing is described together with associated empirical relations used for correcting the parameters evaluated.

## 4.1 Fall cone test

The fall cone test is a laboratory method that can be used for determining the undrained shear strength of a soil. The test is generally performed on fine grained soils and are used for determining the shear strength of both undisturbed core samples and remoulded samples. By dividing the shear strength of an undisturbed soil sample by the shear strength of a remoulded soil sample the sensitivity of the soil can be calculated (SIS, 2017).

The fall cone test is performed by letting a cone fall with its tip first into a soil sample. The penetration of the cone into the soil is measured and the penetration depth can be used to evaluate the shear strength of the soil. The fall cone test is in Europe governed by the standard SS-EN ISO 17892-6:2017. To estimate the undrained shear strength from a fall cone test equation (15) is used (SIS, 2017).

$$c_{ufc}(or\ c_{urfc}) = c \cdot g \cdot \frac{m}{i^2} \tag{15}$$

Where

$c_{ufc}$ is the undrained shear strength of an undisturbed soil sample estimated by the fall cone method [kPa]

$c_{urfc}$ is the undrained shear strength of a remoulded soil sample estimated by the fall cone method [kPa]

$c$ is a constant used that is depending on the tip angle used for the specific test,
- $c$ = 0.80 for cones with 30° tip angle
- $c$ = 0.27 for cones with 60° tip angle

$g$ is the acceleration due to gravity at free fall [m/s$^2$]

$m$ is the mass of the cone [g]

$i$ is the penetration of the cone into the soil sample [mm]

For undisturbed samples $i$ is calculated as the average penetration of at least three test points tested with the same cone. A test is counted as invalid if the penetration depth is deviating more than 0.5 mm from the average penetration depth. If a value deviates more than 0.5 mm a new test should be performed, and the old result should not be counted. For the remoulded samples $i$ is calculated as the average value of the two lowest measurements from two successive pairs of tests which has a penetration depth that is deviating less than 0.5 mm from each other (SIS, 2017).

The shear strength calculated from equation (15), in general needs to be corrected with an empirical relation (Larsson, 2008). The need for a correction factor originates from difficulties in geotechnical practice where the quality of the field investigations performed is not always as good desired (Hov et al., 2021). Equation (16) is showing the empirical relation for correcting the shear strength recommended by the Swedish Geotechnical Institute (SGI) (Larsson, 2008).

$$c_{u,corr} = c_u \cdot \mu \tag{16}$$

Where

$c_u$ is the undrained shear strength of the undisturbed or remoulded sample [kPa]

μ is the empirical correction factor [-]

The empirical correction recommended by SGI is expressed in equation (17), where $w_L$ is the liquid limit of the soil (Larsson, 2008).

$$\mu = \left(\frac{0.43}{w_L}\right)^{0.45} \qquad 1.2 \geq \mu \geq 0.5 \tag{17}$$

This method for correcting the shear strength evaluated from fall cone test was developed in the study by Hansbo (1957). The work is including a theoretical and empirical study with the aim of revising the result so that the shear strength evaluated with the fall cone test would correspond to the shear strength evaluated with the shear vane test. When this method was developed the undrained shear strength was assumed to be dependent on the liquid limit or the plasticity index of the soil (Hov et al., 2021).

Whether the shear strength of the soil is dependent on the liquid limit has however been questioned in recent years. In Hov et al. (2021) the relation between the liquid limit, $w_L$ and the normalised shear strength $(c_u/\sigma_c)$ has been analysed. In the paper, a large number of $c_u$ results from fall cone tests were collected from commercial projects and corrected with equation (17). The database with parameters used for the analysis also contained the liquid limit as well as the preconsolidation pressure obtained from CRS Oedometer tests (Hov et al., 2021). The result of the analysis showed that $(c_u/\sigma_c)$ is increasing with increasing $w_L$ but the correlation is very weak. The results are also containing a large scatter. The scatter is most likely explained by sample disturbance and measurement errors. Additionally, the core samples analysed were taken from a wide variety of locations with different properties. This could have had an impact on the results since it is unlikely that there is a global empirical relation that are valid for all clays (Hov et al., 2021). It is therefore suggested by the author that local empirical relations should be used when available.

## 4.2 Determination of liquid and plastic limits

The liquid limit ($w_L$) defines the transition from liquid to plastic behaviour. The liquid limit can be determined by fall cone testing or the Casagrande method. The Casagrande method has a long history of use for the determination of liquid limit, however the method using the fall cone apparatus is the preferred method of today (SIS, 2018). In the standard SS-EN ISO 17892-12:2018, two different procedures of using the fall cone apparatus as well as the Casagrande method is explained. In this study, the Casagrande method will be excluded. The two procedures for the fall cone test are referred to as four-point test and one-point test (SIS, 2018). The one-point test is the common method for determination of liquid limit in natural Swedish clays (Karlsson, personal communication, February 25, 2022)

For both one-point and four-point test, soil finer than 0.4 mm is required. Sieves can be used for preparation of the sample to remove coarser material. The acceptable penetration depth for determination of the liquid limit ranges from 7-15 mm for a cone with 60° tip angle and 15-25 mm for a cone with 30° tip angle. To enable a penetration depth within this range, it is required to add distilled water or to gently dry the sample in room temperature. When drying the sample, it is important to periodically stir the sample to avoid uneven dryness (SIS, 2018).

The one-point test is performed on one sample and therefore only one water content. The liquid limit corresponds to the water content at a cone penetration depth of 10 mm for a cone with 60° tip angle (SIS, 2018). For the one-point test, the water content is corrected according to equation (18) to correspond to a 10 mm penetration depth (Larsson, 2008).

$$w_L = M \cdot \mathrm{w} + \mathrm{N} \tag{18}$$

Where w is the water content in the soil and $M$ and N are factors that are dependent on the penetration depth of the cone and specifications of the cone used for the specific test. The M and N values when using a cone with 60° tip angle could be obtained from Table 1 (Larsson, 2008).

*Table 1. Correlation between cone penetration depth and the M and N numbers when using a cone with a 60° tip angle* (Larsson, 2008).

| Penetration depth in, [mm], whole numbers | Value | Penetration depth i, [mm], 1/10 of a mm | | | | | | | | | |
|---|---|---|---|---|---|---|---|---|---|---|---|
| | | 0 | 1 | 2 | 3 | 4 | 5 | 6 | 7 | 8 | 9 |
| 7 | M | 1.21 | 1.20 | 1.19 | 1.18 | 1.17 | 1.16 | 1.15 | 1.14 | 1.14 | 1.13 |
| | N | -3.5 | -3.4 | -3.2 | -3.0 | -2.9 | -2.7 | -2.6 | -2.5 | -2.3 | -2.2 |
| 8 | M | 1.12 | 1.11 | 1.11 | 1.10 | 1.10 | 1.09 | 1.08 | 1.07 | 1.07 | 1.06 |
| | N | -2.1 | -1.9 | -1.8 | -1.7 | -1.9 | -1.4 | -1.3 | -1.2 | -1.1 | -1.0 |
| 9 | M | 1.05 | 1.05 | 1.04 | 1.04 | 1.03 | 1.03 | 1.02 | 1.01 | 1.01 | 1.00 |
| | N | -0.9 | -0.8 | -0.7 | -0.6 | -0.5 | -0.4 | -0.3 | -0.3 | -0.2 | -0.1 |
| 10 | M | 1.00 | 1.00 | 0.99 | 0.99 | 0.98 | 0.98 | 0.97 | 0.97 | 0.96 | 0.96 |
| | N | 0 | 0.1 | 0.2 | 0.2 | 0.3 | 0.4 | 0.5 | 0.5 | 0.6 | 0.7 |
| 11 | M | 0.96 | 0.95 | 0.95 | 0.94 | 0.94 | 0.94 | 0.93 | 0.93 | 0.93 | 0.92 |
| | N | 0.7 | 0.8 | 0.9 | 0.9 | 1.0 | 1.1 | 1.1 | 1.2 | 1.3 | 1.3 |
| 12 | M | 0.92 | 0.92 | 0.91 | 0.91 | 0.91 | 0.90 | 0.90 | 0.90 | 0.89 | 0.89 |
| | N | 1.4 | 1.4 | 1.5 | 1.5 | 1.6 | 1.7 | 1.8 | 1.8 | 1.8 | 1.9 |
| 13 | M | 0.89 | 0.88 | 0.88 | 0.88 | 0.88 | 0.87 | 0.87 | 0.87 | 0.87 | 0.86 |
| | N | 1.9 | 2.0 | 2.0 | 2.1 | 2.1 | 2.2 | 2.2 | 2.2 | 2.3 | 2.3 |

In the four-point method, the fall cone apparatus is used to perform the fall cone test four times on a soil sample. Between each test the water content of the soil is either reduced or increased. The penetration depth is then plotted against the corresponding water content, with the penetration depth on the x-axis. If the cone with the 30° tip angle is used, both penetration and water content shall be plotted on linear scale. If the cone with the 60° tip angle is used, the penetration depth shall be plotted on a log10 scale. The points shall be connected with the best straight-line fit. The liquid limit is the water content corresponding to a penetration depth of 10 mm for a 60° cone and 20 mm for a 30° cone (SIS, 2018).

The plastic limit of a soil corresponds to the lowest water content at which the soil is still plastic. The determination of the plastic limit is regulated by the standard SS-EN ISO 17892-12:2018. The plastic limit ($w_P$) is carried out by letting 15-20 g of soil dry until it can be shaped into a ball. The ball is rolled between the palms until it becomes so dry that cracks appear on the surface. The ball is then divided in six portions which are each transformed into a roll using the thumb and forefinger. When the roll is about 6 mm it is placed on a mixing plate. It is important that the mixing plate has no scratches. The rolling motion is continued on the plate until the roll is 3 mm in diameter. The roll is then shaped into a ball again the procedure is repeated until the 3 mm roll just begin to break apart. The water content at this point is the plastic limit (SIS, 2018).

The water content is measured by weighing the soil sample before and after it has been completely dried in an oven with 105-110º for at least 24 hours, regulated by the standard SS-EN ISO 17892-1:2014.

# 5 Principal Component Analysis

Principal component analysis (PCA) is a statistic method for analysing a data set of several dependent variables. PCA will in this project be used as a tool in an attempt to find relations between laboratory data and CPT data. The goal with using PCA is to reduce the number of dimensions and to extract the most important information from the data set (Abdi & Williams, 2010).

Before the analysis, the data is pre-processed. The original data is written as an $i \times j$ matrix. If the data contains various sizes of numbers, the analysis will focus on the larger numbers and important information and connections may be lost. Pre-processing of the data is called autoscaling which gives the parameters the same opportunity of being modelled. The autoscaling is done by centralizing and standardizing the data set (Bro & Smilde, 2014). Centralizing is done by subtracting the mean of the column from each variable. Standardization is done by dividing the centralized values by the standard deviation. It is necessary to standardize the values when the parameters have different units (Abdi & Williams, 2010). The autoscaled data is a matrix with the same dimensions as the original matrix.

The PCA extracts a new set of linear variables from the original data set, called principal components (Ringnér, 2008). The first extracted principal component shall have as large variance as possible, and the second principal component shall be orthogonal to the first component and have a variance as large as possible. A number of principal components are computed similarly (Abdi & Williams, 2010). If the data is autoscaled, the principal components are the normalized eigenvectors of the covariance matrix computed from the autoscaled values. Each eigenvector of the covariance matrix is a principal component. The eigenvalue of each principal component describes how much of the variation of the data that can be associated with the corresponding principal component (Ringnér, 2008).

The data set can be reduced based on the eigenvalues. To extract the important information in the PCA, only components that explains the majority of the variation is analysed. One procedure that is often used to figure out how many of the principal components to consider, is to do a scree plot. In a scree plot, the eigenvalues are plotted and generates a curve. If there is a point in the curve where the curve goes from steep to flat, it is suggested to keep the components represented by the eigenvalues above this point. Another method is to consider the components whose eigenvalues is larger than the average (Abdi & Williams, 2010). An eigenvalue that is larger than 1 for data that is autoscaled means that the component explains the variation of more than one variable and components with eigenvalue larger than one shall therefore be extracted (Bro & Smilde, 2014). It is suggested both by Bro & Smilde (2014) and Abdi & Williams (2010) to combine the mentioned procedures for the evaluation of which principal components to extract.

The variance of each principal component describes how much of the variation in the dataset that is explained by the principal component. Each analysed parameter is more or less associated with the different principal components. The relation between a parameter and a principal component is called loading. The value of the loadings ranges from -1 to 1. If the absolute value of the loading is high, it means that the parameter is highly associated with that specific principal component (Abdi & Williams, 2010).

# 6 Methodology

In his chapter, the methods for the field- and laboratory work conducted in this study is explained as well as deviations from the standardised method descriptions that were described in earlier chapters. How the statistical parameter analysis was conducted along with assumptions made for the analysis is also explained.

## 6.1 Field investigation

Figure 10 is showing the boreholes where the field investigation was performed. The boreholes marked with red are the boreholes primarily used in this project. The decisions on where to perform the modified field methods was based on the drilling depth. The pyramid penetration testing showed larger distance to the glacial till in the boreholes marked with red compared to the boreholes marked with blue in the figure. The distance to glacial till found in the boreholes marked with blue varied between 3 and 5 metres except in the borehole NC2213 where the distance to the glacial till was 14 metres. It was however decided to not perform any further tests in that borehole because of its close proximity to the NC2204 borehole. The field work took place between the 4$^{th}$ and 7$^{th}$ of April 2022. During the field work the weather was rainy, snowy, and sunny and the temperature varied between 2-10$^{o}$.

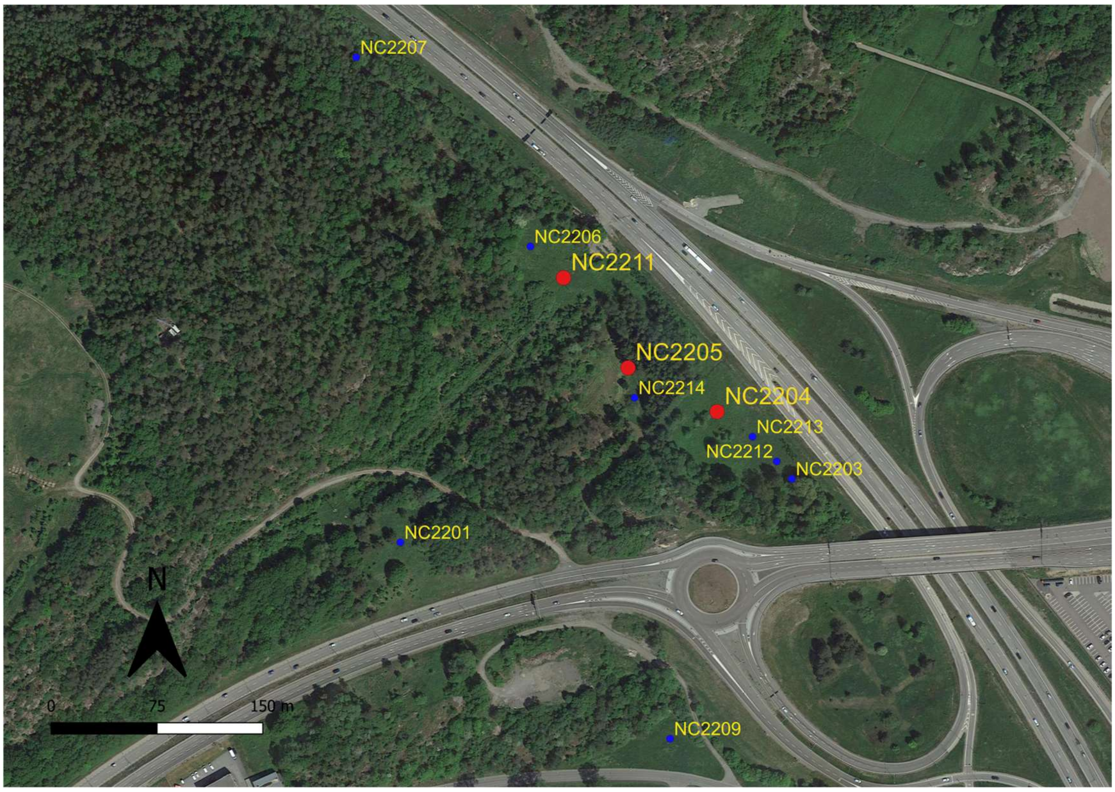


*Figure 10. Map over the boreholes in the project area. Modified from* Google Maps, (n.d.).

Table 2 is showing the borehole ID, the methods used at each borehole and the coordinates for each borehole using the coordinate system SWEREF 99 12 00. From the table it can be seen that the project area is almost entirely flat. The exception being the NC2201 borehole which is located on the slope of the Åseberget bedrock hill.

*Table 2. Methods and coordinates for the boreholes.*

| Borehole ID | Methods | x | y | z |
|---|---|---|---|---|
| NC2201 | JB | 6417391.6039 | 147469.8332 | 24.1469 |
| NC2203 | Skr, Tr | 6417436.3749 | 147747.1810 | 7.2907 |
| NC2204 | Skr, Tr, Kv, 3 x CPTu, TPT, TPTc | 6417483.9219 | 147694.2347 | 7.3924 |
| NC2205 | Skr, Tr, Kv, 3 x CPTu | 6417514.9419 | 147631.1693 | 7.4655 |
| NC2206 | Tr | 6417600.9248 | 147562.0785 | 7.3373 |
| NC2207 | Tr | 6417734.8484 | 147438.8234 | 6.3703 |
| NC2209 | JB | 6417252.5484 | 147660.8400 | 8.9380 |
| NC2211 | Tr, Kv, 3 x CPTu | 6417578.7125 | 147585.4957 | 7.2463 |
| NC2212 | Tr | 6417448.7399 | 147736.5175 | 7.5020 |
| NC2213 | Tr | 6417466.1861 | 147719.3485 | 7.4121 |
| NC2214 | Tr | 6417493.7886 | 147635.8138 | 7.6448 |

JB – Soil/Rock probing
Skr – Auger sampler (disturbed)
Tr – Pyramid penetration test
Kv – Piston sampler (undisturbed)
CPTu – Piezocone penetration test (with pore pressure measurement)
TPT – T-bar penetration test
TPTc – Cyclic T-bar penetration test (self-developed abbreviation)

The triple CPTu penetration was performed in borehole NC2204, NC2205 and NC2211. All the individual soundings were performed according to the standard SS EN-ISO 22476-1:2012 described in chapter 3 (section 3.2) and repeated three times in the exact same position. The purpose of doing three soundings in the same position is to disturb the soil with the aim to achieve a similar state as for the remoulded specimens that is prepared for the fall cone testing. Between each sounding, the penetrometer was disassembled, cleaned, refilled, and reset before the next sounding took place. The time between the soundings was measured to ensure that the breaks was about the same length between the penetrations. Since the intention was to penetrate in the exact same hole, no movements, or changes of angles in the drill rig was done between the penetrations. The used equipment had no capacity for resistivity measurement.

As a part of the project, different approaches to determine the undisturbed shear strength described in chapter 3 (section 3.2.1) were tested. The three consecutive CPTu soundings did also enable a type of remoulded shear strength to be determined. Out of the three consecutive CPTu soundings, the third sounding was the one performed in the most remoulded soil. It was therefore decided that the remoulded shear strength was to be determined from that sounding. To calculate both the undisturbed and remoulded shear strength, four different approaches with different correction factors were tested. Out of those four, three approaches were based on the corrected cone resistance $q_t$ corrected from the measured cone resistance $q_c$, using equation (3). In all of those methods the numerator is equal to the corrected cone resistance $q_t$ subtracted with the *in situ* vertical stress. The first approach tested was to use equation (7), which is the equation recommended method by the SGI for calculating the shear strength of normally consolidated clays. The overconsolidation ratio was evaluated by the preconsolidation stress (obtained using equation (9)) and the *in situ* vertical stress. It was found that the clay was normally consolidated in all depths and all boreholes. To verify the preconsolidation pressure calculated using the CPTu results, a CRS analysis was conducted on a sample from the borehole NC2204 from 4 metres depth by the commercial laboratory Mitta. The preconsolidation pressure obtained from the CRS results was close to the preconsolidation pressure calculated from the CPTu results. Hence it was assumed that the clay was normally consolidated and equation (7) could be used when calculating the shear strength using the SGI method. In the second and third approach, equation (6) were used. The empirical cone factor $N_{kt}$ were in the second approach obtained using the diagram shown in Figure 4 where the cone factor is dependent on the plasticity index. In the third approach $N_{kt}$ were obtained using the diagram shown in Figure 5 where the cone factor is dependent on the pore pressure ratio $B_q$. The fourth approach tested was the method based on the excess pore pressure, $\Delta u$ using equation (11). In this approach the excess pore pressure was divided with the correction factor $N_{\Delta u}$ obtained from the graph shown in Figure 7. In the graph, $N_{\Delta u}$ is dependent on the plasticity index. The approach of using the effective cone resistance $q_e$, described in chapter 3 (section 3.2.1) were not tested. The reason for that was that the effective cone factor $N_{ke}$, used to correct the effective cone resistance could not be obtained for a majority of the sampling depths. Since the pore pressure ratio determined oftentimes were too high, the effective cone factor could not be determined using the graph shown in Figure 6.

The vertical stress used in a majority of the methods to determine the shear strength was calculated based on the density results from the laboratory testing at Chalmers. To obtain the density between the sampling levels, the density was interpolated. The specific weight of the dry crust was unknown and therefore, an assumption was made based on a combination of reference values and the average specific weight of the soil profile. The assumed specific weight of the dry crust was set to 16 kPa/m.

One T-bar penetration test (TPT) and one cyclic T-bar penetration test (TPTc) was performed at NC2204. It was decided to do both tests at NC2204, since the largest continuous clay depth of all investigated boreholes were found there. It was found that the clay depth was 14 metres when performing the pyramid penetration test. The purpose of the cyclic TPT was the same as for the multiple CPT, to achieve a remoulded state similar to the remoulded specimens prepared for fall cone testing. The cycle length in the TPTc was based on the length of the drilling rods and was therefore 2 metres. A cycle will in this project be defined as a penetration of the T-bar two metres into the soil downward followed by an extraction of the T-bar two metres upwards until the T-bar is in the exact position of where the cycle started. A cyclic interval is defined as the depth interval where the cycles are performed. The original idea was to perform two cycles at each cyclic interval, see Figure 11. However, since it turned out that the penetration resistance graph was visible on the field computer when performing the sounding, the number of cycles per level was revised as the penetration went on. It was decided to increase the number of cycles by one for each cycling depth, starting with 2 cycles between 4-6 m and ending with 7 cycles between 12-13.5 m. The drilling rig has no speed regulator for extraction, therefore the extracting rate was regulated manually to be as close to 20 mm/s as possible. Before the penetration started, a 0.2 metre deep and 0.3 x 0.3 metre wide hole was dug with a shovel as a substitute for pre-drilling and to allow the T-bar to be mounted below the drill rig. The T-bar had to be mounted below the drill rig because the stands of the drill rig was to narrow, leading to that the T-bar could not be mounted to the penetrometer as a normal CPTu cone.

The measured penetration resistance from TPTc was corrected according to equation (13) for all cyclic penetrations. The measured extracting resistance was not corrected since the extracting data was not used for calculation of the shear strength. The shear strength was calculated according to equation (14) with $N_T$ and $N_{T,rem}$ values evaluated based on laboratory results and earlier studies.

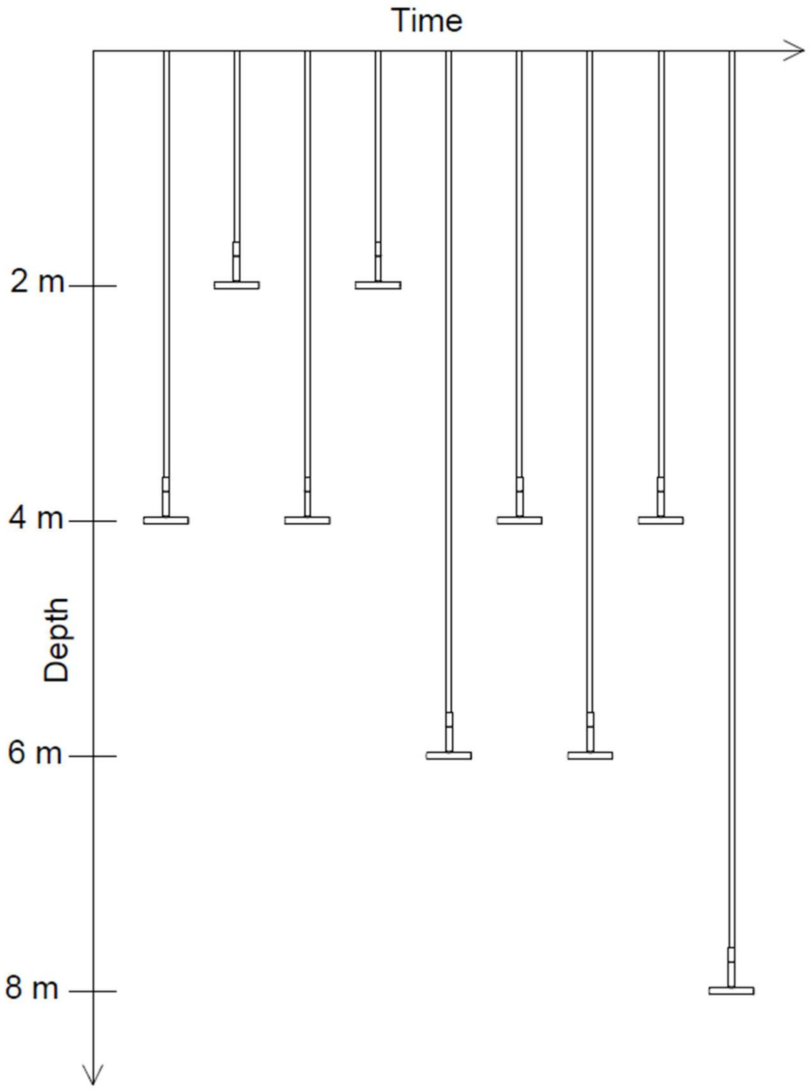


*Figure 11. Cyclic sounding with TPT.*

The standard piston sampling was performed according to the SGF report 1:2009 described in chapter 3 (section 3.1). The used sampler was a St II and the tubes inserted in the sampler were 170 mm long and had a diameter of 50 mm, in line with the SGF report 1:2009. Three samples per depth was recovered and sealed as quickly as possible and placed in the isolated and shock absorbing boxes. The samples were sorted for transportation to the laboratory at Chalmers and Mitta. The middle sample was sent to Chalmers and the top and bottom samples to Mitta.

Six different tests were executed at NC2204, and four different tests were executed at NC2205 and NC2211 respectively. It was made sure that the distance between the different test points were large enough to ensure that the soil was undisturbed when starting a new test.

## 6.2 Laboratory work

Laboratory testing was part of this project to determine reference values for the evaluated parameters from the field methods. The laboratory testing was performed by the authors of this thesis at the Chalmers geomechanics laboratory. The middle tubes from borehole NC2204, NC2205 and NC2211 was used for the testing. The methods used were fall cone test for determination of the undisturbed shear strength, the remoulded shear strength, and the liquid limit. Additional testing conducted was determination of density, natural water content ( $w_n$ ) and plastic limit. The determination of undisturbed and remoulded shear strength as well as the liquid and plastic limit were conducted according to the SS EN-ISO standards described in chapter 4 (section 4.1 and 4.2). No correction of the shear strength with equation (16) was done since it is not praxis to correct the shear strength for sensitivity analysis. The determination of the density was done by weighing the tube containing the soil sample and then subtract the weight of the empty tube. The weight of the soil was then divided by the volume of the tube. The natural water content was evaluated by weighing at least 30 g of the soil before and after it was dried in 105°C for at least 24 hours. For the liquid limit determination, both the four-point and the one-point method was performed on the samples from the borehole NC2205. This was done to validate the use of the one-point method for the other two boreholes. The laboratory work at Chalmers took place 8-14 of April, 2-9 days after sampling.

The same testing was conducted at the commercial laboratory Mitta for the upper and lower tube at each depth for the three boreholes, except from the four-point method for liquid limit determination. CRS-testing for two depths in borehole NC2204 were also performed at Mitta. The testing took place the 21$^{st}$ and 27$^{th}$ of April, 15-22 days after sampling.

## 6.3 Statistical parameter analysis

A part of this project has been to conduct three different statistical parameter analyses. In all three analyses a wide variety of data obtained from laboratory tests performed on core samples and CPT soundings has been analysed. Two of the analyses was done using the statistical method PCA and the third analysis was done comparing two of the parameters collected. The data used in all analyses was collected from a great number of already performed geotechnical site investigations where core samples has been recovered in close proximity to where CPTu soundings had been performed. Locations where quick clay had been confirmed as well as locations where quick clay had not been found or confirmed were both chosen to be included in the analysis. The prerequisites for the selected boreholes were that they had to be located in the south-west part of Sweden and that the sampling and CPTu sounding had been performed in the same borehole. Furthermore it was decided that data from depths less than five metres below the ground surface were excluded from the analysis. This was decided since near the ground surface it is more likely that the soil is impacted by recent geological- or anthropogenic processes.

### 6.3.1 Principal component analysis

In the PCA conducted, using the statistical software IBM SPSS, seven parameters were analysed. This analysis was divided into two parts. One analysis including all data collected and one similar analysis where only the depths where quick clay had been confirmed was included. In the first PCA a total of 41 boreholes were selected, and 311 depths were analysed. For the analysis performed where quick clay had been confirmed, the original dataset was filtered, resulting in 30 boreholes and 110 depths being included in the analysis.

The data was partly collected from the geotechnical archive compiled by SGI (SGI, n.d.). The data used for the analysis were downloaded in GeoSuite format from the website https://bga.sgi.se/. Data was also collected from the project database of the consultant company Norconsult. The borehole ID and coordinates for all used boreholes can be found in Appendix D. The parameters collected for the analyses were partly collected from CPTu soundings and partly collected from laboratory tests performed on soil samples. From the CPTu results the corrected cone resistance $q_t$, the uncorrected sleeve friction $f_s$, and the measured pore pressure from the $u_2$ location were collected. The cone resistance was chosen as a parameter for the analysis because of its possibility to distinguish variation in stiffness in the soil. The sleeve friction was collected for the analysis because of its possibility to observe variations in the friction acting on the sleeve of the cone penetrometer. Generally, the friction acting on the sleeve of the penetrometer is changing drastically depending on if the penetrometer is driven through a cohesive or non-cohesive soil. By collecting the pore pressure at the $u_2$ location of the penetrometer, the depths where the pore pressures deviated from the hydrostatic pore pressure could be made visible. Those depth were of interest for the analysis since it was perceived that it could be of significance to find where quick clay could be expected. To collect the data from the same depths as core samples had been recovered from, the software Conrad 3.1 developed by the Swedish geotechnical institute (SGI) was used. Parameters from laboratory results were obtained from the collected GeoSuite data files and from geotechnical reports (MUR) for the Norconsult projects. The parameters collected from laboratory results were the remoulded shear strength, sensitivity, liquid limit and density. The remoulded shear strengths collected had been evaluated using the fall cone method and so had the undisturbed shear strength used to calculate the sensitivity. The remoulded shear strength and the sensitivity was included in the analysis because in Sweden it is the two parameters that are required to verify if a clay is quick. The liquid limit was included in the analysis mainly because it has been debated whether it is correlated to the shear strength or not. The density was included in the analysis as well. If several densities (normally three) had been evaluated from the same depth, the density with the value in the middle was chosen. Figure 12 is showing a map of the location in south-west Sweden of the boreholes used for the analysis.

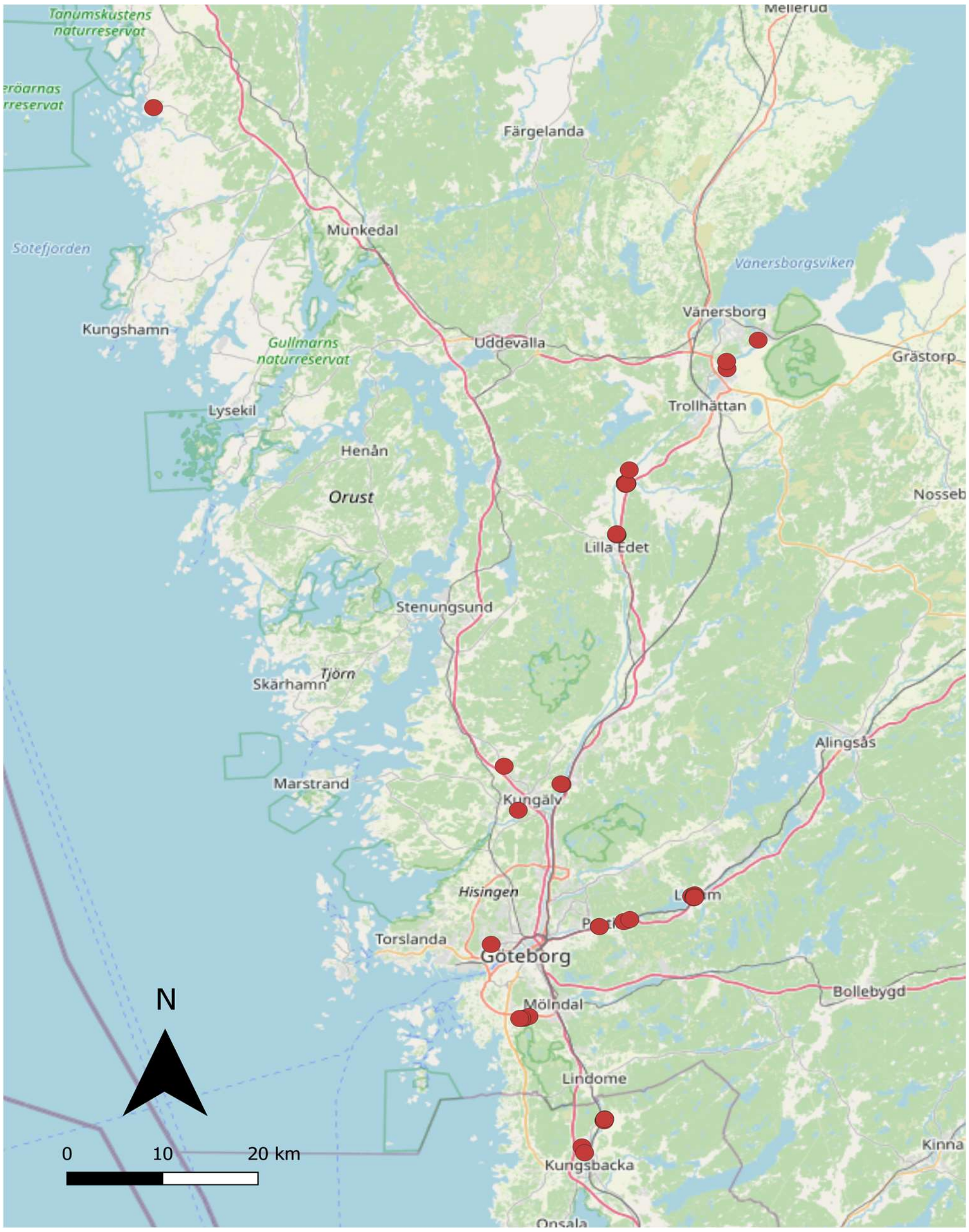


*Figure 12. Map over the observed boreholes.*

## 6.3.2 Distance to a draining layer

The third statistical analysis was a comparative analysis was where the distance to the closest draining layer for a specific depth was compared with the corresponding remoulded shear strength of that depth. This analysis was done to assess the impact a draining layer has on the formation of quick clay. Prior to performing the analysis the hypothesis was that if a low remoulded shear strength was to be observed at depths near a draining layer, it could be argued that the distance to a draining layer could be an important parameter to assess when mapping quick clay.

This analysis was decided to be done separate from the PCA. That was decided because when the distance to the draining layer was included that analysis, the results showed that the parameter was not statistically significant. The values of the extracted communalities were low, and it had low correlation with all other parameters included in the PCA. Another reason for doing this analysis separate from the PCA was related to the difficulties with identifying draining layers in the soil strata in the different boreholes. For this reason, it was only possible to do the comparison in boreholes where evidence of a draining layer was clear, which resulted in a significant reduction of depth when performing the PCA.

One of the methods used to identify a draining layer was to observe parameters obtained from CPTu results. When looking at the CPTu data a draining layer was defined as a level where the cone resistance and sleeve friction drastically changed, simultaneously as the pore pressure drastically decreased. A drastic change in the cone resistance and sleeve friction is likely to imply a change in soil material. A drastic decrease in pore pressure is perceived to imply a more permeable soil layer.

The soil material identified in soil samples were in some cases used to motivate a draining layer. Coarser material in general has a higher hydraulic conductivity. If for example sand or silt were found in the samples and the CPT results indicated a draining layer around that depth a draining layer was assumed there.

The stop code marked for the different CPT soundings were in some cases used to motivate the position of a draining layer. A description of the different stop codes is shown in Table 3 (SGF & BGS, 2001).

*Table 3. Stop codes used for CPT soundings, modified from SGF & BGS, (2001).*

| Stop code | Description |
|---|---|
| 90 | Sounding terminated without reaching refusal |
| 91 | The probe cannot be driven deeper down by normal procedure |
| 92 | Stop against stone, boulder or bedrock |
| 93 | Stop against stone or boulder |
| 94 | Stop against assumed bedrock |
| 95 | Drilling into assumed bedrock |

If the CPT sounding was marked with code 91, 92, 93, 94 or 95 a draining layer was assumed if evidence of a draining layer was shown in the CPT results or soil samples. If the CPT sounding was marked with stop code 90, that borehole was excluded from the analysis if no other significant evidence of a draining layer was observed.

# 7 Results and Discussion

Results and discussion regarding the modified field methods is presented in the following chapter as well as a discussion of the deviating laboratory results from the two laboratories. The laboratory results from Chalmers and Mitta are used as a reference to the evaluated shear strength obtained from the modified field methods. The laboratory results from both laboratories can be found in Appendix A The results and discussion regarding the statistical analysis will also be presented in this chapter.

## 7.1 General characterisation

The results of the first CPTu soundings for borehole NC2204, NC2205 and NC2211 is shown in Figure 13, Figure 14 and Figure 15 respectively. The figures are showing the measured cone resistance, sleeve friction and pore pressure from the $u_2$ location. It can be seen that a slight increase with depth is observed in the measured cone resistance. The exception being the dry crust located between the ground surface and one to two metres below the ground surface, where $q_c$ is considerably higher. The sounding was stopped before where the pyramid penetration test indicated rock or till to prevent damage on the piezocone. That depth is clearly visible in all graphs, showing a significant increase in measured cone resistance. The measured sleeve friction, $f_s$ registered was in general constant with depth with significantly higher sleeve friction at the level of the dry crust. Based on the assessment from the Mitta laboratory all samples were categorised as clays except for the samples from the depths of two and four metres in the borehole NC2204, which was categorised as gyttja. The laboratory results and the CPTu results are both indicating that the soil in the project area constitutes of a continuous and homogenous clay layer.

The cone resistance registered at the level of the dry crust in the borehole NC2205 is very high. Because of that, it is in the graph difficult to see the measured cone resistance at depths below the dry crust. When studying the numbers, it is however evident that the measured cone resistance is similar to the measured cone resistance in the boreholes NC2204 and NC2211. In all three boreholes a measured cone resistance of around 150 kPa was registered below the dry crust at around 1.5 metres depth. This is followed by an in general slight increase with depth. A measured cone resistance of around 250 kPa was registered at a depth of around six metres below the ground surface in all boreholes. In the borehole NC2211 the cone resistance is deviating extensively at depths between four to six metres below the ground surface. The deviating values are most likely caused by the abundant number of shells found at these depths.

Based on the CPTu results the ground water level was assumed to be positioned at a level of 1.5 metres below the ground surface in all boreholes analysed. The measured pore pressure showed values well above the hydrostatic pore pressure. No dissipation test has been performed. Therefore, the in situ excess pore water pressure is not evaluated. In the NC2205 and NC2211 boreholes, the measured pore pressure is increasing with depth at a rate similar to the rate of the hydrostatic pore pressure. Meanwhile in the NC2204 borehole the pore pressure is increasing with a rate much higher than the hydrostatic pore pressure between two and four metres from the ground surface. Followed by a phase where the pore pressure is relatively constant with depth. In two of the three boreholes the pore pressure measured is considerably larger than zero at the position of the groundwater level. This could possibly be explained by that the boreholes were not pre-drilled through the dry-crust or by in general wet conditions in the clay the days the CPTu-soundings were performed.

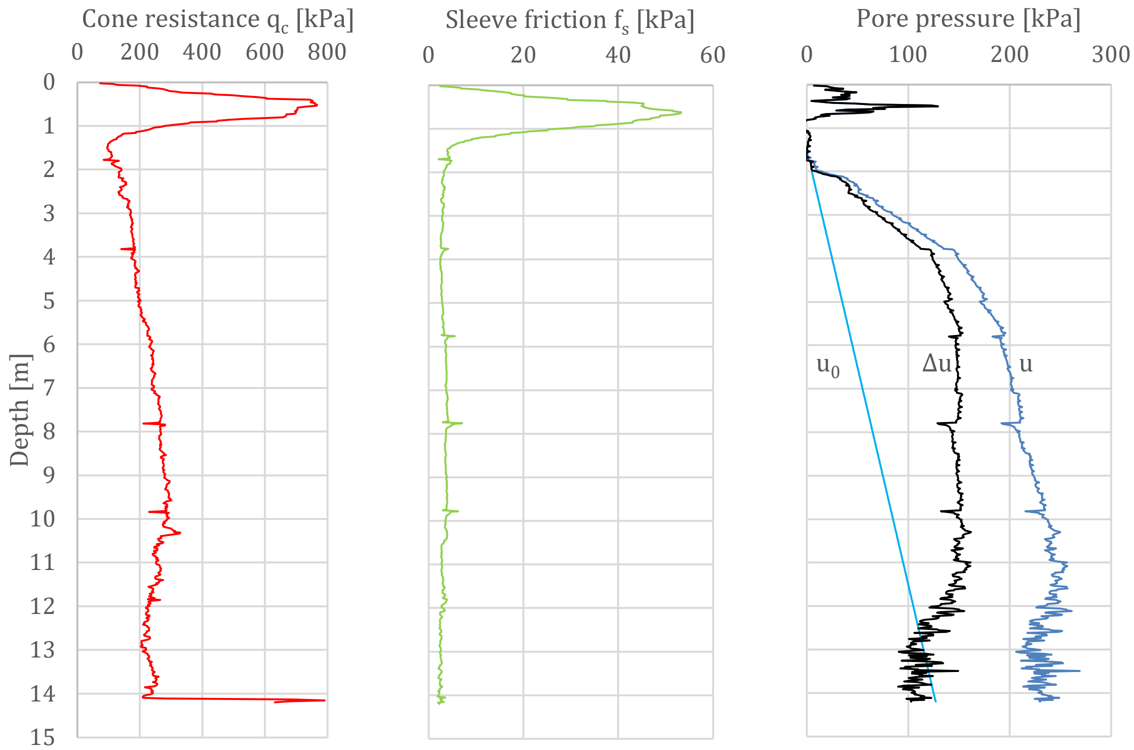


*Figure 13. Measured cone resistance, sleeve friction and pore pressure in the initial sounding in NC2204.*

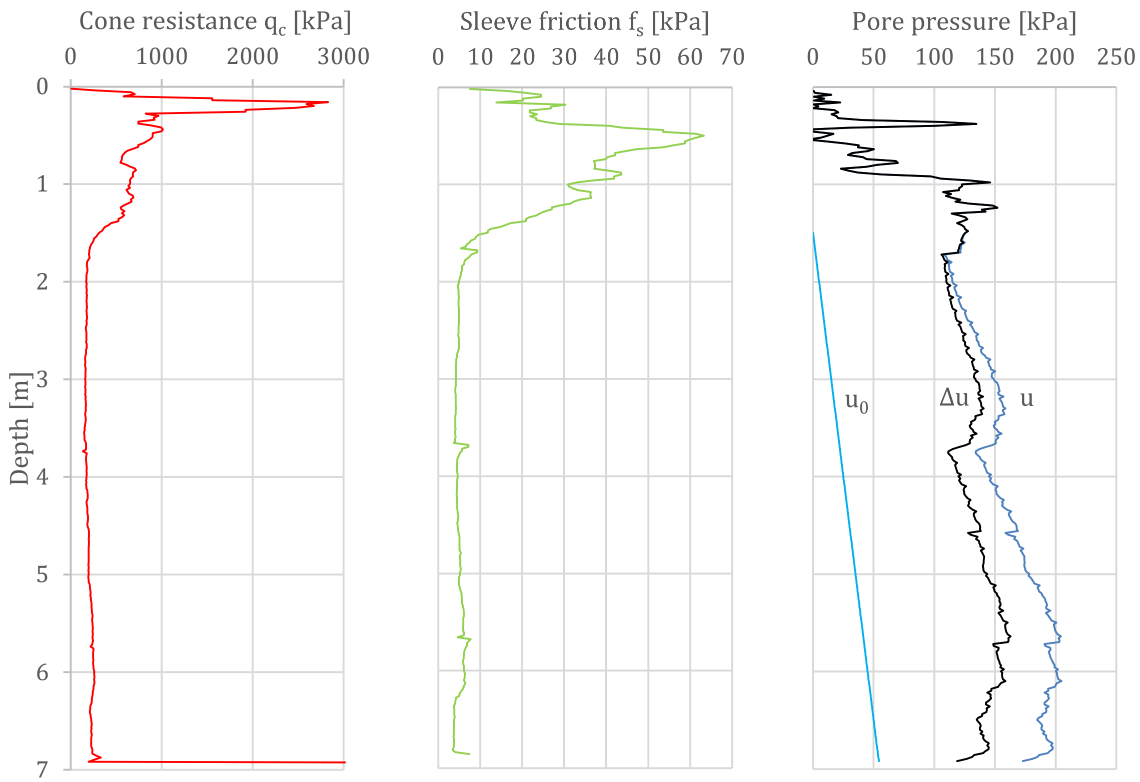


*Figure 14. Measured cone resistance, sleeve friction and pore pressure in the initial sounding in NC2205.*

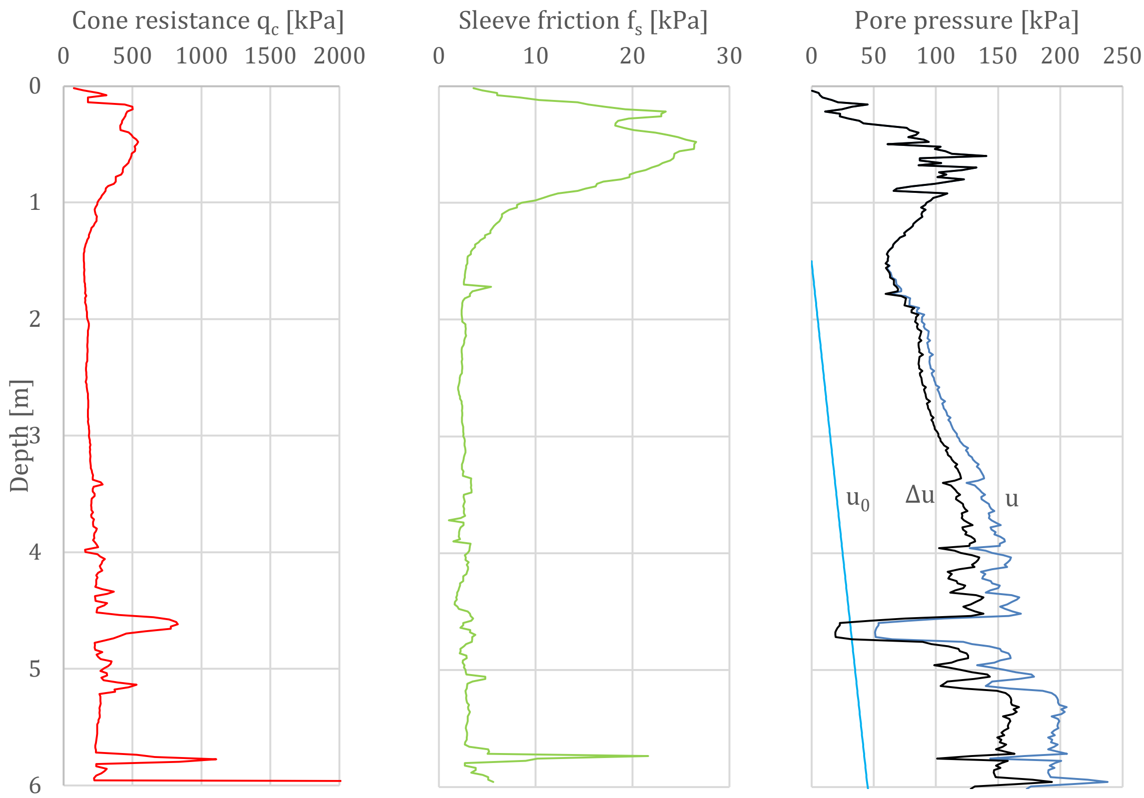


*Figure 15. Measured cone resistance, sleeve friction and pore pressure in the initial sounding in NC2211.*

## 7.2 Multiple CPTu-soundings in the same borehole

Figure 16-Figure 21 are showing the measured cone resistance, sleeve friction and pore pressure of the three CPTu-soundings that were performed in each of the boreholes named NC2204, NC2205 and NC2211. The measurements are plotted from below the dry crust. When comparing the parameters in the first, second and third sounding it is noted that most parameters in most boreholes are decreasing when compared to the preceding sounding. Exceptions from this are in a few cases found. For example, when the sounding is stopped for adding new rods, or in some cases where the measured data of two consecutive soundings (often the second and third) is largely similar.

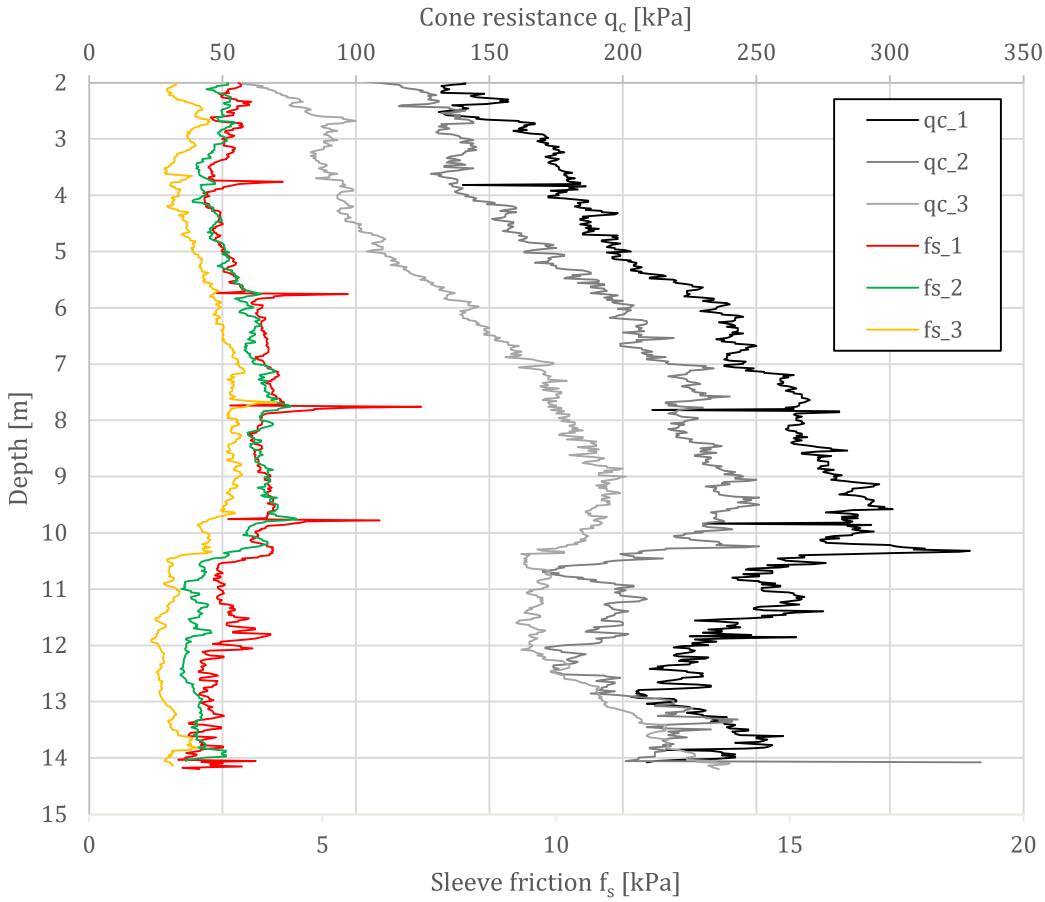


*Figure 16. Measured cone resistance and sleeve friction in the NC2204 borehole.*

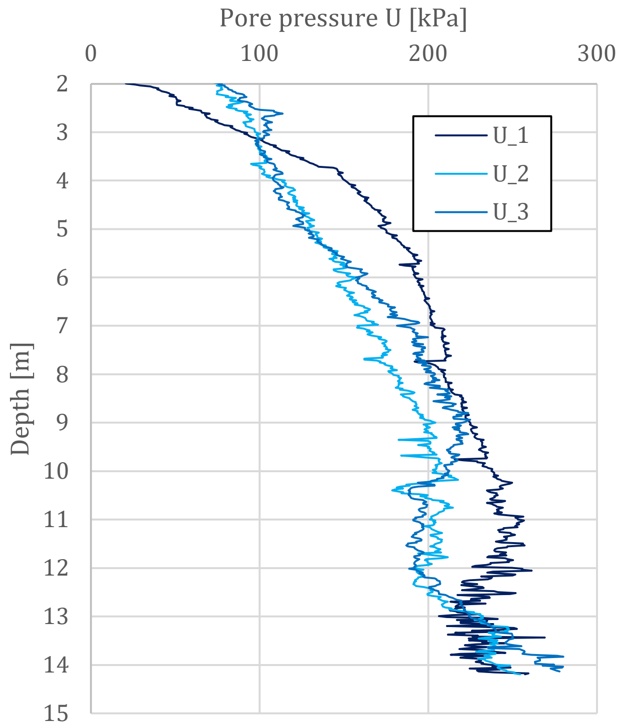


*Figure 17. Measured pore pressure at the $u_2$ location in the NC2204 borehole.*

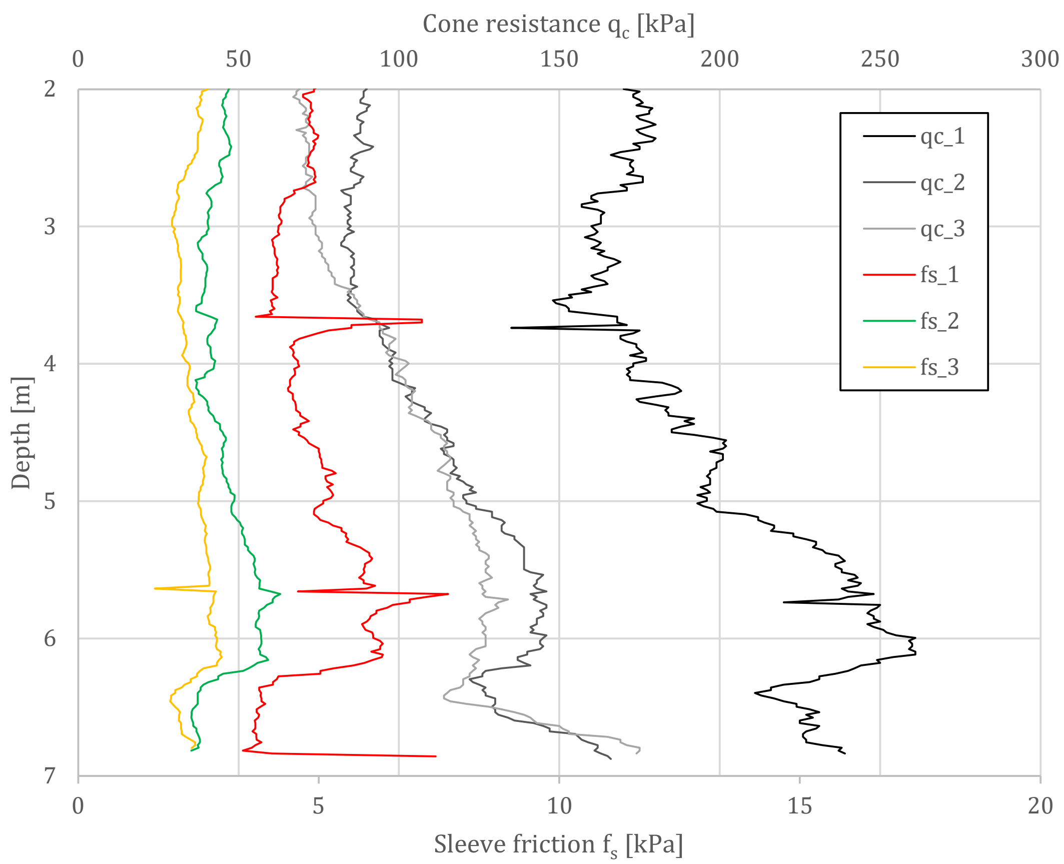


*Figure 18. Measured cone resistance and sleeve friction in the NC2205 borehole.*

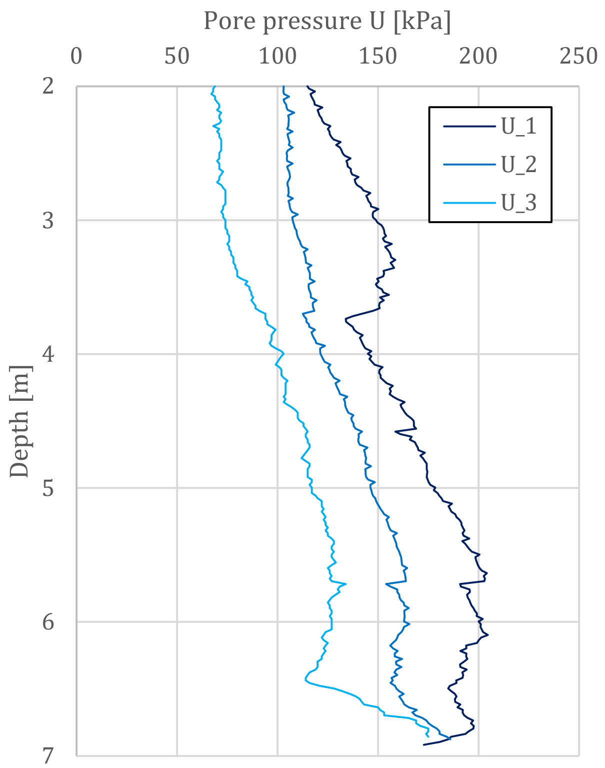


*Figure 19. Measured pore pressure at the $u_2$ location in the NC2205 borehole.*

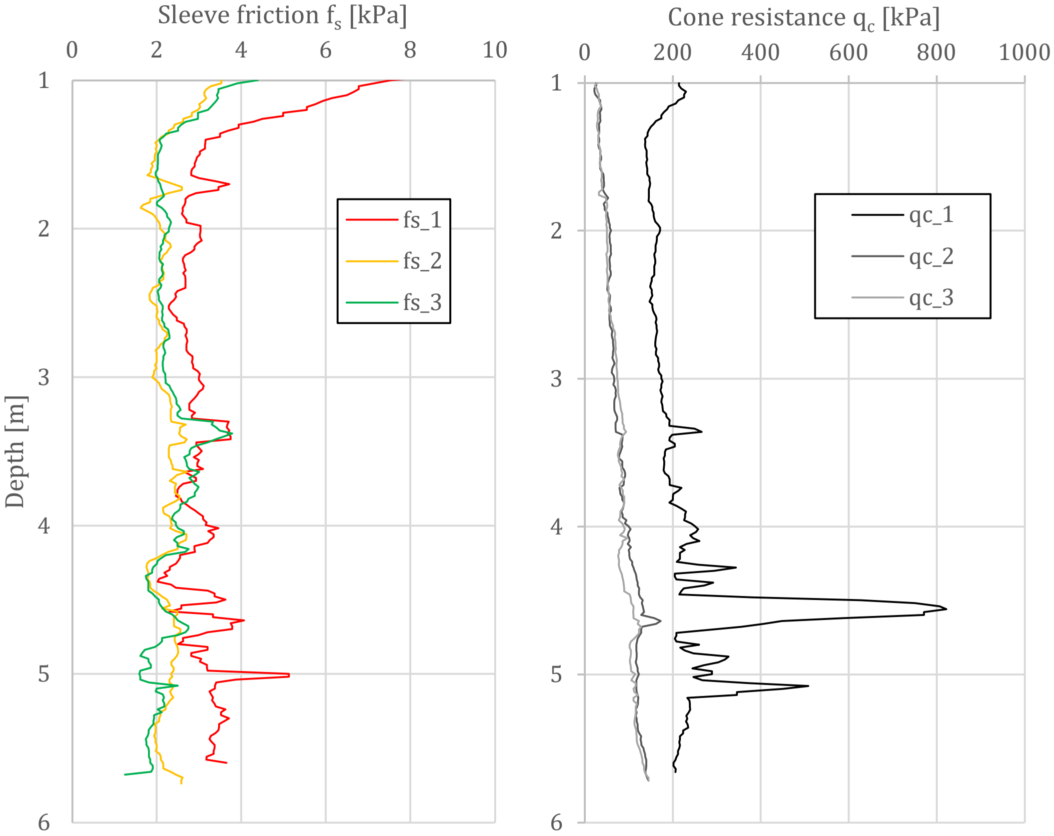


*Figure 20. Measured cone resistance and sleeve friction in the NC2211 borehole.*

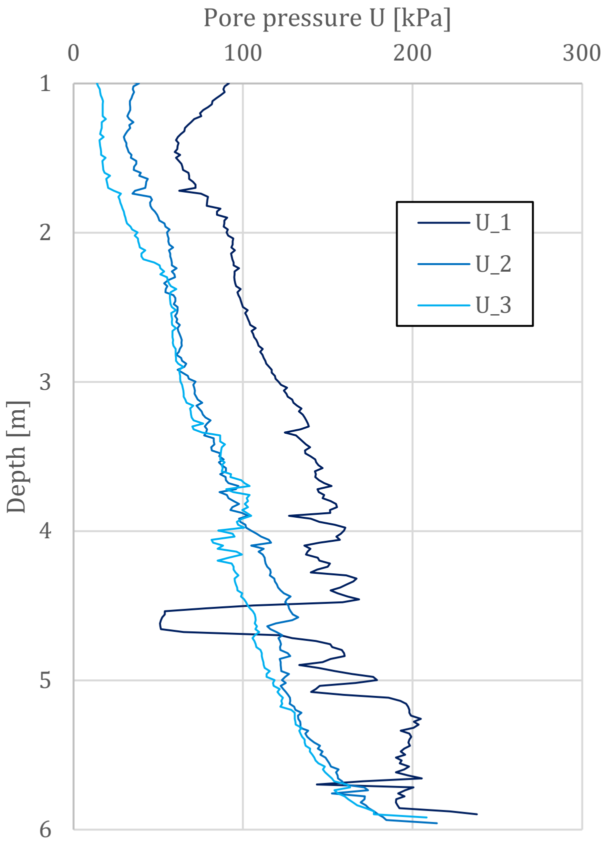


*Figure 21. Measured pore pressure at the $u_2$ location in the NC2211 borehole.*

The general trend when observing all three parameters is that the largest decrease is found between the first and second sounding. A lower decrease is in general found between the second and third sounding. Which is suggesting that the penetrometer to some degree is remoulding the clay. Graphs showing the difference between the three measured CPTu parameters comparing the first and second sounding and second and third sounding in percentage is shown in Appendix B in Figure B1, Figure B2Figure B3. The trend of having the largest decrease between the first and second sounding when comparing the different parameters is most clearly visible in the data showing the measured cone resistance. It is least clearly visible when comparing the measured pore pressure. The trend is most pronounced in the NC2205 and NC2211 boreholes. Meanwhile in the NC2204 borehole, the decrease between the second and third sounding was about equally large and at some depths larger than the decrease observed between the first and second sounding. A possible explanation to the differences between boreholes could be how well the CPTu penetrometer is driven following the same path as the proceeding sounding. In Figure 22 the tilt angles of the cone penetrometer for the three soundings of the three boreholes is plotted against depth. The tilt angle shown in the figure is the inclination of the penetrometer in relation to the vertical axis. When looking at the graphs it is important to have in mind that they are not showing the direction of the inclination of the penetrometer, only the inclination. From the figure it can be seen that the tilt angles of the borehole NC2204 is varying more than the NC2205 and NC2211 boreholes. A possible explanation to this could be that the path of the second or third sounding partly or fully missed the path made by the preceding sounding or soundings. If the CPTu is driven following the same path, it should be expected that the decrease in measured cone resistance and sleeve friction will decline exponentially as more soundings are performed. That could be an explanation to the lower than expected decrease in measured cone resistance and sleeve friction between the first and second sounding in the NC2204 borehole. A following higher than expected decrease between the second and third sounding could then be explained by that the path made by the first and second sounding is not followed until the third sounding is performed. These results are showing that in order to develop a method that could be repeated and give comparable results, it is important that the soundings following the first sounding is performed with great accuracy. No movements of the drill rig should be done between the penetrations. Another uncertainty with performing multiple CPTu soundings in the exact same location is that it is difficult to assess whether the hole created after the penetrometer is withdrawn collapses or not. The method therefore has best potential to work in soft clays where the likelihood of the hole created by the cone penetrometer collapsing is large.

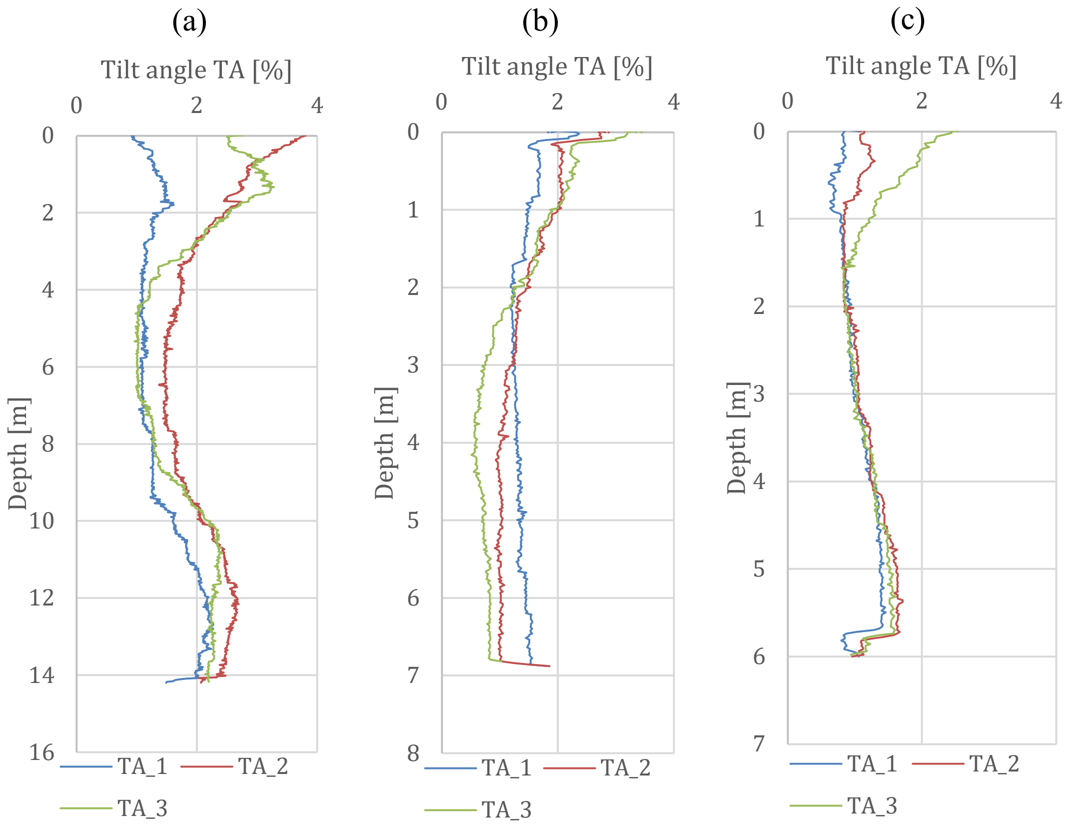


*Figure 22. Tilt angles of the three CPTu-soundings in NC2204 (a), NC2205 (b) and NC2211 (c).*

### 7.2.1 Evaluated shear strength from multiple CPTu-soundings

Figure 23 is showing the shear strength calculated using the results from the three consecutive CPTu soundings performed in the borehole NC2204. The shear strength was calculated using equation (7) which is Swedish standard praxis for normally consolidated clays. The undisturbed and remoulded shear strength evaluated with the fall cone test at the Chalmers geomechanics laboratory, and the commercial laboratory Mitta is also included in the figure.

From the Figure 23 it can also be seen that both undisturbed shear strengths evaluated in laboratory is higher than the shear strength evaluated from the first CPTu sounding. The remoulded shear strength evaluated in the laboratories is in general much lower than the shear strength evaluated from the third CPTu sounding. The undisturbed as well as the remoulded shear strength is to a certain degree following the same trend with depth as the shear strengths evaluated from the CPTu soundings.

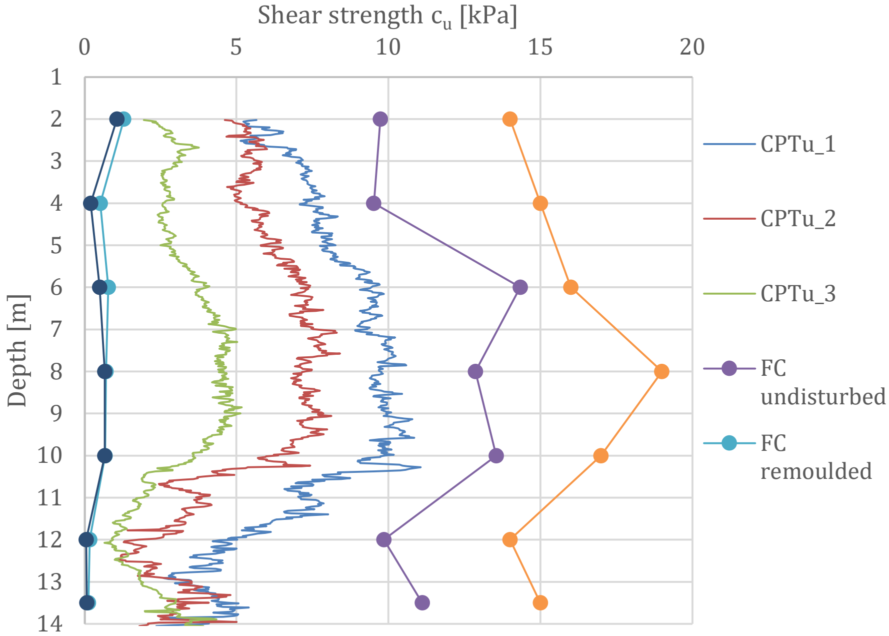


*Figure 23. Undisturbed and remoulded shear strength evaluated in the borehole NC2204 from three consecutive CPTu soundings and from two different laboratories with the fall cone test.*

Figure 24 is showing corresponding results as Figure 23 but for the borehole NC2205. Similarly to the results in the borehole NC2204, the undisturbed shear strength from the laboratories is higher and the remoulded shear strength is lower compared to all shear strengths evaluated from all CPTu soundings. The shear strengths evaluated from the laboratories and the CPTu results are to a certain degree following the same trend with depth. An exception from this is however noted at the depth five metres below the ground level. At this level the undisturbed shear strength is decreasing drastically, whilst no decrease is observed in the shear strength evaluated from the first CPTu sounding.

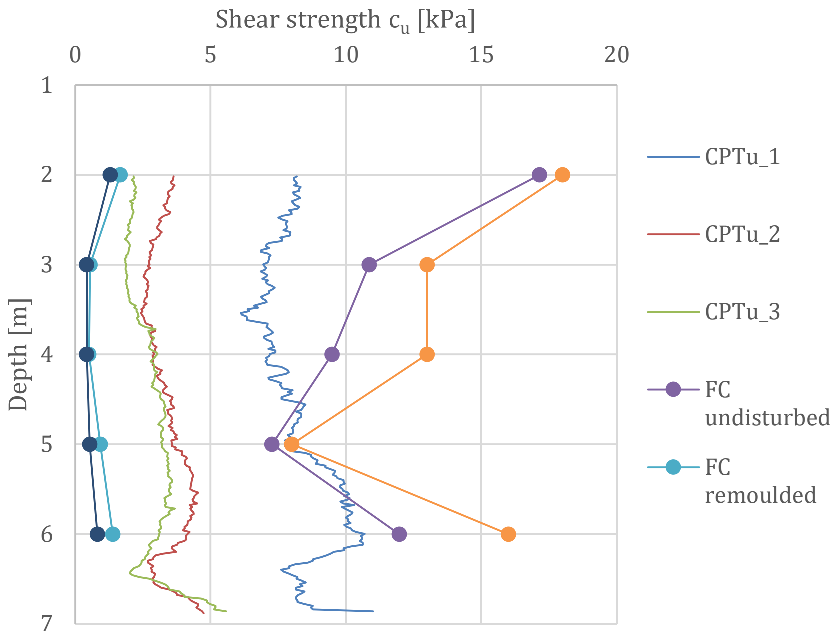


*Figure 24. Undisturbed and remoulded shear strength evaluated in the borehole NC2205 from three consecutive CPTu soundings and from two different laboratories with the fall cone test.*

Figure 25 is showing corresponding results as Figure 23 and Figure 24 but for the borehole NC2211. The CPTu soundings and sampling in NC2211 was impacted by an abundant number of shells which impacted the quality of the CPTu sounding and piston sampling negatively. Noted in this borehole is that the shear strength evaluated from the laboratories and from the CPTu sounding is not matching each other particularly well.

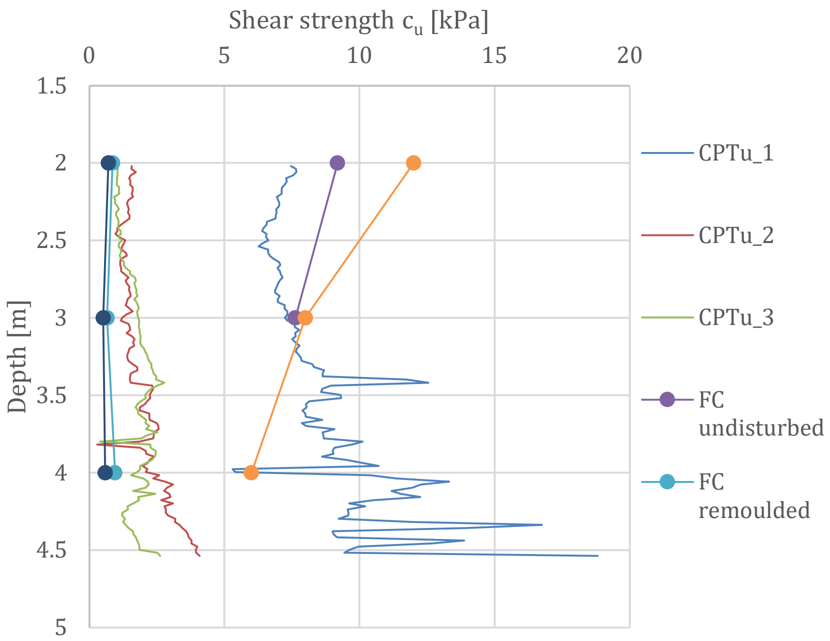


*Figure 25. Undisturbed and remoulded shear strength evaluated in the borehole NC2211 from three consecutive CPTu soundings and from two different laboratories with the fall cone test.*

When comparing the shear strength evaluated in all three boreholes from the CPTu soundings using the method that is Swedish praxis, it was found that the undisturbed shear strength evaluated from the CPTu result in almost all cases was lower than the corresponding shear strength determined in the laboratories. Furthermore, the remoulded shear strength evaluated in the laboratories in all boreholes and all levels is lower than the strength evaluated from the third sounding. This is suggesting that the three soundings are not remoulding the clay fully. Fully remoulded in this context refers to the state of remoulding achieved in laboratory when preparing a specimen for evaluation of the remoulded shear strength with the fall cone test.

When calculating the shear strength using the different approaches described in chapter 3 (section 3.2.1), it was shown that the shear strength varied a lot depending on which method was used. Figure 26 is showing the different shear strengths calculated from the first CPTu sounding performed in the NC2204 borehole. The shear strength for each depth shown in the graph is the average shear strength of one metre, starting half a metre above and half a metre below the depth specified in the table. Included in the graph is also the undisturbed shear strength evaluated in the two laboratories. As shown in the graph, the shear strength has not been evaluated at all sampling levels. That is because some of the methods could not be applied for all depths. Because at some depths, the plasticity limit and pore pressure ratio were too high, which resulted in that the shear strength could not be evaluated.

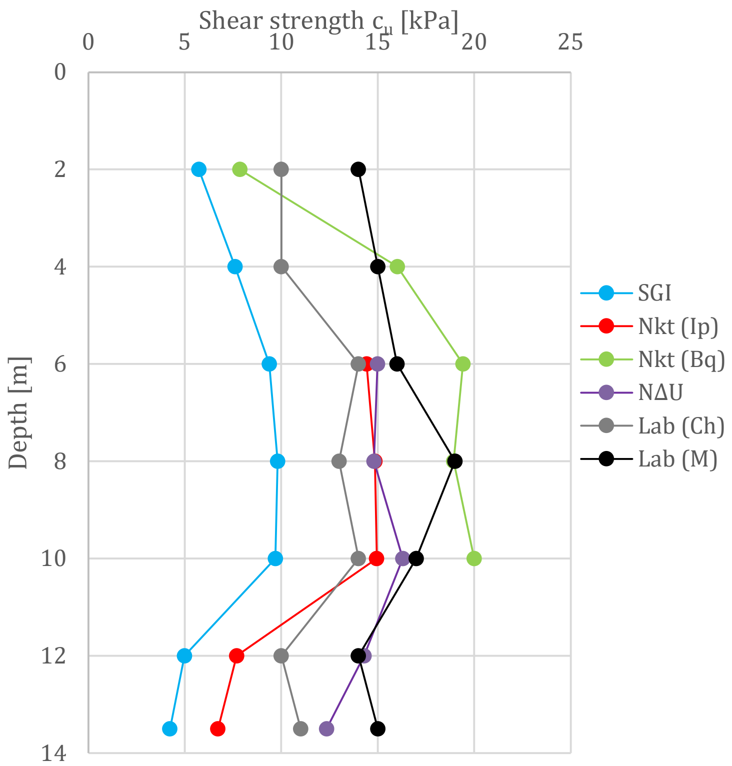


*Figure 26. Undisturbed shear strength [kPa] calculated from CPTu results using different approaches. Including the two laboratory results. Borehole NC2204.*

The method yielding the lowest shear strength in all depths is the method recommended by the SGI. The SGI method (denoted SGI in the graph) is depending on the liquid limit of the soil. A high liquid limit will result in a low shear strength. Both methods using equation (6) (denoted $N_{kt}(I_p)$ and $N_{kt}(B_q)$ in the graph) results in a considerably higher shear strength compared to the SGI method. When comparing the shear strength from the $N_{kt}(I_p)$ and $N_{kt}(B_q)$ methods it is found that the method where $N_{kt}$ is determined using the plasticity index ($N_{kt}(I_p)$) is resulting in a lower shear strength compared to when the pore pressure ratio is used ($N_{kt}(B_q)$). A high liquid limit will result in a high plasticity index which in turn results in a low shear strength. The method where $N_{kt}$ is calculated using the pore pressure ratio is yielding the highest undisturbed shear strength of all tested methods. The method where the shear strength is determined using the excess pore pressure ($N_{\Delta U}$) is yielding shear stresses close to the $N_{kt}(I_p)$ method. These two methods are giving results that are closest to the undisturbed shear strength evaluated in the laboratories.

The undisturbed shear strength evaluated in the laboratory at Chalmers is denoted Lab (Ch) and the undisturbed shear strength in the laboratory of Mitta is denoted Lab (M) in Figure 26. One should however be careful when comparing the shear strength determined using the CPTu results with the laboratory results. That is partially because the cone factor used to calculate the shear strength using the $N_{kt}(I_p)$, $N_{kt}(B_q)$ and the $N_{\Delta U}$ method is correlated to a shear strength determined from results of anisotropically consolidated triaxial tests sheared in compression (Karlsrud et al., 1997, 2005). The shear strength determined by using the fall cone test is therefore not completely comparable to those results. Another factor that is important to have in mind is that the sampling method the cone factors are based upon, could not be directly compared to the sampling method performed during the field investigation that was part of this project. That is because the specimens that were triaxially tested to obtain the different cone factors were performed on samples recovered using the Sherbrooke 250 mm block sampler (Karlsrud et al., 2005). The specimens recovered using the Sherbrooke 250 mm block sampler is expected to be of higher quality (less disturbed) compared to the samples recovered using the standard piston sampler used during the field investigation in this project. The triaxial test performed on the high quality block samples will most likely give a higher shear strength, which results in a lower cone factor compared to a cone factor evaluated on core samples recovered using the piston sampler. To test this hypothesis, the cone factor $N_{kt}$ was determined using the undisturbed shear strength evaluated with the fall cone test at the Chalmers laboratory. The results showed that a higher cone factor than all cone factors used when calculating the shear strength with the $N_{kt}(I_p)$, $N_{kt}(B_q)$ and the $N_{\Delta U}$ method was indeed obtained for all depths except for the sampling depths 12 and 13.5 metres below the ground surface. A graph showing the cone factor against depth for the tested methods can be seen in Figure B4 in Appendix B. In summary it can be said that the shear strength evaluated using those methods is not directly comparable to the shear strength determined using the fall cone test.

Figure 27 is similarly to Figure 26 showing the shear strength evaluated from the borehole NC2204 using the different approaches described. But in this graph, the CPTu results of the third sounding, which is performed in a partially remoulded soil is shown. Included in the graph is also the remoulded shear strength from the two laboratories.

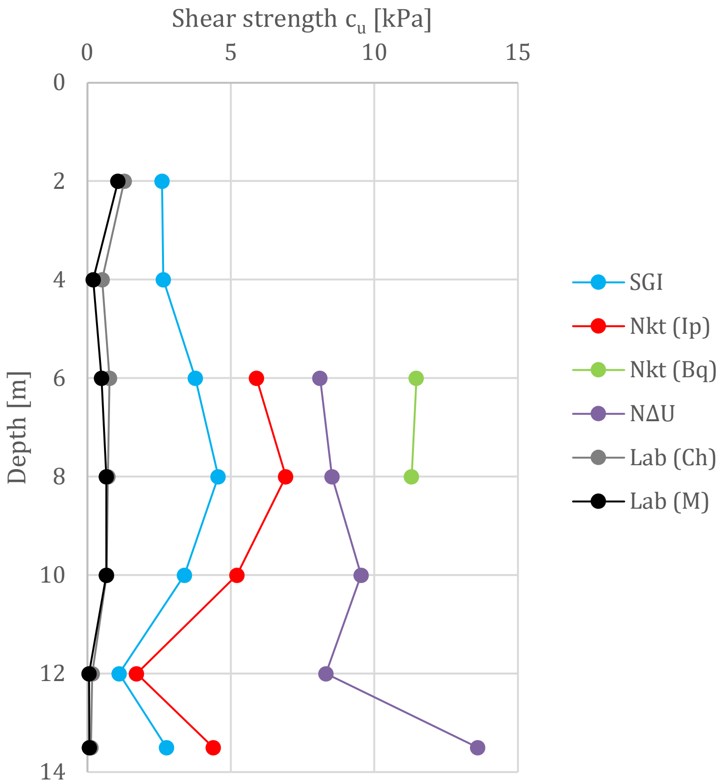


*Figure 27. Remoulded shear strength [kPa] calculated from CPTu results using different approaches. Including the two laboratory results. Borehole NC2204.*

The shear strength from the third consecutive CPTu sounding is for almost all methods and depths lower than the shear strength evaluated from the first sounding. It is also noted that the methods based on the total cone resistance (SGI, $N_{kt}$ $(I_p)$ $N_{kt}(B_q)$) is decreasing more in comparison to the method based on the excess pore pressure. This is mainly because the corrected cone resistance is decreasing more than the measured pore pressure the excess pore pressure is based upon when comparing the first and the third CPTu sounding. The method based on the excess pore pressure is the only method where an increase in shear strength has occurred, comparing the first and third sounding. That increase is occurring at the depth of 13.5 metres. The graph is also showing that all shear strengths evaluated from the third sounding is considerably higher than the remoulded shear strength evaluated in the laboratories. This is again suggesting that the three consecutive CPTu soundings is not remoulding the clay fully.

When doing the same analysis in other boreholes similar trends to the results in the borehole NC2204 is observed. The results of the undisturbed and remoulded shear strength evaluated with the different methods described is for borehole NC2205 shown in Figure B5Figure B6 in Appendix B. The method giving the highest undisturbed shear strength in NC2205 ($N_{kt}$ calculated using $B_q$) is the same method yielding the highest shear strength in NC2204. Similarly, the method giving the lowest shear strength (the SGI method) is the same in both boreholes. When comparing the undisturbed shear strength evaluated in the laboratory to the undisturbed shear strength evaluated with CPTu data it was noted that they are not following the same trend at a depth of five metres below the ground surface. The undisturbed shear strengths evaluated from both laboratories at this depth is decreasing drastically meanwhile no drastic decrease is observed for any of the methods based on the CPTu data. A possible explanation to this could be that the shear strength evaluated from the registered cone resistance, for unknown reasons is not yielding the low shear strength the clay possibly has at that depth. Another explanation could be that the undisturbed sample recovered at that depth has been disturbed, and thus yielding a lower undisturbed shear strength. This could be true since no significant decrease in remoulded shear strength evaluated at both laboratories was observed when comparing that depth to the other depths in the studied borehole.

When reflecting over the results a note should be made that the different methods used to calculate the shear strength from the CPTu results is not intended to be used on soils that has been disturbed. This has the effect that for the methods based on the total cone resistance, the vertical stress is getting an increasingly high impact on the results. In the borehole NC2204 at a depth of 12 metres, it was for example observed that the difference between the corrected cone resistance and the vertical stress was very small. If the procedure of doing multiple CPTu soundings at the exact same location were to be used in larger scale, the possibility of the vertical stress becoming higher than the corrected cone resistance cannot be excluded. The impact of that would be that the shear strength becomes negative which in that case would not reflect what is happening in practice.

Considering the fact that the shear strength evaluated from the third CPTu sounding is much higher than the remoulded shear strength evaluated with the fall cone test, a possible option to obtain a more reasonable value for the shear strength could be to correct the remoulded CPTu sounding with a cone factor exclusively developed for remoulded conditions. A cone factor for remoulded conditions has previously been tested and assessed in Low et al. (2010) when evaluating shear strength from cyclic T-bar penetration tests. A similar approach could possibly be adopted for determining the shear strength with CPTu in remoulded soils. To determine the cone factor for remoulded conditions it would be preferable that it is based on the last CPTu sounding out of more than three consecutive soundings. Preferably should soundings be made until the point where the decrease in registered cone resistance is insignificant small. A type of correction might also be necessary to add in the numerator of equation (6) to minimise the risk of the vertical stress having too much impact on the evaluated shear strength. A possible development of both these corrections is however not within the scope of this project.

## 7.3 Cyclic T-bar penetration test

The measured penetration and extraction resistance $q_{c.T-bar}$ for the TPTc performed in NC2204 is plotted against depth in Figure 28. In the graph each colour is representing one cyclic level (except the line between 0-4 metre, where no cyclic penetrations were performed). The solid lines (mainly on the positive side of the x-axis) are the resistance when penetrating down in the soil and the dotted lines (mainly on the negative side on the x-axis) are the resistance when extracting the penetrometer. Deviating values registered when additional rods were attached has been removed. The extraction resistance was logged as negative values, however the actual resistance when extracting the T-bar is the absolute values of the logged resistance. One can see that the first penetration resistance for each cyclic interval is significantly larger than the resistance of the other penetrations at the same cyclic interval. The same phenomena are visible for the extracting resistance but not to the same extent. The penetration and extraction resistance decreases for each cycle. When the first penetration takes place at each cyclic interval, the clay is undisturbed and then it gets more and more remoulded which explains the decrease in resistance. For the first three cyclic intervals, the resistance is continuing to decrease for each cycle (there is a gap between the last and second last $q_c$ curves). For the cycles between 10-12 and 12-13.5 metres there is no visual gap between the last $q_c$ curves. This indicates that the clay is not completely remoulded between 4-10 metres but may be considered as remoulded between 10-13.5 metres. The clay should theoretically be more remoulded further down since the number of cycles increased by the depth. One can argue that a preferable scenario for this analysis would have been to increase the number of cycles for all cyclic intervals until there were no gap between the resistance curves.

The first cycle at each cyclic interval is considered as undisturbed. The soil just below the depth at which one cycle ends and the penetrometer is extracted, may be disturbed by the pressure of multiple cycles. A regular TPT, where the penetrometer was driven to 13.5 metres and extracted to the surface without any cycles, was performed at NC2204. A comparison between the measured resistance of the TPT and the resistance from the first cycle at each cyclic interval from the TPTc (found in Appendix C, Figure C1) showed that there were no differences in resistance between the two soundings. This indicates that the soil below a cyclic interval is still undisturbed when multiple cycles have been performed above.

The probability that the T-bar penetrometer is following the same path as the previous sounding is most likely higher than for the CPT. Since the TPT tip is cylindrical, the likelihood reduces that it will take another path than the previous sounding. Compared with the sharp pointed CPT that more easily creates a new path. The effect of the full-flow penetrometer is that since the clay is flowing around the cylindrical T-bar it gets remoulded in the driven path and therefore the clay is softer than in the surroundings.

The two-metre cyclic intervals may as well reduce the uncertainty of whether the penetrometer following the same path as the previous sounding or not. Since the time required for one cycle is relatively short, the clay does not have much time to recover. From Figure 28 it is evident that the penetration (and extraction) resistance is reducing between each cycle. Even if the order of cycles for each cyclic interval is not visible in this graph, the cycles come in ascending order. Meaning that the first line (from the left-hand side in the graph) for each cyclic interval is the resistance of the penetration of the first cycle. The second line for each cyclic interval is the resistance of the penetration of the second cycle and so on. The fact that the cycles come in order in the resistance graph, together with the fact that the resistance is decreasing for each cycle, indicates that the penetrometer was driven through the same path as the previous cycles. If the order of cycles in the graph would have varied, i.e., if cycle 3 would have had higher resistance than cycle 4 for an arbitrary cyclic interval, it could have indicated that the penetration was not driven through the same path as the previous.

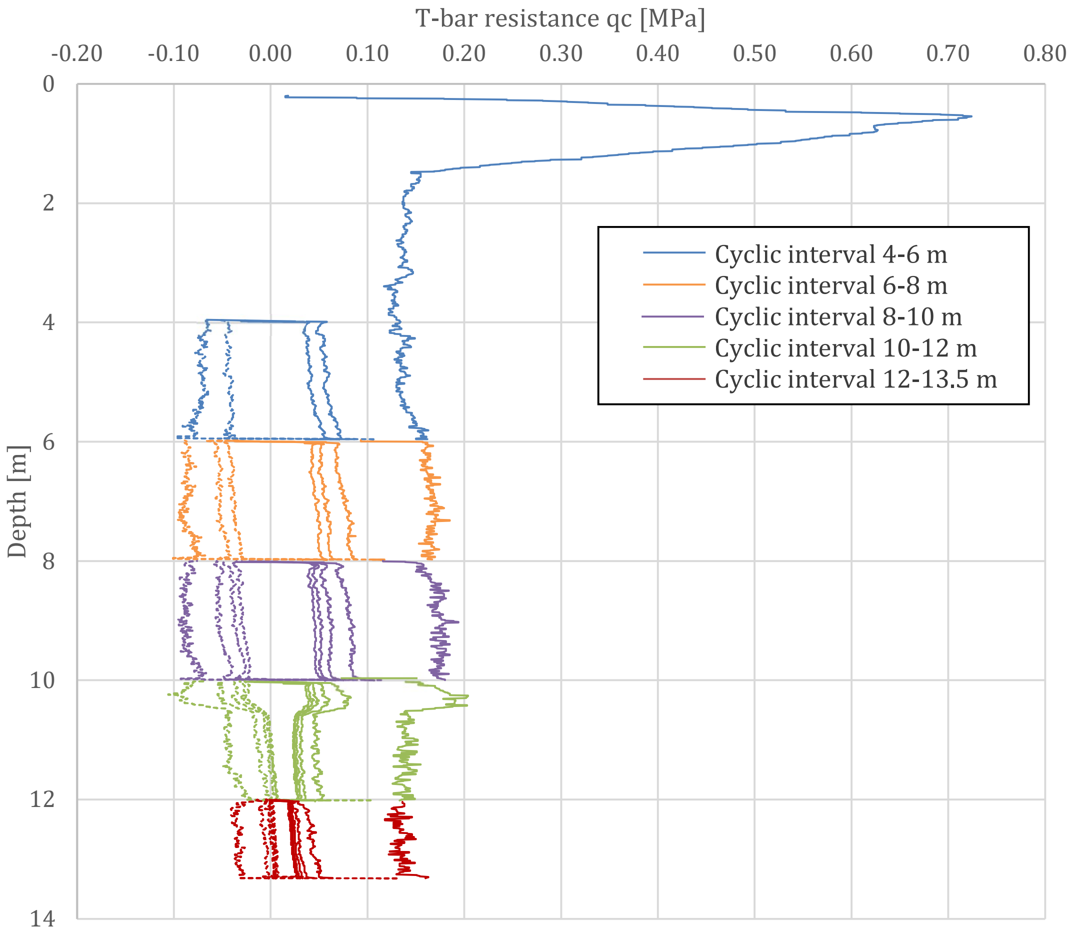

*Figure 28. Penetration and extraction resistance for TPTc in NC2204.*

### 7.3.1 Evaluated shear strength from TPTc

The evaluated shear strengths from the TPTc are plotted together with the shear strengths determined using the fall cone test at both the Chalmers and the Mitta laboratories (Figure 29). It is only the penetrations that are considered, not the extraction. The extraction of the T-bar is seen as further remoulding of the clay and the measured resistance from the extraction is not relevant for determination of shear strength. The shear strength from the first penetration (TPTc 1) is considered as undisturbed and is therefore compared with the undisturbed shear strength from the fall cone tests. As described in chapter 3 (section 3.3), the $N_T$ values from earlier studies ranged between 7.1-14.3. A $N_T$ factor of 10 was used in this analysis to represent the undisturbed shear strength from fall cone test. A $N_T$ factor of 12 generated a shear strength curve that corresponds better to the Chalmers laboratory values and a $N_T$ factor of 9 generates a shear strength curve that corresponds to Mitta's shear strength values to a greater extent. Even though the $N_T$ factors evaluated in earlier studies are based on the shear strength obtained from triaxial tests, direct simple shear tests and field vane shear tests, the $N_T$ factor used in this study to simulate the shear strength from fall cone test lies within the same range. For the purpose of determining the sensitivity of a clay, a lower $N_T$ factor is considered conservative since that will generate a higher undisturbed shear strength. Reasons for the differences in undisturbed shear strength between the two laboratories is discussed in section 7.4.

The shear strength from the last TPTc curve for each cyclic interval is the most remoulded shear strength at that specific interval. It is therefore reasonable to compare the shear strength obtained from the last TPTc penetration at each cyclic interval with the remoulded shear strength from the fall cone tests performed in the laboratories. The $N_{T.rem}$ factor was chosen to be 17 for evaluation of the shear strength for all cycles except for the first undisturbed cycle at all intervals. The $N_{T.rem}$ value is based on earlier studies where the evaluated factor ranges between 11.61-16.98 for remoulded shear strength evaluated from fall cone tests. The $N_{T.rem}$ value of 16.98 was obtained based on a clay sample with a sensitivity of 8.5, which was the highest sensitivity of the tested soil samples (Low et al., 2010). The laboratory results from the site investigated in this project, showed that the sensitivity is above 18 for all considered depths. At the lower depths where more cycles have remoulded the soil, the shear strength from the fall cone test and the evaluated shear strength from TPTc are more similar than in the upper part of the soil profile. A higher $N_{T.rem}$ factor will decrease the remoulded shear strength evaluated from the TPTc. The highest value of $N_{T.rem}$ mentioned in chapter 3 (section 3.3) was 32. The shear strength used in order to evaluate the $N_{T.rem}$ of 32 was obtained from an unconsolidated undrained triaxial test in compression on a clay sample with a sensitivity of 5.5 (Low et al., 2010). When using a $N_{T.rem}$ of 32 in this project, the remoulded shear strength from the TPTc is more in line with the results from the fall cone tests for 4-10 metres as well. However, since the clay between 4-10 metres may not be considered as totally remoulded, as high $N_{T.rem}$ for these depths are misleading. An increased $N_{T.rem}$, to about 25, will in the lower part of the profile generate shear strength that corresponds better to the fall cone results. It can be argued that this confirms the hypothesis that a higher $N_{T.rem}$ is needed for more sensitive soils, as was one of the conclusions in the report by Low et al., (2010). However, in this study only one borehole has been evaluated.

The shear strength evaluated from the TPTc is based on equation (14) where the $q_{t,T-bar}$ is evaluated according to equation (13). The $A_s/A_p$ term in the equation (13), which determines how much the vertical stress and hydrostatical pore pressure is affecting the corrected resistance, is 0.1. For the hydrostatical pore pressure, the term $(1-a)$ is also included. Which results in that it is 1.5% of the hydrostatical pore pressure that is affecting the corrected resistance and may be seen as negligible. Whereas 10% of the vertical stress is subtracted from the measured resistance. The vertical stress has low influence on the corrected resistance for the initial penetration when the measured resistance is high. But at lower depths and after multiple cycles, when the vertical stress is high and the measured resistance is low, the $A_s/A_p$ term has significant influence on the corrected resistance. Thereby also on the evaluated shear strength. The decrease in shear strength is therefore larger than the decrease in measured resistance between two consecutive cycles. Even if the measured resistance is showing some deviation in the measurement between the last cycles at a cyclic interval, the shear strength may not have as large variance as the measured resistance. However, since it is the measured resistance that can be seen on the field computer when performing the TPTc, it is still reasonable to continue the cycles until no further decrease in resistance is shown for a cyclic interval.

According to the laboratory results, both from Chalmers and from Mitta, quick clay is confirmed at 12 and 13.5 metres depth. It was no core samples recovered from between 10 to 12 metres depths. From Figure 29 it is visible that there is a gap in the remoulded shear strength at 12 metres depth. This indicated that there is no quick clay above 12 metres depth. However, there is a gap in shear strength at all points where a new cyclic level begins. It would be preferable to have recovered the core samples from the middle of each cyclic interval instead of in the transitions between the cycles to get better comparable results.

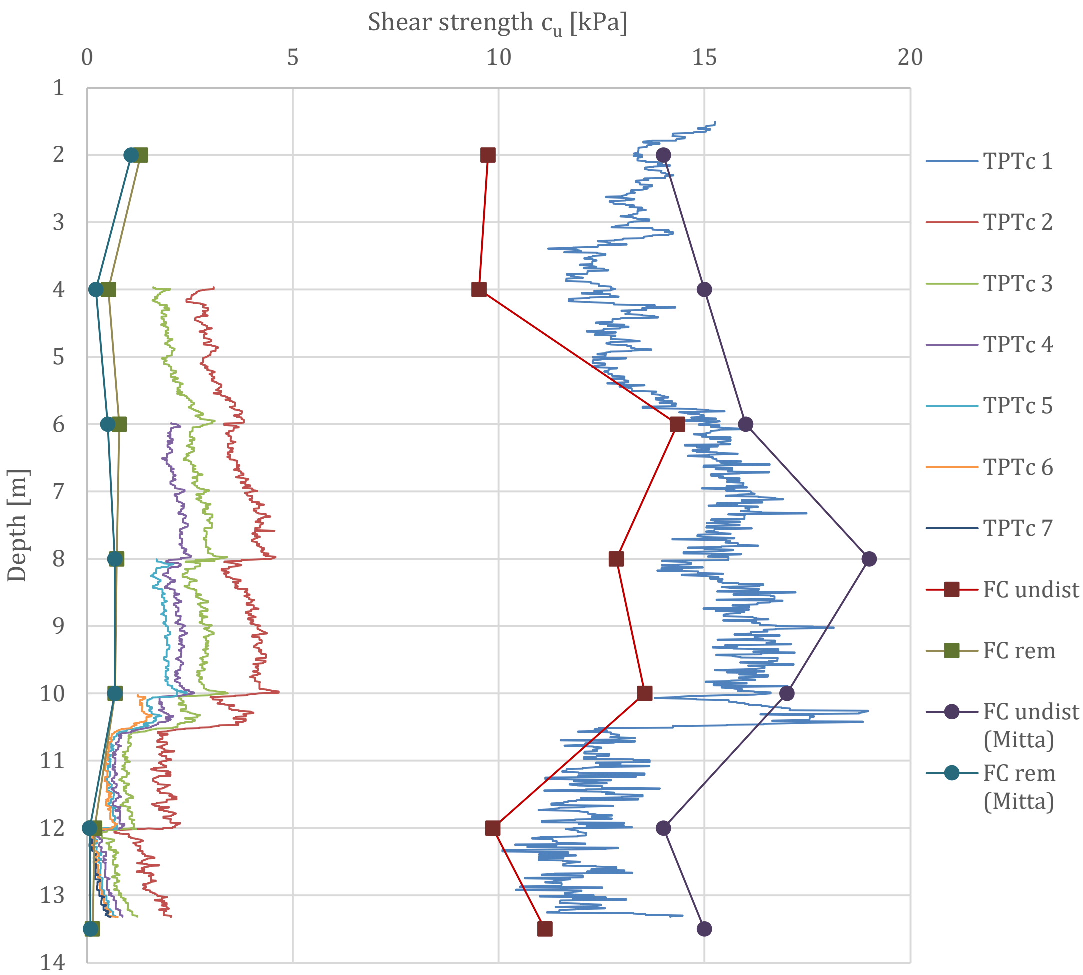


*Figure 29. Shear strength from TPTc and from fall cone test conducted at Chalmers and at Mitta.*

Figure 30 is presenting the remaining shear strength (in percentage) after each cycle, compared with the first cycle. The portion of shear strength that is left (for each cycle interval) is plotted against the number of penetrations. The remaining shear strength is calculated as the average shear strength for each cyclic interval divided by the initial average shear strength at each cyclic interval. The deviating values due to attaching additional rods has been removed in the graph.

At 10-12 and 12-13.5 metres depth, the remaining shear strength after the second penetration is 17% and 12% of the initial shear strength respectively. While for 4-6, 6-8 and 8-10 metres depth interval, the remaining shear strength is about 25% of the initial shear strength. Meaning that the soil below 12 metres depth loses more of its shear strength between the first and second penetration than the soil in the upper part of the profile. Besides the varying loss of shear strength between the initial and the second penetration, the inclination of the curves differs. The curves representing the intervals 6-8 and 8-10 metres are more or less identical and the soil in this interval loses equal amount of shear strength between the penetrations and may be assumed to have the same characteristics. The curves representing 8-10 metre is not as steep as the curves representing 10-12 and 12-13.5 metres. This is indicating that the soil between 6-10 metres and the soil between 10-13.5 metres have different characteristics. The soil between 6-10 metres loses more of its strength between penetration 3-4 and 4-5 compared to the soil below 10 metres. It could be argued that it takes more energy to remould the clay in the upper part of the profile compared to what it takes to remould the soil below 12 metres depth.

It is visible that none of the intervals have been fully remoulded since the curves are not completely vertical. However, the decrease in shear strength is very small for the last penetrations for both the 10-12 and the 12-13.5 metres interval. The change between the last and second last penetration for the depth 12-13.5 metres is 0.46 percentage points. With a $N_{T.rem}$ factor of 25, which was discussed earlier, the change between the last and second last penetration is 0.36 percentage points. Meaning that the clay gets closer to be considered as fully remoulded.

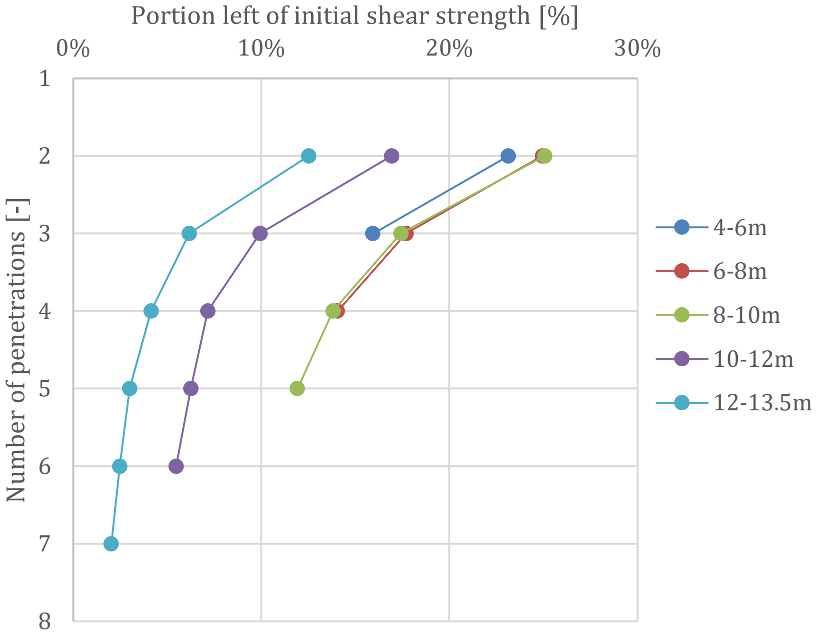


*Figure 30. Shear strength for TPTc per penetration cycle compared with the first penetration.*

Even if the shape of the curves in Figure 30 are not completely identical, the trends are almost similar. If a weighted assessment is made with respect to the trend of all curves combined, the remaining shear strength after seven penetrations can be predicted for all cyclic intervals. The predicted remaining shear strength can in turn be used to evaluate the shear strength after seven penetrations for all penetration interval, using the initial shear strength. A combined assessment was made and the predicted shear strength after seven penetrations was plotted for all cyclic intervals (found in Appendix C, Figure C2). It was found that the shear strength was closer to the laboratory results even for the depth between 4-10 meters, but not to a completely desirable extent. More cycles are required for all cyclic intervals to reach a remoulded state, especially for the depths between 4-10 metres. If more cycles were made, the predicted shear strength would most probably coincide with the remoulded shear strength evaluated in the laboratories to a greater extent. However, it is uncertain whether a remoulded state corresponding to that which can be reached in the laboratory can be reached using TPTc. One should keep in mind that in this study, only one borehole has been analysed and the number of penetrations is specific for this study and borehole.

To repeat the TPTc until there are no visible gaps in the resistance graph is very time consuming in practice. With further studies performing TPTc with a large number of cycles per interval, it might be possible to create empirical curves/relations describing the loss or remaining shear strength after a certain number of cycles, similar to the curves in Figure 30. Then only two or three cycles are needed for each interval to get the starting value and the empirical curve/relation can be used to generate a curve for each interval. The remoulded shear strength can be calculated based of the remaining portion of the initial shear strength obtained where the curve no longer changes in inclination. The various need of energy required to remould clay with different characteristics may be a source of error.

If the clay is quick, it may be of interest to know how much energy that is required for the clay to lose its shear strength. A clay that is quick but requires a lot of energy to lose its shear strength may not be considered as dangerous as a quick clay that loses its shear strength using less energy. The penetration rate shall be kept constant at 20 mm/s. Meaning that the force is varying when a constant velocity is maintained, dependent on the resistance of the clay. It may be possible to use this relation to evaluate the energy that is required to remould the clay to an extent where the loss of shear strength is critical.

## 7.4 Laboratory results

The laboratory results from the Mitta laboratory states that the soil profile to a varying degree consists of gyttja-like silty clay with some plant and shell residues. In the borehole NC2205 plenty of shells at 4 and 5 metres depth were observed. This had the effect that the fall cone test could not easily be performed with good results. The results show that from the tests performed at Chalmers laboratory, quick clay is per the Swedish definition confirmed at 12 and 13.5 metres depth in the borehole NC2204. Mitta's results showed the same, but they also obtained quick clay at 4 metres depth in NC2204. The Norwegian definition states that it is quick clay if the remoulded shear strength is below 0.5 kPa. Then there is quick clay at 6 metres depth in NC2204 and at 3 and 4 metres depth in NC2205. Regardless, the remoulded shear strength is low in many levels which would mean that care has to be taken in practical work preceding construction.

The density, natural water content and liquid limit matched well between the two laboratories for all three boreholes. The undisturbed and remoulded shear strength on the other hand did not correspond as good. The undisturbed shear strength was higher for all boreholes and depths from the tests conducted at Mitta. While the remoulded shear strength was lower for all boreholes and depths from the tests conducted at Mitta. This generates higher sensitivity for all examined points for the results from Mitta compared with the results from Chalmers. There could be several reasons why the results differ between the laboratories. The middle tube was tested at Chalmers and the lower tube was tested at Mitta and there could be natural variations in the samples. The samples were treated and stored in the same box in field and transported from the testing site to the place for storage in field where they were sorted depending on testing location. The transportation from the field storage to the two different laboratories was done on separate days. The transportation routes differed and one or the other may had more speed bumps, sharp curves or other traffic situations that could have disturbed the samples. One major difference is that the testing at Chalmers was conducted 2-9 days after sampling while the testing at Mitta took place 15-22 days after sampling. A consequence of the laboratory testing taking place later at the Mitta laboratory could be that an increase in shear strength possibly could have occurred (Persson, personal communication, June 3, 2022). This could possibly explain the higher undisturbed shear strength evaluated at the Mitta laboratory. Although both laboratories have worked according to the standard, small differences in equipment or differences in the experience of the staff may affect the results. The authors of this report, who performed the testing at Chalmers with supervision from the laboratory staff, did the tests for the first time. Unexperienced people that have never performed the tests before will probably read and follow the regulating standards carefully. At the same time, small but important details could possibly be missed when having no experience in the field. People who have done the tests many times before, have good routine on the procedures but may do several things at once, small mistakes could therefore possibly be made. The choice of cone (angle and weight) may affect the results. Since the shear strength from fall cone tests is determined by the empirical relation explained by equation (15) where $c$ is a constant depending on the cone angle, the choice of cone can affect the result. A preferable cone to use for the very soft remoulded clay would be a wider and lighter cone than the 60° and 60 g cone that was used at Chalmers. Most likely, Mitta used a more suitable cone for the very soft remoulded clay samples, which then gives more trustworthy results for the remoulded shear strength. As a comparison to the shear strength evaluated from the field methods, the results from both laboratories will be presented as reference values.

## 7.5 PCA including non-quick and quick clay

The correlation between the analysed parameters from a depth of 5 metre and downward is presented in Table 4. The colour coding of the correlation matrix is based on the absolute values, and the definitions can be found in Table 5. There is a relatively strong correlation between the parameters measured from CPTu, especially between the measured pore pressure and the cone resistance. High correlation between the measured pore pressure and cone resistance was expected based on the visual judgment from the CPTu results. There is relatively strong correlation between the density and the liquid limit. When the liquid limit decreases, the density increases. It could be argued that the sensitivity and the remoulded shear strength should have stronger correlation since the remoulded shear strength is used when calculating the sensitivity. The accuracy when determining the shear strength of remoulded samples with fall cone test is however considered to be low for highly sensitive clays. Because in some cases the remoulded soil sample may be too fluid to be used in the fall cone test. This will have the effect that the fall cone apparatus is determining an inaccurate and oftentimes too low remoulded shear strength. The accuracy is at the same time often higher when determining the undisturbed shear strength (Persson, personal communication, Mars 16, 2022). This difference in accuracy will in some cases yield sensitivities that are very high. This could possibly explain why the correlation between the sensitivity and the remoulded shear strength was lower than expected.

*Table 4. Correlation matrix generated from IBM SPSS for all depth from 5 m.*

| Parameters | $S_t$ | $c_{urfc}$ | $w_L$ | ρ | $q_t$ | $f_s$ | $u_2$ |
|---|---|---|---|---|---|---|---|
| $S_t$ | 1 | -0.449 | -0.374 | 0.028 | 0.186 | 0.079 | 0.221 |
| $c_{urfc}$ | -0.449 | 1 | 0.332 | 0.194 | 0.375 | 0.445 | 0.357 |
| $w_L$ | -0.374 | 0.332 | 1 | -0.646 | -0.237 | -0.007 | -0.202 |
| ρ | 0.028 | 0.164 | -0.646 | 1 | 0.497 | 0.274 | 0.461 |
| $q_t$ | 0.186 | 0.375 | -0.237 | 0.497 | 1 | 0.636 | 0.974 |
| $f_s$ | 0.079 | 0.445 | -0.007 | 0.279 | 0.636 | 1 | 0.636 |
| $u_2$ | 0.221 | 0.357 | -0.202 | 0.461 | 0.974 | 0.636 | 1 |

*Table 5. Colour coding for the correlation matrix.*

| | |
|---|---|
| 0.9-0.999 | |
| 0.8-0.899 | |
| 0.7-0.799 | |
| 0.6-0.699 | |
| 0.5-0.599 | |
| 0.4-0.499 | |
| 0.3-0.399 | |
| 0.0-0.299 | |

The principal components generated from IBM SPSS for the dataset with all depth from 5 m and downward is presented in Table 6. The table also presents the eigenvalues for the principal components and how much of the variance in the dataset each of the principal components accounts for as well as the cumulative variance. In this analysis, the first three principal components were selected to be analysed further. The first three principal components have eigenvalues larger than 1 and accounts for 86% of the variance in the dataset.

*Table 6. Generated principal components and their eigenvalues and total variance from IBM SPSS.*

| Principal component | Eigenvalue | % of variance | Cumulative % |
|---|---|---|---|
| 1 | 3.125 | 44.643 | 44.643 |
| 2 | 1.875 | 26.790 | 71.433 |
| 3 | 1.050 | 15.002 | 86.436 |
| 4 | 0.426 | 6.090 | 92.526 |
| 5 | 0.322 | 4.600 | 97.126 |
| 6 | 0.177 | 2.532 | 99.658 |
| 7 | 0.024 | 0.342 | 100.00 |

With the three principal components extracted, Table 7 describes the communalities between the principal components and the original dataset. In the table, it can be seen that the three chosen principal components combined describes 87.5% of the sensitivity values in the original dataset. A low value of the extracted communality indicates that a parameter is not suitable for the analysis. It is evident that the extracted components and the original dataset have great communalities.

*Table 7. Communalities of the extracted principal components and the original data from IBM SPSS.*

| Parameters | Extraction [%] |
|---|---|
| $S_t$ | 87.5 |
| $c_{urfc}$ | 82.8 |
| $w_L$ | 90.8 |
| ρ | 91.4 |
| $q_t$ | 91.2 |
| $f_s$ | 70.5 |
| $u_2$ | 90.9 |

The absolute value of the loadings of the parameters associated with each principal component is presented in Figure 31. The cone resistance, sleeve friction, measured pore pressure and to some extent the density are the key parameters for component 1. According to Table 6, component 1 explains roughly 45% of the variance in the dataset. The sensitivity, the remoulded shear strength and the liquid limit are mostly associated with component 2 which account for roughly 27% of the variance in the dataset. The sensitivity and density are also associated with component 3 and component 3 accounts for 15% of the variance. Prior to the analysis, a desired scenario was that the sensitivity or remoulded shear strength together with more than one parameter from the CPTu soundings, were to be associated with the same principal component. Preferably a component that accounts for the majority of the variation in the dataset. Had this been the case, further investigations of that relation would potentially result in useful findings when mapping quick or highly sensitive clays. However, the fact that no clear relation between the field measurements and the sensitivity or the remoulded shear strength were found was not entirely unexpected. A possible explanation to the low correlation between the parameters collected from laboratory results and from CPTu soundings could be linked to local geological differences. Local differences in the sedimentation environment will affect the properties of the clay and may vary within the region.

A source of error when collecting the data to the PCA is that the values retrieved from the CPTu results is the measured values at specific depths based on where the core samples had been recovered. Significant variations in the CPTu measurements near such a depth may thus have led to a non-representative choice of value.

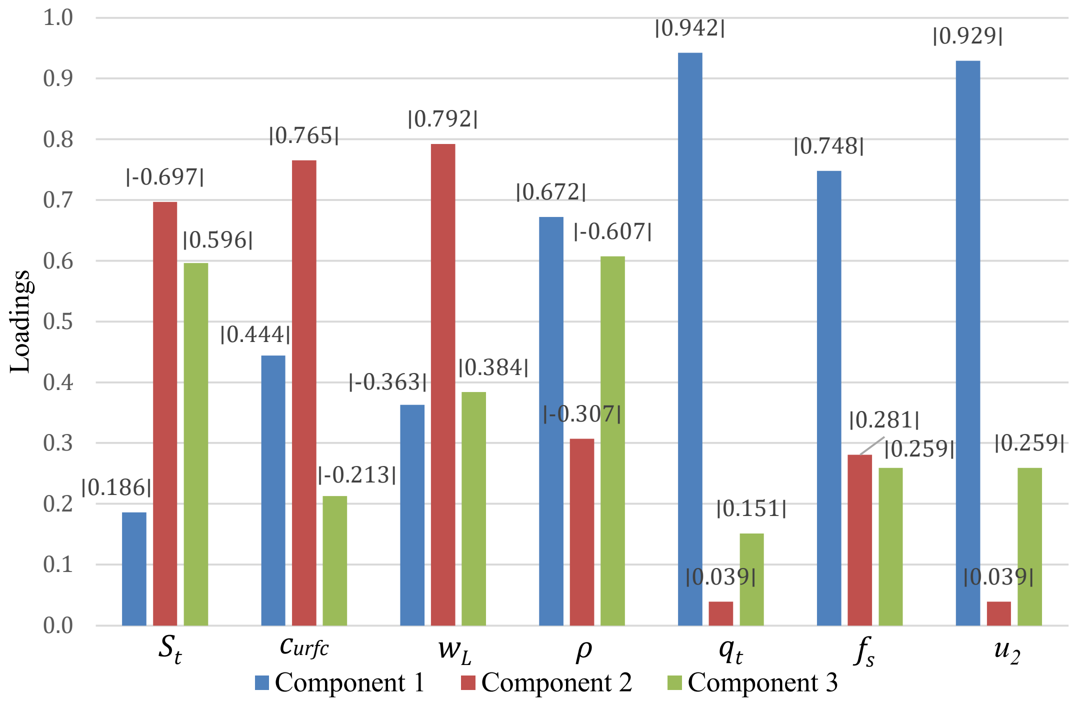


*Figure 31. Absolute values of the loadings.*

## 7.6 PCA including only quick clay

The correlation matrix for the depths where quick clay is confirmed i.e., the sensitivity is greater than 50 and the remoulded shear strength is lower than 0.4 kPa, is presented in Table 8. There is a significant difference between the correlation matrix for the depths where quick clay is confirmed and the correlation matrix including all depths shown in Table 4. The major difference is that sensitivity has increased correlation with the parameters from the field measurement, especially the measured pore pressure and the cone resistance. The absolute value of the correlation between the sensitivity and the remoulded shear strength has also increased compared to Table 4.

*Table 8. Correlation matrix generated from IBM SPSS for depth with quick clay.*

| Parameter | $S_t$ | $c_{urfc}$ | $w_L$ | ρ | $q_t$ | $f_s$ | $u_2$ |
|---|---|---|---|---|---|---|---|
| $S_t$ | 1 | -0.639 | -0.286 | 0.182 | 0.655 | 0.488 | 0.702 |
| $c_{urfc}$ | -0.639 | 1 | 0.155 | 0.029 | -0.054 | -0.043 | -0.121 |
| $w_L$ | -0.286 | 0.155 | 1 | -0.766 | -0.401 | -0.145 | -0.372 |
| ρ | 0.182 | 0.029 | -0.766 | 1 | 0.425 | 0.231 | 0.366 |
| $q_t$ | 0.655 | -0.054 | -0.401 | 0.425 | 1 | 0.615 | 0.978 |
| $f_s$ | 0.488 | -0.043 | -0.145 | 0.231 | 0.615 | 1 | 0.647 |
| $u_2$ | 0.702 | -0.121 | -0.372 | 0.366 | 0.978 | 0.647 | 1 |

In conformity with the analysis performed for all depths, it is the first three principal components that is used for further analysis. In Table 9 it can be seen that their eigenvalues are larger than 1 and that they account for 89% of the variance in the dataset.

*Table 9. Generated principal components and their eigenvalues and total variance for only quick clay from IBM SPSS.*

| Principal component | Eigenvalue | % of variance | Cumulative % |
|---|---|---|---|
| 1 | 3.570 | 51.006 | 51.006 |
| 2 | 1.439 | 20.560 | 71.566 |
| 3 | 1.196 | 17.092 | 88.658 |
| 4 | 0.453 | 6.477 | 95.135 |
| 5 | 0.206 | 2.945 | 98.080 |
| 6 | 0.118 | 1.680 | 99.760 |
| 7 | 0.017 | 0.240 | 100.00 |

Figure 32 is showing the absolute values of the loadings between the parameters and the principal components for the depths where quick clay is confirmed. Several parameters are less clearly associated with one specific component than what was the case in Figure 31. However, the cone resistance, measured pore pressure and sensitivity are the key parameters associated with component 1. Component 1 accounts for 51% of the variance in the dataset. Since the cone resistance and the measured pore pressure has such a strong correlation, it is expected that those parameters are associated with the same component and might be a reason for component 1 explaining the majority of the variance. When quick clay is confirmed, there is a correlation between sensitivity and CPTu measurement results. Both the correlation matrix and the loadings indicate the same trend when combining fall cone results and CPTu measurements. However, since this analysis is based on the fact that quick clay is confirmed, it is difficult to come to any conclusions if those relations can facilitate mapping of quick clay.

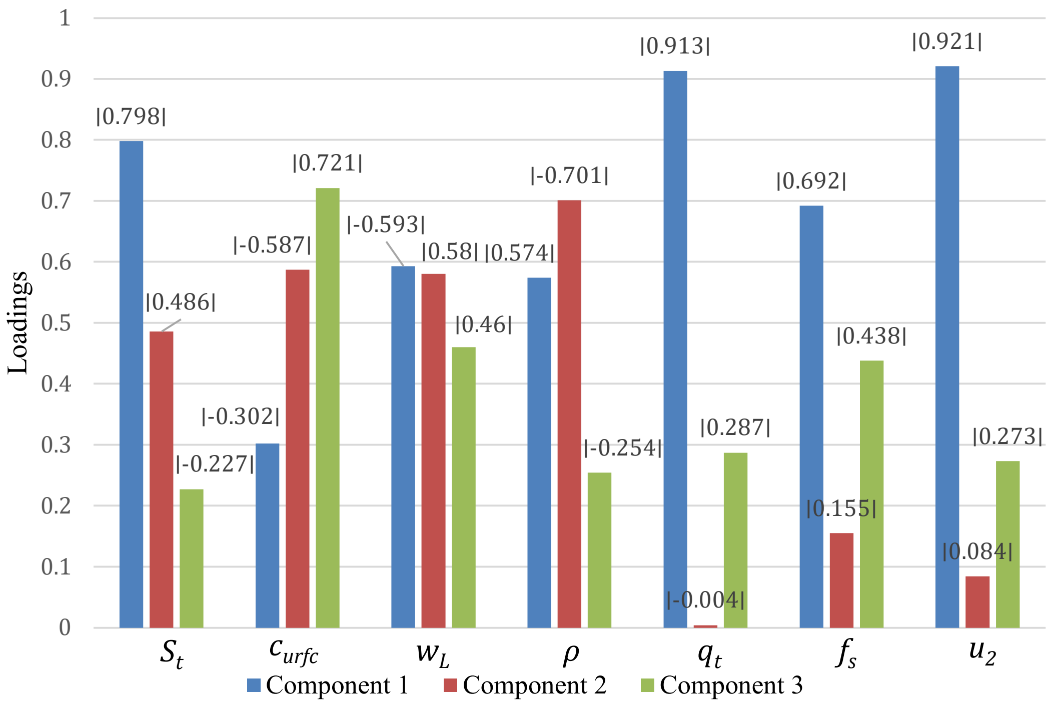


*Figure 32. Absolute values for the loadings for only quick clay.*

## 7.7 Distance to a draining layer

The relation between the remoulded shear strength and the distance to a draining layer is presented in Figure 33. The depths with a distance of below one metre from a draining layer has been excluded from the analysis. The lower values of the remoulded shear strengths (<0.4 kPa) are all closer than 13 metres from a draining layer and the majority is below 10 metres. At longer distances from a draining layer, higher remoulded shear strength is observed. However, high values of the remoulded shear strengths were also observed at distances very close to an assumed draining layer. A correlation between the distance to a draining layer and the remoulded shear strength therefore could not be found in this analysis. There might however be a relation between the distance to a draining layer and a low remoulded shear strength, but the used method (identifying draining layers based on CPTu results) did not confirm the hypothesis. One contributing reason for that is assumed to be linked to difficulties in identifying draining layers using CPTu data. The low correlation could be explained by that the local differences in the geology at the sites tested were neglected. In the method adopted a defined draining layer could for example either be of high or low hydraulic conductivity. The method is not taking into consideration the hydraulic conductivity neither in the draining layer nor in the surrounding soil. As mentioned in chapter 2 (section 2.2) the ion composition of the infiltrating water is crucial for the leaching effect. Hence, one cannot argue that all water flowing in a draining layer has a leaching effect on the clay. Furthermore, the CPTu is a one dimensional evaluating method. Therefore, only the potentially draining layers in the vertical direction is taken into consideration. What happens in the horizontal plane cannot be evaluated based on CPTu.

Another possible reason to the non-correlative response could also be that no clear correlation exists. That could in turn possibly be explained by a phenomenon called restabilisation. Restabilisation is the process in a clay sediment where the clay goes from being quick to not being quick. Restabilisation of clay could occur as a consequence of change in ion composition in the pore water (Suer et al., 2014). This change in ion composition could be caused by weathering of minerals in the clay particles occurring in the clay sediment near the ground surface. Positive ions previously bonded to the negatively charged clay particles could then be released into the pore water and increase the concentration of such ions (Rankka et al., 2004). If a draining layer is directly connected to infiltrating water originating from the ground surface, restabilisation of quick clay could occur depending on the ion composition. In Moum et al., (1971, 1972) the process of restabilisation has been examined in a project site near Drammen in Norway. On the site, quick clay was only found in the central parts of the studied clay deposit. The explanation for that given by the authors was that the clay most likely had been quick in the lower lying parts of the deposit located closer to a more permeable soil. But had been restabilised through release of $Mg^{2+}$ and $K^{+}$ ions into the pore water caused by mineral weathering of the clay particles occurring in the clay sediment near the ground surface.

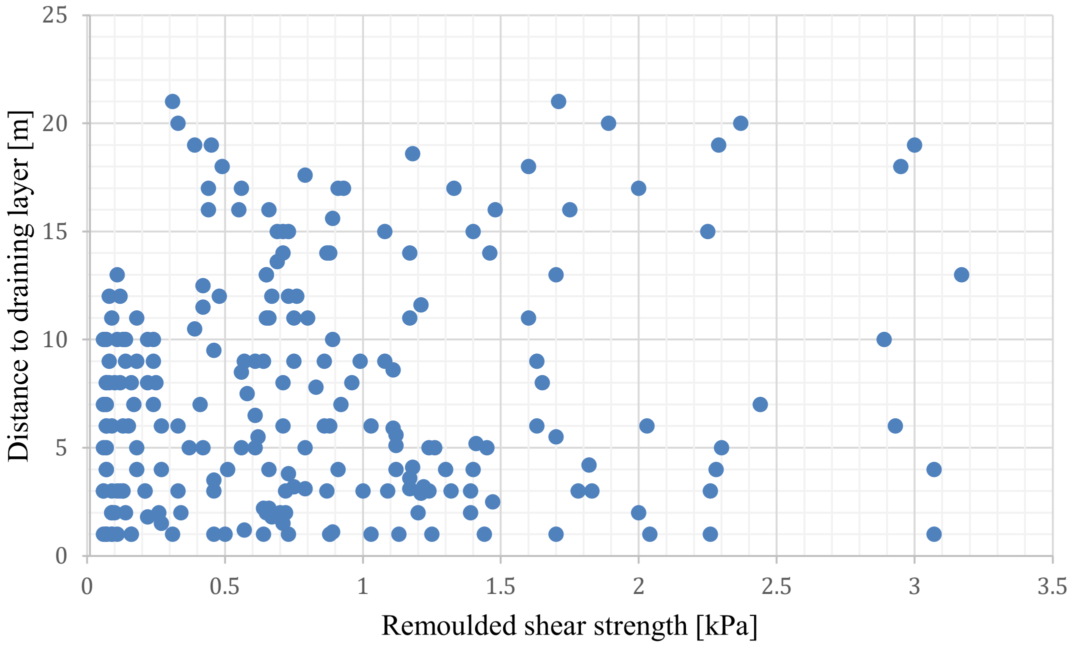


*Figure 33. Relation between the remoulded shear strength and the distance to a draining layer.*

# 8 Conclusions – Recommendations

When performing the multiple CPTu soundings in the exact same positions it was found that all evaluated parameters in general is decreasing as more soundings are performed. If the method were to be used in larger scale as a method for evaluating the remoulded shear strength directly in field, several uncertainties and sources of errors can be addressed. One major uncertainty with the method is to assess whether the penetrometer is following the same path made by the preceding sounding. It is therefore difficult to tell if the parameters are registered in a remoulded soil or not. Another uncertainty is whether it is possible for the consecutive soundings to remould the clay enough so that a fully remoulded state is reached. In order to determine the remoulded shear strength from CPTu soundings performed in remoulded clay, a revision of the empirical relation is furthermore recommended to be developed.

The TPTc showed useful results for evaluation of the shear strength. Foremost for the undisturbed shear strength where the results when using correction factors from earlier studies, corresponded well to the laboratory results. The remoulded shear strength evaluated from cyclic intervals where many cycles was performed, showed results in line with the laboratory results. It is therefore recommended to continue the cycles until no further decrease in measured penetration resistance is shown, to evaluate more reliable results of the remoulded shear strength. Furter studies of correction factors for remoulded shear strength in soft soil may as well be required in order to achieve more correct results of the remoulded shear strength from TPTc. The loss in shear strength between the cycles indicated that the TPTc can be used for remoulding of soft soil in field. The probability is shown to be high that the T-bar penetrometer is driven through the same path as the previous.

The statistical analysis using PCA, showed no clear relations between the parameters collected from laboratory results and parameters collected from the CPTu results. In the analysis where only sampling depths where quick clay had been confirmed was included, a correlation between the sensitivity and CPTu parameters were found. However, since this analysis was based on the fact that quick clay was confirmed, the relation cannot be used to facilitate the mapping of quick clay. The statistical analysis assessing the impact the distance to a draining layer has on an arbitrary point in a clay deposit, did not yield a strong correlation with the corresponding remoulded shear strength. Reasons for the lack of correlation could possibly be explained by difficulties with identifying draining layers using CPTu data. Another explanation may be that it is not possible to find any regional correlations using this method.

Of the three methods tested, it was concluded that the TPTc has best potential to facilitate mapping of quick clay without relying on the evaluation of undisturbed soil samples. The TPTc as a method is preferred before the multiple CPTu soundings primarily because of the fewer sources of errors linked to the execution of the method. It is however recommended to perform the two field geotechnical methods at several locations and in different geological conditions, for further evaluation of the utility of the methods. An interesting aspect to note from the results of the undisturbed and remoulded shear strength evaluated in the two laboratories is that the results differed when compared to each other. This demonstrates that even though uncertainties for determining the shear strength from geotechnical field methods exists, uncertainties in the laboratory evaluation are to some extent present too.

# 9 References


Abdi, H., & Williams, L. J. (2010). Principal component analysis. *Wiley Interdisciplinary Reviews: Computational Statistics*, *2*(4), 433–459. https://doi.org/10.1002/wics.101

Bergh, I., & Rengemo, H. (2021). *Förstudie Åseberget*. Kungälvs kommun. https://www.kungalv.se/siteassets/dokument/bygga-och-bo/dokument/planer-och-byggprojekt/aseberget-forstudie/forstudie-aseberget-ks2021_0772-2.pdf

Bergström, U., Pile, O., Curtis, P., & Eliasson, T. (2022). *Göteborgsområdets berggrund, jordarter och geologiska utveckling*. (SGU-rapport 2021:31) Geological Survey of Sweden. https://resource.sgu.se/dokument/publikation/sgurapport/sgurapport202131rapport/s2131-rapport.pdf

Bro, R., & Smilde, A. K. (2014). Principal component analysis. *Anal. Methods*, *6*(9), 2812–2831. https://doi.org/10.1039/C3AY41907J

Craig, R. F., & Knappet, J. A. (2012). Craig's Soil Mechanics. (8th edition). Spon Press.

Google maps. (n.d.). *[Google maps showing the area around Åseberget]*. Retrieved April 25, 2022, from https://www.google.no/maps/@57.8772002,11.9555457,816m/data=!3m1!1e3?hl=se

Hansbo, S. (1957). *A new approach to the determination of the shear strength of clay by the fall-cone test*. (No. 14) Royal Swedish Geotechnical Institute. Stockholm.

Hov, S., Prästings, A., Persson, E., & Larsson, S. (2021). On Empirical Correlations for Normalised Shear Strengths from Fall Cone and Direct Simple Shear Tests in Soft Swedish Clays. *Geotechnical and Geological Engineering*, *39*(7), 4843–4854. https://doi.org/10.1007/s10706-021-01797-w

Jannuzzi, G. M. F., Danziger, F. A. B., Martins, I. S. M., & Lunne, T. (2021). Penetration and retrieval forces during sampling in a very soft clay. *Soils and Foundations*, *61*(2), 303–317. https://doi.org/10.1016/j.sandf.2020.09.012

Karlsrud, K., Lunne, T., & Brattlien, K. (1997). *Improved CPTU interpretations based on block samples*. Norwegian Geotechnical Institute. Oslo.

Karlsrud, K., Lunne, T., & Strandvik, S. O. (2005). CPTU correlations for clays. *Proceedings of the International Conference on Soil Mechanics and Geotechnical Engineering.*, 693–702. https://doi.org/10.3233/978-1-61499-656-9-693

Larsson, R. (2008). *Jords egenskaper* (Issue 5). Swedish Geotechnical Institute. Linköping. https://www.sgi.se/globalassets/publikationer/info/pdf/sgi-i1.pdf

Larsson, R., & Sällfors, G. (1995). *Sättningsegenskaper i lös lera på grund av geologisk avsättning och "åldring."* Swedish Geotechnical Institute. Linköping.

Larsson, R., Sällfors, G., Bengtsson, P.-E., Alén, C., Bergdahl, U., & Eriksson, L. (2007). *Skjuvhållfasthet -utvärdering i kohesionsjord*. Swedish Geotechnical Institute. Linköping.

Löfroth, H., Suer, P., Dahlin, T., Leroux, V., & Schälin, D. (2011). *Quick clay mapping by resistivity-Surface resistivity, CPTU-R and chemistry to complement other geotechnical sounding and sampling*. (GÄU - Delrapport 30) Swedish Geotechnical Institute. Linköping. https://www.researchgate.net/publication/239794128

Low, H. E., Lunne, T., Andersen, K. H., Sjursen, M. A., Li, X., & Randolph, M. F. (2010). Estimation of intact and remoulded undrained shear strengths from penetration tests in soft clays. *Géotechnique*, *60*(11), 843–859. https://doi.org/10.1680/geot.9.P.017

Lundström, K., Larsson, R., & Dahlin, T. (2009). Mapping of quick clay formations using geotechnical and geophysical methods. *Landslides*, *6*(1), 1–15. https://doi.org/10.1007/s10346-009-0144-9

Lunne, T., Randolph, M. F., Chung, S. F., Andersen, K. H., & Sjursen, M. (2005). Comparison of cone and T-bar factors in two onshore and one offshore clay sediments. In M. J. Cassidy, & S. Gourvenec (Eds.),. *Proceedings of the International Symposium on Frontiers in Offshore Geotechnics (Perth, Australia*, *n/a*, 981-989). CRC Press/Balkema.

Lunne, T., Robertson, P. K., & Powell, J. J. M. (1997). *Cone Penetration Testing in Geotechnical Practice*. E & FN Spon. Abingdon.

Möller, B., & Bergdahl, U. (1982). *Estimation of the sensitivity of soft clays from static and weight sounding tests* (1st Edition). Taylor & Francis Group. Amsterdam.

Moum, J., Löken, K., & Torrance, J. K. (1972). Discussion: A geochemical investigation of the sensitivity of a normally consolidated clay from Drammen, Norway. *Géotechnique*, *22*(4), 675–676. https://doi.org/10.1680/geot.1972.22.4.675

Moum, J., Løken, T., & Torrance, J. K. (1971). A Geochemical Investigation of The Sensitivity of a Normally Consolidated Clay From Drammen, Norway. *Géotechnique*, *21*(4), 329–340. https://doi.org/10.1680/geot.1971.21.4.329

MSB. (2009). *Analys av samhällsekonomisk kostnad - Skredet vid E6 i Småröd, 2006*. Swedish Civil Continguencies Agency. Karlstad.

Nakamura, A., Tanaka, H., & Fukasawa, T. (2009). Applicability of T-bar and ball penetration tests to soft clayey grounds. In *Soils and Foundations* (Vol. 49, Issue 5, pp. 729–738). Japanese Geotechnical Society. https://doi.org/https://doi.org/10.3208/sandf.49.729

NGS. (2011). *Veiledning for symboler og definisjoner i geoteknikk, identifisering og klassifisering av jord* (Vol. 2). Norwegian Geotechnical Society. http://www.ngf.no/

Randolph, M. F. (2004). *Characterisation of soft sediments for offshore application* (pp. 209–232). Millpress. Rotterdam.

Rankka, K., Andersson-Sköld, Y., Hulten, C., Larsson, R., Leroux, V., & Torleif, D. (2004). *Quick clay in Sweden*. Swedish Geotechnical Institute. Linköpng.

Ringnér, M. (2008). What is principal component analysis? In *NATURE BIOTECHNOLOGY* (Vol. 26). http://www.nature.com/naturebiotechnology

SGF. (2009). Metodbeskrivning för provtagning med standardprovtagare - Ostörd provtagning i finkornig jord. In *Rapport 1:2009*. Swedish Geotechnical Society. Linköping.

SGF. (2013). Geoteknisk fälthandbok. In *Rapport 1:2013* (Issue 1). Swedish Geotechnical Society. Gothenburg.

SGF, & BGS. (2001). System of notations: for geotechnical investigations. In *Version 2001:2*. Swedish Geotechnical Society & Society of Engineering Geology. http://www.sgf.net/web/page.aspx?refid=2674

SGI. (n.d.). *Geotechnical archive*. Retrieved March 10, 2022, from https://bga.sgi.se

SGI. (1961). *Standard Piston Sampling - A report by the Swedish Committee on Piston Sampling* (Vol. 19). Swedish Geotechnical Institute. Stockholm.

SGI. (2012). Landslide risks in the Göta River valley in a changing climate. In *Final report: Part 2 - Mapping*. Swedish Geotechnical Institute. Linköping. www.swedgeo.se

SGI. (2018). Metodik för kartläggning av kvicklera, Vägledning. In *SGI Publication 46*. Swedish Geotechnical Institute. Linköping.

SGU. (n.d.). *Jordarter 1:25 000 - 1:100 000*. Geological Survey of Sweden. Retrieved April 5, 2022, from https://apps.sgu.se/kartvisare/kartvisare-jordarter-25-100.html

SIS. (2012). *Geotechnical investigation and testing-Field testing-Part 1: Electrical cone and piezocone penetration test*. (SS-EN ISO 22476-1:2012). Swedish Institute for Standards. https://www.sis.se/produkter/anlaggningsarbete/markarbete-utgravning-grundlaggning-arbete-under-jord/sseniso2247612012/

SIS. (2014). *Geotechnical investigation and testing – Laboratory testing of soil – Part 1: Determination of water content*. (SS-EN ISO 17892-1:2014). Swedish Institute for Standards. https://www.sis.se/produkter/miljo-och-halsoskydd-sakerhet/jordkvalitet-pedologi/fysiska-egenskaper-hos-jord/iso1789212014/

SIS. (2017). *Geotechnical investigation and testing– Laboratory testing of soil ± Part 6: Fall cone test*. (SS-EN ISO 17892-6:2017). Swedish Institute for Standards. https://www.sis.se/produkter/miljo-och-halsoskydd-sakerhet/jordkvalitet-pedologi/fysiska-egenskaper-hos-jord/sseniso1789262017/

SIS. (2018). *Geotechnical investigation and testing-Laboratory testing of soil-Part 12: Determination of liquid and plastic limits*. (SS-EN ISO 17892-12:2018). Swedish Institute for Standards. https://www.sis.se/produkter/miljo-och-halsoskydd-sakerhet/jordkvalitet-pedologi/fysiska-egenskaper-hos-jord/ss-en-iso-17892-122018/

Solberg, I.-L., Hansen, L., Rønning, J. S., & Dalsegg, E. (2011). *Veileder for bruk av resistivitetsmålinger i potensielle kvikkleireområder*. Norges Geotekniske Undersøkelse (NGU). Publication nr: 2010.048. Trondheim.

Stevens, R., Hellgren, L.-G., & Häger, K.-O. (1984). Depositional Environments and General Stratigraphy of Clay Sequences in South Western Sweden. In *Glaciomorine Fine Sediments in Southwestern Sweden: Vol. A 54* (pp. 13–18).

Stewart, D. P., & Randolph, M. F. (1994). T-Bar Penetration Testing in Soft Clay. *Journal of Geotechnical Engineering*, *120*(12), 2230–2235. https://doi.org/10.1061/(ASCE)0733-9410(1994)120:12(2230)

Suer, P., Löfroth, H., & Andersson-Sköld, Y. (2014). Ion Exchange as a Cause of Natural Restabilisation of Quick Clay – A Model Study. In J.-S. L'Heureux, A. Locat, S. Leroueil, D. Demers, & J. Locat (Eds.), *Landslides in Sensitive Clays - From Geosciences to Risk Management: Vol. Volume 36* (pp. 51–62). Springer. https://doi.org/10.1007/978-94-007-7079-9_5

# Appendix A

Results from laboratory testing at Chalmers and Mitta.

*Table A1. Borehole NC2204. Tested at Chalmers.*

| Depth [m] | Density [t/m$^3$] | $W_n$ [%] | $W_L$ (4P) [%] | $W_L$ (1P) [%] | $W_P$ [%] | $S_t$ [-] | $c_{ufc}$ [kPa] | $c_{urfc}$ [kPa] |
|---|---|---|---|---|---|---|---|---|
| 2 | 1.46 | 110 | - | 98 | 33 | 8 | 10 | 1.29 |
| 4 | 1.43 | 115 | - | 86 | - | 18 | 10 | 0.52 |
| 6 | 1.48 | 102 | 81 | 81 | 31 | 18 | 14 | 0.78 |
| 8 | 1.50 | 91 | - | 78 | - | 18 | 13 | 0.72 |
| 10 | 1.55 | 84 | - | 69 | 28 | 20 | 14 | 0.68 |
| 12 | 1.46 | 122 | - | 74 | - | 54 | 10 | 0.18 |
| 13.5 | 1.45 | 105 | - | 66 | 31 | 86 | 11 | 0.13 |

*Table A2. Borehole NC2204. Tested at Mitta.*

| Depth [m] | Density [t/m$^3$] | $W_n$ [%] | $W_L$ (4P) [%] | $W_L$ (1P) [%] | $W_P$ [%] | $S_t$ [-] | $c_{ufc}$ [kPa] | $c_{urfc}$ [kPa] |
|---|---|---|---|---|---|---|---|---|
| 2 | 1.48<br>1.45 | 102<br>107 | - | 96 | - | 13 | 14 | 1.07 |
| 4 | 1.43<br>1.43 | 117<br>114 | - | 84 | - | 71 | 15 | 0.21 |
| 6 | 1.46<br>- | 106<br>- | - | 80 | - | 33 | 16 | 0.50 |
| 8 | 1.45<br>1.51 | 94<br>91 | - | 77 | - | 29 | 19 | 0.67 |
| 10 | 1.55<br>1.54 | 82<br>85 | - | 71 | - | 26 | 17 | 0.67 |
| 12 | 1.44<br>1.46 | 117<br>122 | - | 70 | - | 217 | 14 | 0.06 |
| 13.5 | 1.51<br>1.47 | 94<br>69 | - | 70 | - | 194 | 15 | 0.08 |

*Table A3. Borehole NC2205. Tested at Chalmers.*

| Depth [m] | Density [t/m$^3$] | $W_n$ [%] | $W_L$ (4P) [%] | $W_L$ (1P) [%] | $W_P$ [%] | $S_t$ [-] | $c_{ufc}$ [kPa] | $c_{urfc}$ [kPa] |
|---|---|---|---|---|---|---|---|---|
| 2 | 1.50 | 86 | 86 | 89 | 31 | 10 | 17 | 1.66 |
| 3 | 1.42 | 113 | 87 | 89 | 33 | 20 | 11 | 0.54 |
| 4 | 1.47 | 98 | 75 | 76 | 32 | 19 | 9 | 0.50 |
| 5 | 1.51 | 90 | 75 | 76 | 35 | 8 | 7 | 0.93 |
| 6 | 1.54 | 84 | 78 | 79 | 32 | 9 | 12 | 1.39 |

*Table A4. Borehole NC2205. Tested at Mitta.*

| Depth [m] | Density [t/m$^3$] | $W_n$ [%] | $W_L$ (4P) [%] | $W_L$ (1P) [%] | $W_P$ [%] | $S_t$ [-] | $c_{ufc}$ [kPa] | $c_{urfc}$ [kPa] |
|---|---|---|---|---|---|---|---|---|
| 2 | 1.55<br>1.47 | 82<br>99 | - | 84 | - | 14 | 18 | 1.29 |
| 3 | 1.42<br>1.43 | 112<br>110 | - | 97 | - | 32 | 13 | 0.42 |
| 4 | 1.45<br>1.49 | 105<br>93 | - | 86 | - | 32 | 13 | 0.42 |
| 5 | 1.51<br>1.47 | 91<br>89 | - | 81 | - | 16 | 8 | 0.54 |
| 6 | 1.53<br>1.55 | 86<br>83 | - | 76 | - | 19 | 16 | 0.82 |

*Table A5. Borehole NC2211. Tested at Chalmers.*

| Depth [m] | Density [t/m$^3$] | $W_n$ [%] | $W_L$ (4P) [%] | $W_L$ (1P) [%] | $W_P$ [%] | $S_t$ [-] | $c_{ufc}$ [kPa] | $c_{urfc}$ [kPa] |
|---|---|---|---|---|---|---|---|---|
| 2 | 1.44 | 111 | - | 93 | - | 11 | 9 | 0.86 |
| 3 | 1.47 | 102 | 82 | 82 | 30 | 12 | 8 | 0.66 |
| 4 | 1.68 | 72 | - | 64 | - | - | - | 0.95 |
| 5 | 1.81 | 53 | - | - | - | - | - | - |

*Table A6. Borehole NC2211. Tested at Mitta.*

| Depth [m] | Density [t/m$^3$] | $W_n$ [%] | $W_L$ (4P) [%] | $W_L$ (1P) [%] | $W_P$ [%] | $S_t$ [-] | $c_{ufc}$ [kPa] | $c_{urfc}$ [kPa] |
|---|---|---|---|---|---|---|---|---|
| 2 | 1.45<br>1.43 | 100<br>112 | - | 92 | - | 17 | 12 | 0.71 |
| 3 | 1.46<br>1.48 | 104<br>89 | - | 88 | - | 16 | 8 | 0.52 |
| 4 | 1.68<br>1.63 | 75<br>66 | - | 60 | - | 11 | 6 | 0.59 |
| 5 | 1.76 | 49 | - | - | - | - | 6 | - |

*Table A7. Borehole NC2204. Assessment from Mitta.*

| Depth [m] | Comment |
|---|---|
| 2 | Gray-green clayey GYTTJA. plant residues |
| 4 | Gray-green clayey GYTTJA. plant residues |
| 6 | Gray gyttja-like CLAY. shell- and plant residues |
| 8 | Gray gyttja-like silty CLAY. shell- and plant residues |
| 10 | Gray gyttja-like silty CLAY. shell- and plant residues |
| 12 | Gray gyttja-like silty CLAY. single plant residues<br>Note: Disturbed. air pockets may exist |
| 13.5 | Gray sandy silty CLAY. shell residues |

*Table A8. Borehole NC2205. Assessment from Mitta.*

| Depth [m] | Comment |
|---|---|
| 2 | Gray partly gyttja-like silty CLAY. elements of plant residues |
| 3 | Gray gyttja-like silty CLAY. elements of plant residues |
| 4 | Gray gyttja-like silty CLAY. single plant residues |
| 5 | Gray gyttja-like silty CLAY. single plant- and shell residues |
| 6 | Gray gyttja-like silty CLAY. shell residues |

*Table A9. Borehole NC2211. Assessment from Mitta.*

| Depth [m] | Comment |
|---|---|
| 2 | Gray gyttja-like CLAY. shell residues |
| 3 | Gray gyttja-like CLAY. shell residues |
| 4 | Gray partly gyttja-like silty CLAY. plenty of shell residues |
| 5 | Gray sandy silty CLAY. plenty of shell residues |

# Appendix B

Multiple CPTu soundings performed at the same position.

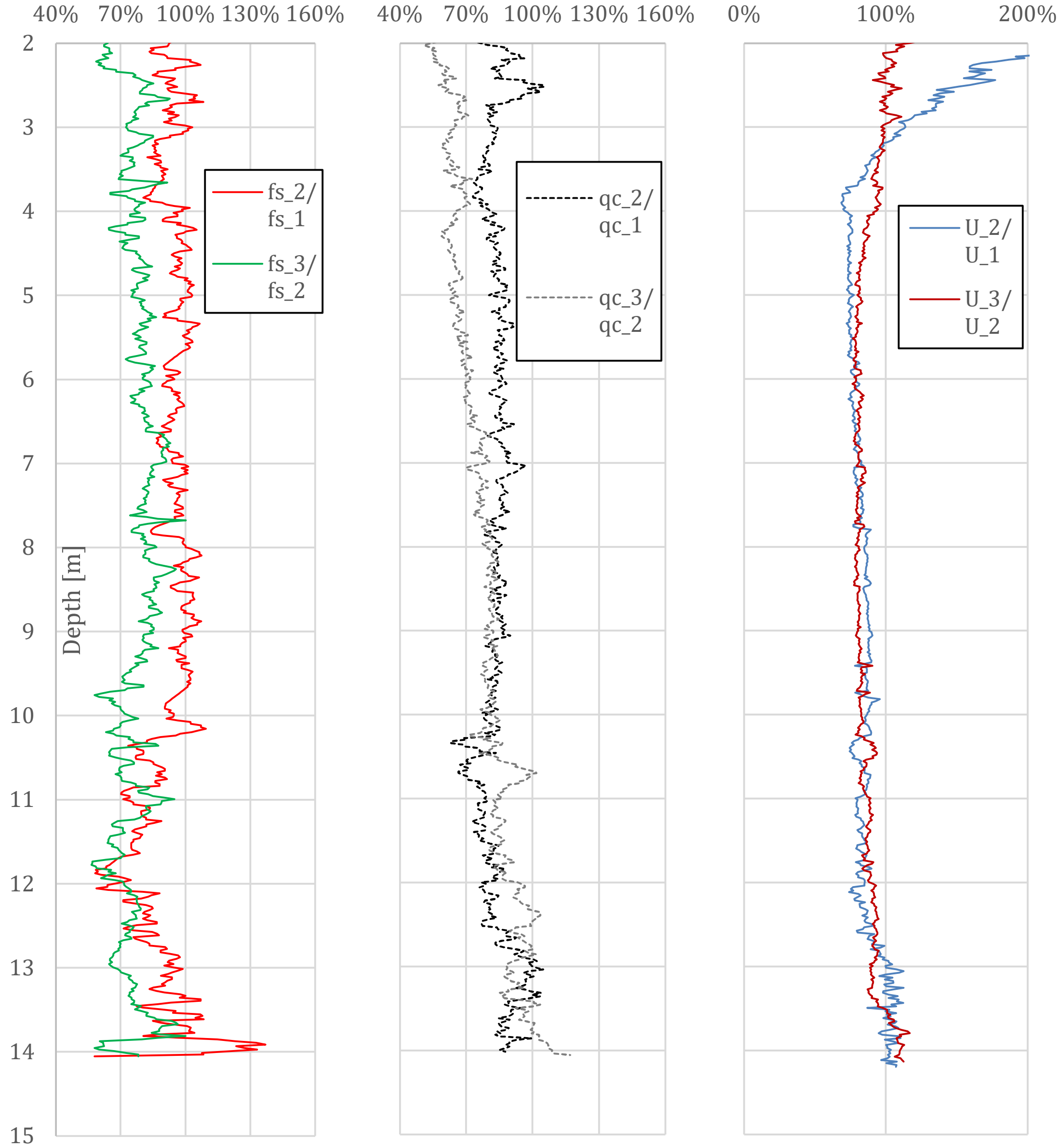


*Figure B1. Percentage of second to first and second to third CPTu sounding for the NC2204 borehole.*

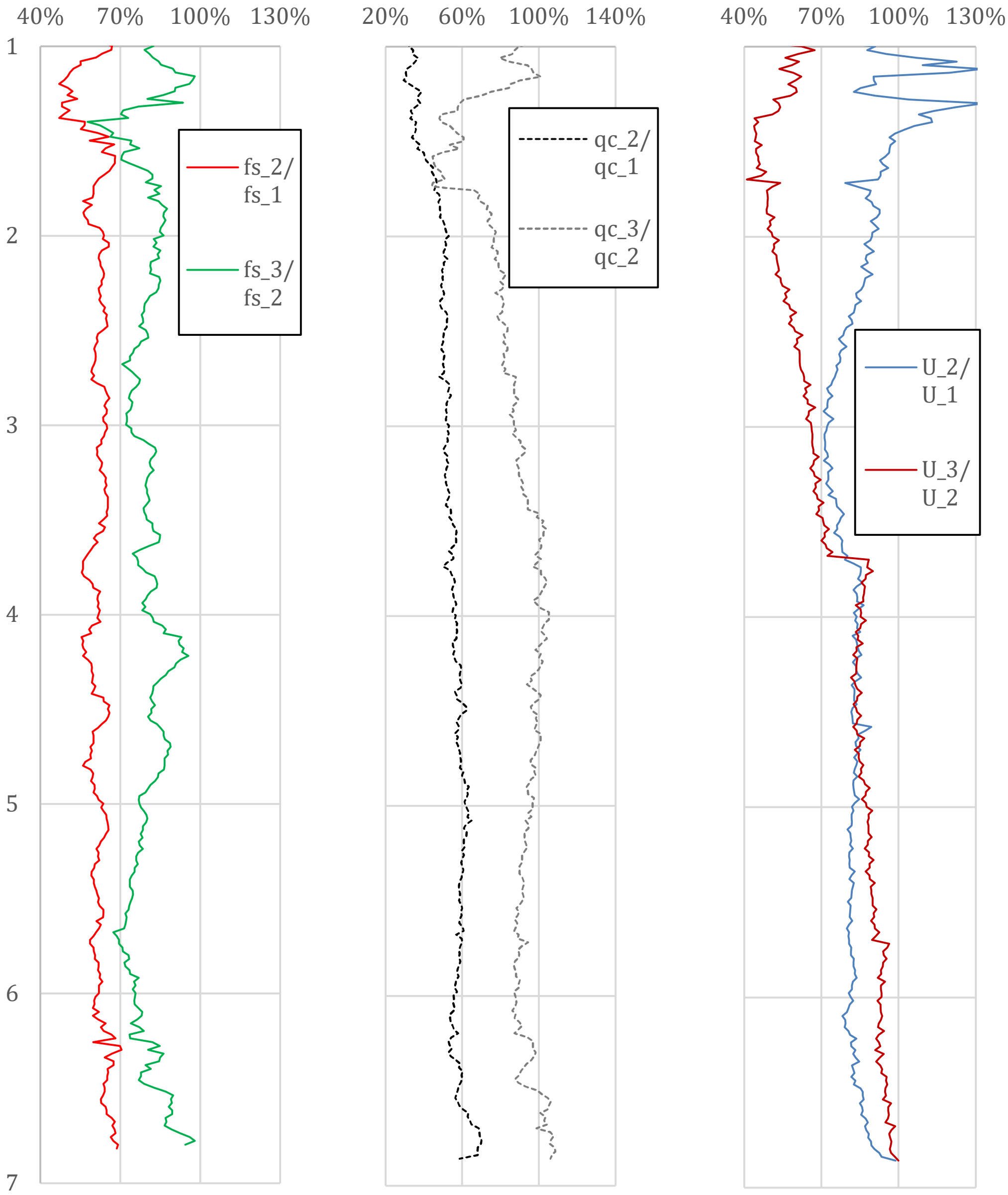


*Figure B2. Percentage of second to first and second to third CPTu sounding for the NC2205 borehole.*

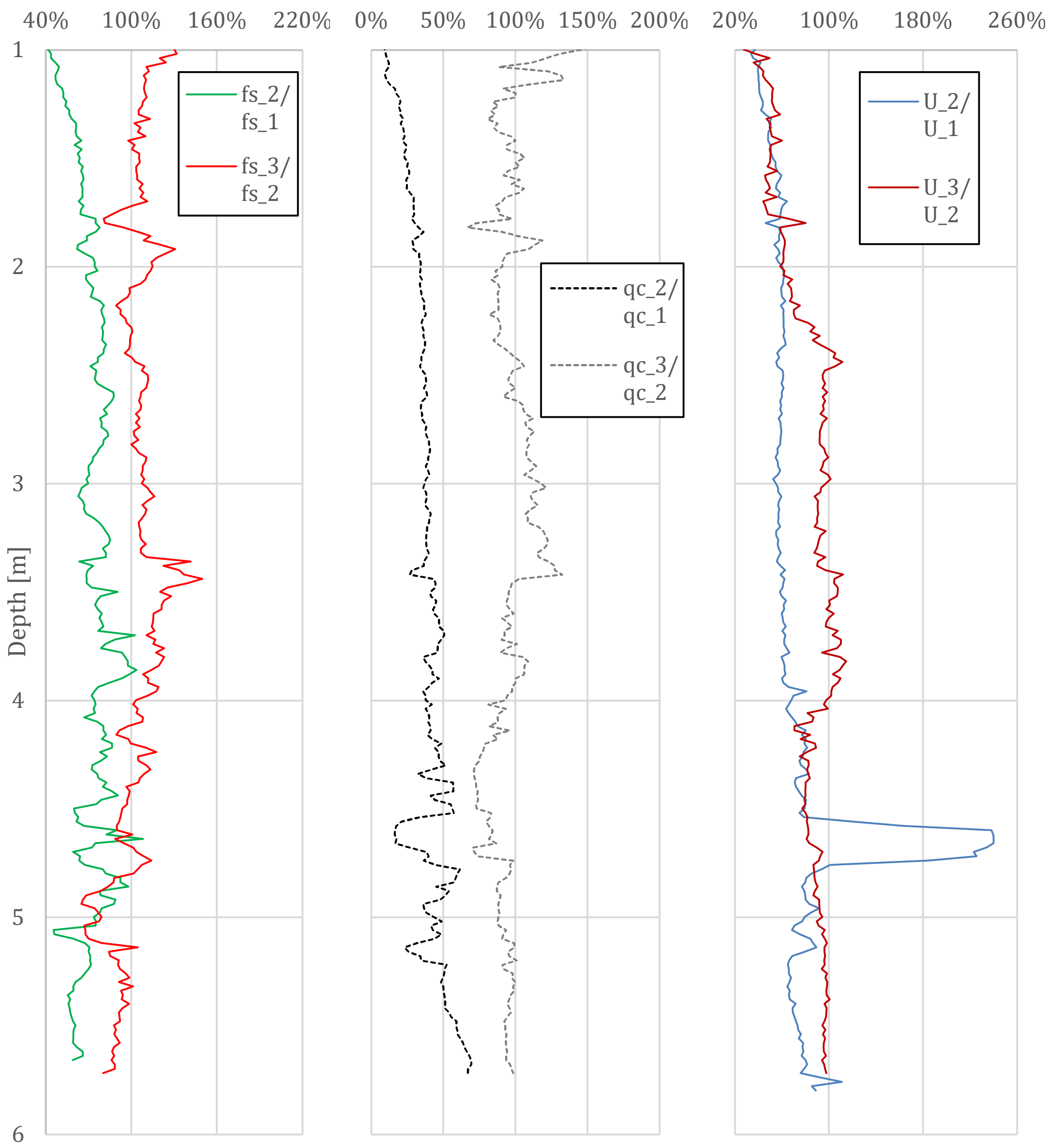


*Figure B3. Percentage of second to first and second to third CPTu sounding for the NC2211 borehole.*

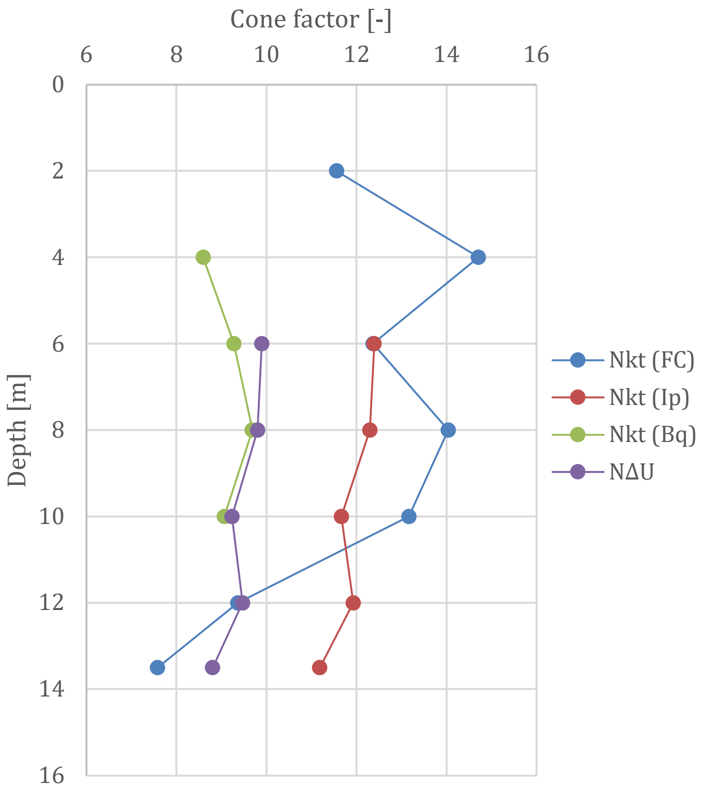


*Figure B4. $N_{kt}$ determined using the undisturbed shear strength evaluated with the fall cone test on the samples from borehole NC2204 at the Chalmers laboratory. Compared with the other cone factors used.*

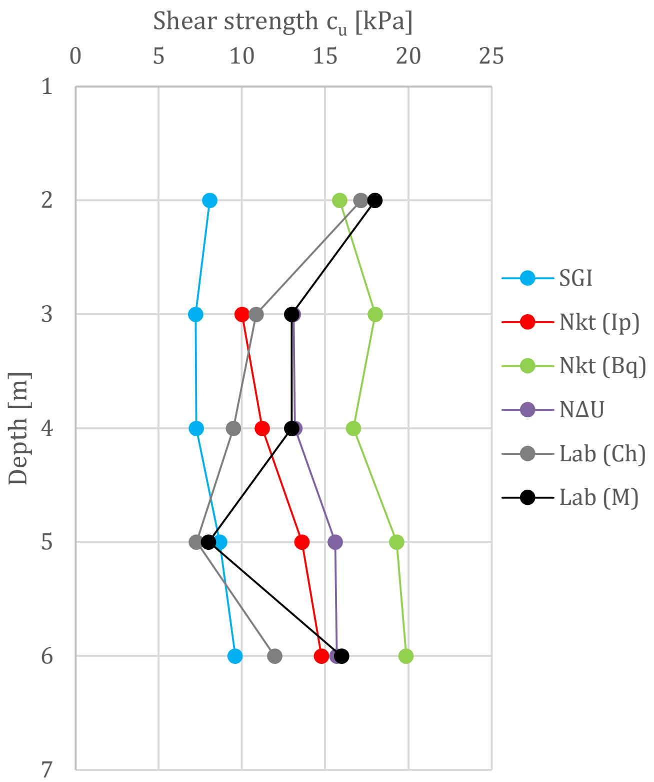


*Figure B5. Undisturbed shear strength [kPa] evaluated from CPTu results using different approaches. Including the two laboratory results. Borehole NC2205.*

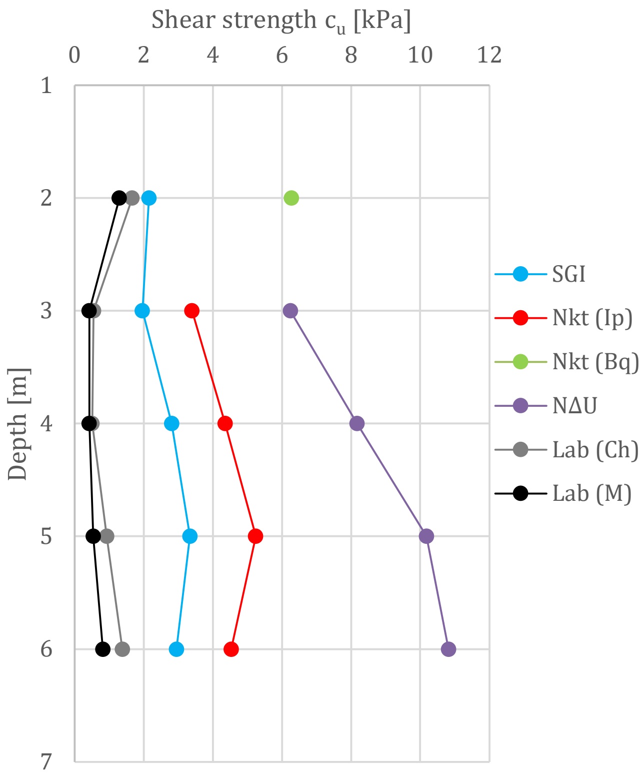


*Figure B6. Remoulded shear strength [kPa] calculated from CPTu results using different approaches. Including the two laboratory results. Borehole NC2205.*

# Appendix C

Additional results from T-bar.

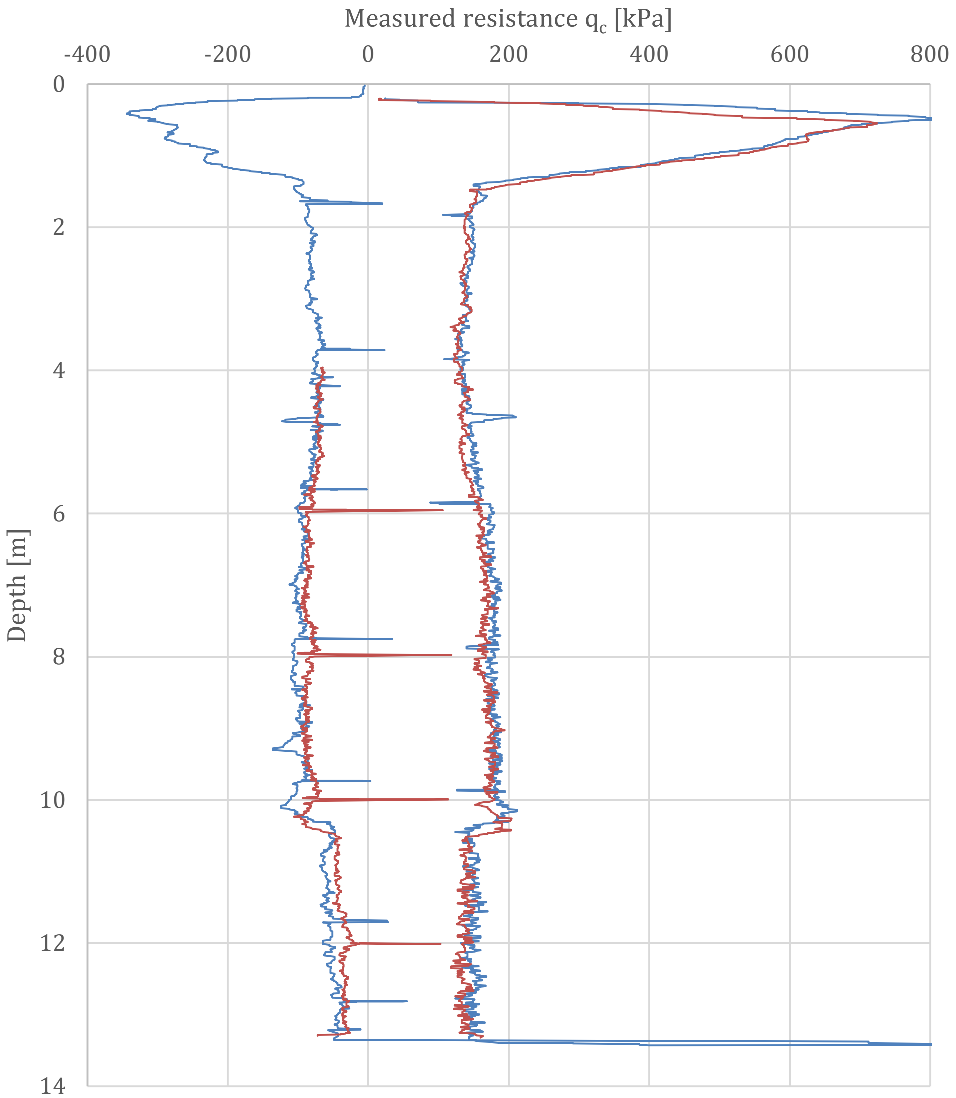


*Figure C1. Measured penetration and extracting resistance for TPT and TPTc in NC2204.*

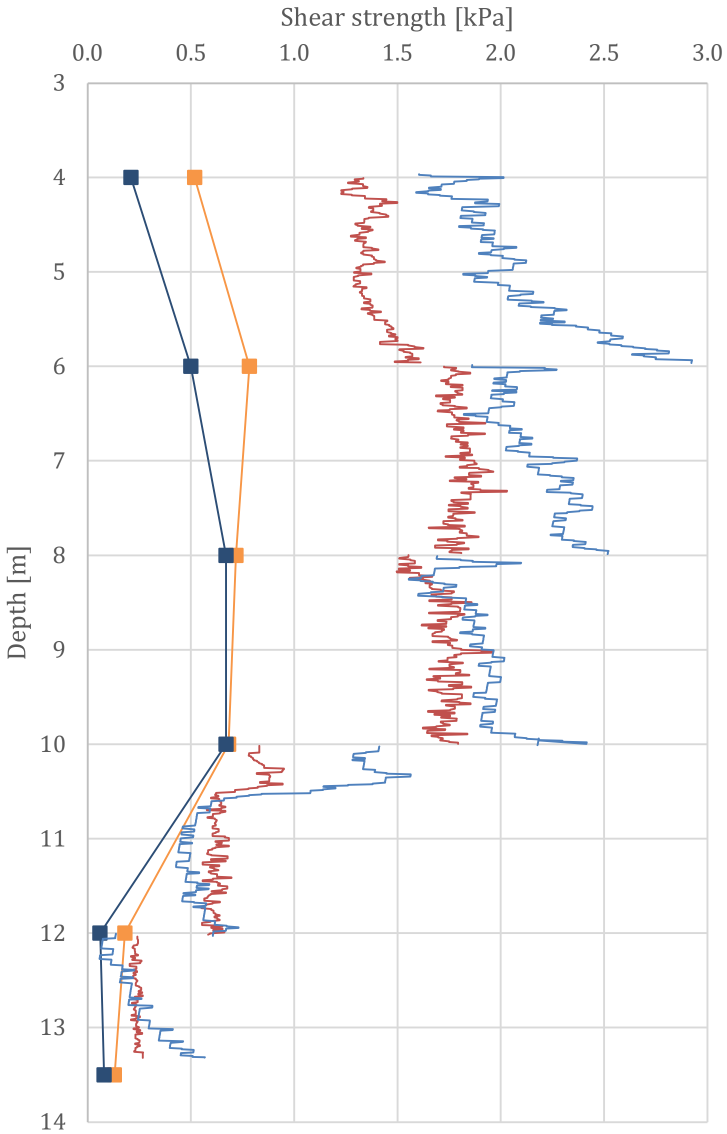


*Figure C2. Predicted shear strength after seven penetrations (red line), shear strength from last cycle at each penetration interval (blue line), shear strength from Chalmers (orange line and markers) and shear strength from Mitta (dark blue line and markers).*

# Appendix D

Field and laboratory data collected from borehole dataset available in the geotechnical archive compiled by SGI (SGI. n.d.). retrieved from: https://bga.sgi.se/. The coordinates are expressed using the SWEREF 99 12 00 coordinate system.

*Table D1. Boreholes retrieved from SGI.*

| Borehole ID | X | Y |
|---:|---:|---:|
| 19SW64 | 6447725.336 | 157574.093 |
| 19SW61 | 6447856.748 | 157631.105 |
| 19SW62 | 6447848.514 | 157581.988 |
| U07047 | 6453651.391 | 158630.800 |
| U07048 | 6453685.409 | 158667.580 |
| U07052 | 6453755.197 | 158491.959 |
| U07053 | 6453725.788 | 158501.298 |
| U07054 | 6453646.802 | 158527.865 |
| 20G036 | 6453722.788 | 158475.601 |
| 20G035 | 6453620.026 | 158499.458 |
| 20G038 | 6453671.361 | 158622.420 |
| 16TY061 | 6402038.790 | 155755.337 |
| 16TY062 | 6402024.113 | 155785.541 |
| U02291 | 6415617.144 | 147274.513 |
| U03019 | 6418633.081 | 151860.223 |
| U03021 | 6418682.698 | 151747.795 |
| U05094 | 6455313.792 | 158869.235 |
| U05095 | 6455305.659 | 158908.923 |
| U06271 | 6467105.087 | 169142.308 |
| U06491 | 6467955.579 | 169101.709 |
| U06131 | 6470430.342 | 172410.320 |
| 16TY091 | 6402602.889 | 158332.560 |
| 16TY101 | 6402847.536 | 158959.940 |

*Table D2. Field and laboratory data collected from projects the consultant company Norconsult AB has been involved in.*

| Project name and ID | Borehole ID | X | Y |
|---|---|---|---|
| Anneberg/Skårby (106 34 10) | NC06 | 6379465.900 | 156254.600 |
| Anneberg/Skårby (106 34 10) | NC05 | 6379450.600 | 156286.000 |
| Anneberg/Skårby (106 34 10) | NC08 | 6379669.800 | 156334.500 |
| Anneberg/Skårby (106 34 10) | NC10 | 6379630.054 | 156333.207 |
| Rishammar 2:2. Kareby (104 34 24) | NC1621 | 6420996.717 | 145993.398 |
| Rishammar 2:2. Kareby (104 34 24) | NC1603 | 6420744.436 | 145800.420 |
| Lunnagården (104 37 66) | NC14B | 6391538.360 | 148783.130 |
| Lunnagården (104 37 66) | NC25 | 6391386.880 | 147932.070 |
| Lunnagården (104 37 66) | NC26 | 6391581.690 | 148390.750 |
| Lunnagården (104 37 66) | NC31 | 6391354.161 | 147651.298 |
| Lunnagården (104 37 66) | NC40 | 6391339.568 | 147420.223 |
| Lunnemyren. Tanum (107 33 89) | NC2110 | 6497552.178 | 109074.614 |
| Varla (106 26 68) | NC02 | 6376417.500 | 153957.979 |
| Varla (106 26 68) | NC05 | 6375735.260 | 154227.801 |
| Åtorps udde (107 39 72) | 17S02 | 6405564.686 | 165432.811 |
| Åtorps udde (107 39 72) | 17S04 | 6405370.589 | 165647.750 |
| Åtorps udde (107 39 72) | 1407 | 6405494.953 | 165731.253 |
| Åtorps udde (107 39 72) | 107-NC05 | 6405722.738 | 165772.743 |
| Åtorps udde (107 39 72) | PEH2-206 | 6405532.455 | 165729.789 |
| Åtorps udde (107 39 72) | PEH2-211 | 6405421.669 | 165743.700 |
| Göteborg. Jättesten (106 11 21) | Gb-Js:NC8 | 6399960.072 | 144437.271 |

DEPARTMENT OF ARCHITECTURE AND
CIVIL ENGINEERING
CHALMERS UNIVERSITY OF TECHNOLOGY
Gothenburg, Sweden 2022
www.chalmers.se

CHALMERS
UNIVERSITY OF TECHNOLOGY